Thermodynamic properties of ionic liquids

Dissertation

zur

Erlangung des akademischen Grades

doctor rerum naturalium (Dr. rer. nat.)

der Mathematisch-Naturwissenschaftlichen Fakultät

der Universität Rostock

vorgelegt von

Andrei Yermalayeu

aus Rostock

Rostock, 07.08.2013

urn:nbn:de:gbv:28-diss2014-0021-2

Gutachter:

1. Gutachter:
   Prof. Dr. Sergey Verevkin
   Universität Rostock, Institut für Chemie

2. Gutachter:
   Prof. Dr. Ingo Krossing
   Universität Freiburg,
   Institut für Anorganische und Analytische Chemie

Datum der Einreichung: 07.08.2013

Datum der Verteidigung: 19.11.2013

Content

1. Introduction and motivation

1.1 Introduction

Ionic Liquids (ILs) are a new class of materials, which has attracted a lot attention in scientific and industrial research recently. Due to their combination of chemical and physical properties they significantly differ from common molecular liquids. ILs are often defined as salts with low melting point, usually below 373 K [1]. More broad definition is given by K. Seddon: ionic liquid is an organic salt that exists in the liquid state below the temperature of decomposition.

First IL was reported by Gabriel and Weiner (ethanolammonium nitrate with m.p. c.a. 276 K) in 1888 [2]. Really liquid IL was first reported by Paul Walden (ethylammonium nitrate with m.p. 285 K) in 1910 [3]. After that ILs were forgotten for almost 70 years. In 1982 Wilkes et al [4] published an article, where they described 1-alkyl-3-imidazolium salts with $[Cl]^-$, $[Br]^-$, $[I]^-$, $[AlCl_4]^-$ etc. anions. These compounds were considered as 1-st generation ILs. They barely found a practical application, due to instability in the presence of water. Ten years later the 2-nd generation of ILs was synthesized [5] by anion exchange (to $[BF_4]^-$, $[PF_6]^-$, $[NTf_2]^-$ etc.). Their stability in air, and in the presence of water, made ILs interesting for practical applications. As an example one of the most studied ILs $[C_2mim][NTf_2]$ is shown in Figure 1.1. The 2-nd generation ILs were attractive with a combination of unique properties: low volatility [6], thermal stability [7] etc.

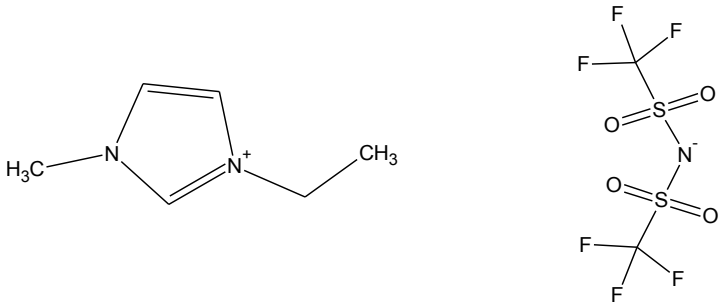

Figure 1.1 1-ethyl-3-methylimidazolium bis(trifluoromethylsulfonyl)imide or $[C_2mim][NTf_2]$.

The development of task specific ILs with a number of functional groups attached to the cation or anion [8] lead to the creation 3-rd generation ILs, that are being synthesized with the aim to achieve specific desired physical and chemical properties. At least 4 degrees of freedom can be tuned in the IL structure:

- cation
- anion
- alkyl chains in the cation or anion
- attachment of specific functional groups

The simple combinatory analysis indicates that about 10^{18} ILs can be possibly synthesized. This variety opens wide opportunities in the tailoring of ILs suitable for practical applications.

ILs have already found a way to practical applications in various fields. Due to their low volatility and thermal stability they are considered as an alternative for traditional volatile organic solvents [9] in the processes of synthesis, extraction, for "green chemistry", and as a heat transfer media [10]. ILs are also interesting for different electrochemical applications as electrolytes [11]. The combination of the stability, low volatility, and tribological properties has stimulated attempts to apply them as a lubricants and greases [12]. Another novel application is the use of IL in the pharmaceutical industry, e.g for topical drug delivery [13]. IBM has recently reported about the potential application of ILs in future generation logic and memory units [14].

The understanding of the behavior of ILs and their properties is crucial for any practical application. But the available chemical and physical data are unfortunately scarce in comparison to the amount of already commercially available ILs. Moreover, the existing data are often inconsistent. In this work we focused on the reliable determination of thermodynamic properties of ILs using different independent methods. The molar vaporization enthalpy $\Delta_l^g H_m^0$ of ILs has been the key value throughout this study.

Initially it was assumed that ILs had no measurable vapor pressure at ambient temperature. Surprisingly, Earle et al [6] showed, that IL could be distilled at low pressures and elevated temperatures. Thus, an experimental study of ILs vapor pressure and vaporization enthalpies was required. Several techniques were developed or adjusted for $\Delta_l^g H_m^0$ measurements: transpiration method [15], [16], Knudsen method [17], [18], thermogravimetrical analysis (TGA) [19]–[21], temperature-programmed desorption with line of sight mass spectrometry (TPD-LOSMS) [22]–[25], high-temperature spectroscopic technique (HT-UV) [26], drop-calorimetry [27], Langmuir method combined with quartz micro balance (QCM) [28].

1.2 General Motivation

1) One of the potential areas of application of ILs is the usage as alternative solvents due to their low volatility. The study of temperature volatility dependence and vaporization enthalpy is required for successful application of ILs in industrial processes. The measurements of volatility and vaporization enthalpy of extremely low-volatile compounds are a challenging task. This task requires the development of new methods as well as modification of existing methods. To produce reliable experimental values for vaporization enthalpy of ILs, simultaneous application of several independent methods is required.

2) The experimental values of enthalpies of vaporization provide direct access to the intermolecular interactions, thus they are especially desired for quantum calculations and molecular dynamic methods as reference data.

3) Studies of structure-property relations of thermodynamic properties of ILs are important to assess consistency of the experimental data, as well as to predict these properties for ILs not studied yet.

In this work we analyzed structure-property relations in ILs vaporization enthalpy using data available in the literature together with own experimental results. This study focused on the development of practical procedures for reliable adjustment of vaporization enthalpies measured at elevated temperatures to the conventionally acknowledged reference temperature T = 298.15 K, where available experimental and theoretical values could be compared and correlated. We analyzed experimental vaporization enthalpies measured by the Langmuir method combined with quartz micro balance (QCM), and the thermogravimetrical analysis (TGA) in order to understand the problems with adjustment of the values to the reference temperature (298 K). We introduced and tested three practical methods of the adjustment. For validation of experimental data measured by "direct" methods (QCM and TGA) we additionally used "indirect" methods (solution calorimetry, and DSC). In this work we developed a new method to derive vaporization enthalpies "indirectly" – solution calorimetry. We have introduced and tested an approach of the determination of liquid enthalpies of formation for ILs based on results of solution and combustion calorimetry. This approach, combined with quantum chemical calculations, allows to assess the vaporization enthalpies of ILs. Finally, some useful trends and structure-property dependencies on different structure variations: cation, anion, alkyl chain length, were found and used for development of group contribution method for prediction of thermodynamic properties of ILs.

2. Determination of vaporization enthalpies of ionic liquids with QCM and TGA techniques.

2.1 Review of available vaporization enthalpies of ILs.

Experimental measurements of the vaporization enthalpies are extremely challenging because of two main problems. The vapor pressure of ILs at ambient temperature is negligible, whereas at high temperatures where vapor pressures can be measured, possible thermal decomposition process can distort the results. As a matter of fact, with the exception for the Knudsen method [17], [29] traditional experimental techniques for vapor pressure measurement have not been developed for the extremely low volatile liquids such as ILs. This fact has stimulated the development of new direct experimental methods: TPD-LOSMS [22], [23], TGA [19], [20], [30], HT-UV [26], and QCM [28], [31]. As a rule, the vaporization studies of ILs were performed at temperatures between 360 and 600 K [19], [22], [23], [26], [28], [30]–[32]. Most frequently studied ILs are imidazolium (Im), pyrrolidinium (Pyrr), pyridinium (Py) and ammonium (N) based with typical anions $[NTf_2]^-$, $[BF_4]^-$, $[PF_6]^-$ etc.

A homological series of the 1-alkyl-3-methylimidazolium bis(tri-fluoromethane-sulfonyl)imides or $[C_n\text{mim}][NTf2]$ is beyond any doubt the most frequently investigated class of IL for the study of vaporization enthalpies. There are at least two reasons for this intense interest. First, it is well known that these ILs have such a remarkable thermal stability, that they can be distillated without decomposition at elevated temperatures of 473 to 573 K [6], [33]. The second aspect is that the increasing length of the cation alkyl chain should lead to predictable monotonic structure-property relations such as those exhibited by molecular liquids like alkanes. However, it remains unclear, whether ionic liquids follow the same monotonic pattern or not, especially for the vaporization enthalpy. We have collected the available literature data on vaporization enthalpies of $[C_n\text{mim}][NTf_2]$ and present them graphically in Figure 2.1.

It is apparent that the available vaporization enthalpies of $[C_n\text{mim}][NTf_2]$ are in total disarray. However, not without bias, some definite trends in the $\Delta_l^g H_m^0$ values of $[C_n\text{mim}][NTf_2]$ (see Figure 2.2) can be suggested and even justified. For example, a very unusual (for a homologous series) and noticeably non-linear and even "bent up" dependence of $\Delta_l^g H_m^0$ on alkyl chain length (in the imidazolium cation) was observed (see Figure 2.2) for ethyl-, butyl-, hexyl-, and octyl-derivatives determined by the Knudsen method [29] and by LOSMS [22]. In contrast, the direct calorimetrically measured values of vaporization enthalpies [27] for the same set of ILs demonstrated (see Figure 2.2) the expected linear dependence of the $\Delta_l^g H_m^0$ on the chain length. What is curious about the calorimetry data, is the unusually high contribution each additional CH_2 group makes to the vaporization enthalpy (8.9±0.6 kJ·mol^{-1}) [27]. For comparison, in

alkanes the incremental increase in vaporization enthalpy per CH_2 group (4.95±0.10 kJ·mol^{-1}) [34] is twice lower.

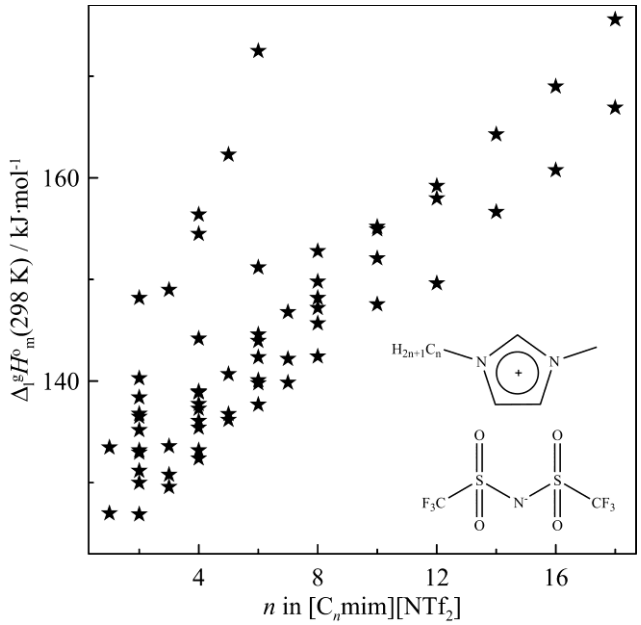

Figure 2.1 Available literature data on the enthalpy of vaporization, $\Delta_l^g H_m^0$ (298 K) chain length (n) dependence for [C$_n$mim][NTf$_2$].

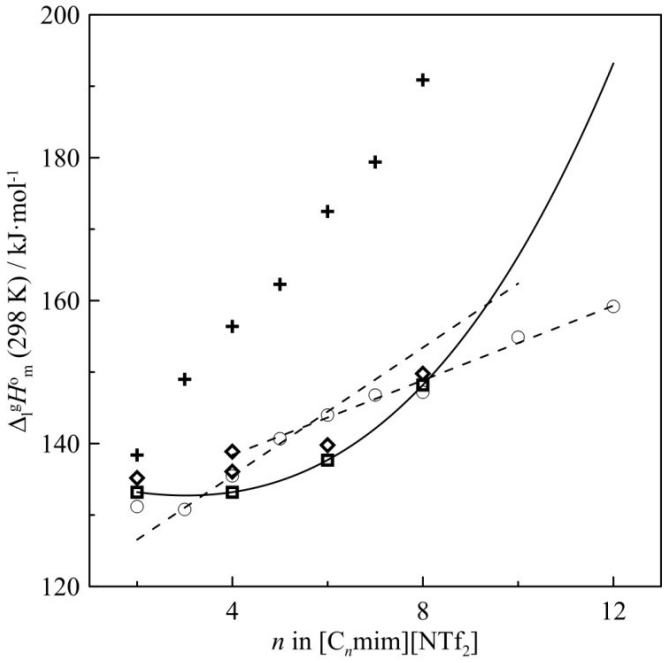

Figure 2.2 Some possible trends in the vaporization enthalpy chain-length dependence. ◊ – Knudsen effusion method [29], □ – LOSMS [22], + - calorimetry [27]; ○- QCM-Knudsen [31]

Another and more sophisticated dependence of vaporization enthalpies was reported recently based on the data obtained with the Knudsen effusion cell, combined with a quartz crystal microbalance [31]. Two distinct slopes in the vaporization enthalpy versus alkyl chain length curve were clearly observed for the [$C_n$mim][NTf_2] ILs series, with the change in slope occurring at [C_6mim][NTf_2] (see Figure 2.2). This behavior was explained in terms of a structural percolation phenomenon in which the longer alkyl chains form aggregates in the liquid phase, thereby lowering the vaporization enthalpy for the longer alkyl chains [31]. Such an aggregation phenomenon has been reported in several simulations [35], [36] and experimental studies of volumetric properties [1], but this was the first time such a phenomenon was observed [31] for the enthalpy of vaporization trend.

Considering these conflicting results, the following questions arise:

1. What is the reasonable trend within the spread of the experimental results in Fig 2.1?
2. Are the observed in the literature shapes of the vaporization enthalpy dependence on the alkyl chain length a consequence of the ionic interactions?
3. What makes the vaporization enthalpy dependence of ILs different in comparison with the molecular liquids?

We attempted to answer these questions using a combination of precise experimental measurements and atomistic simulations to examine the vaporization enthalpies for the [$C_n$mim][NTf_2] family with odd and even chain length of the alkyl-imidazolium cation. Two recently developed methods QCM and TGA [28], [30], were used for the experimental investigation. A short description of both methods is given below. The detailed description is given in Chapter 6.

2.2 Langmuir method in combination with quartz micro balance (QCM)

The experimental procedure was reported elsewhere [28]. In short, a sample of IL placed in an open cavity of a thermostated metal block is exposed to vacuum system (at 10^{-5} Pa). The quartz crystal microbalance was placed directly over the measuring cavity containing the IL. The change in the vibrational frequency of the crystal Δf is a measure of the amount of IL deposited on the cold QCM. The value of Δf was measured as a function of time at different temperatures. The change of the vibrational frequency Δf is directly related to the mass deposition Δm on the crystal surface according to equation [28], [37]:

$$\Delta f = -C \cdot f^2 \cdot \Delta m \cdot S_C^{-1} \tag{2.1}$$

where f is the fundamental frequency of the crystal (5 MHz in this case) with $\Delta f << f$, S_C is the area of the crystal, and C is a constant [28], [37]. Using the frequency change rate df/dt measured by the QCM the molar enthalpy of vaporization, $\Delta_l^g H_m^0$ (T_0), is obtained [28] by:

$$ln\left(\frac{df}{dt}\sqrt{T}\right) = A' - \frac{\Delta_l^g H_m^0(T_0) - \Delta_l^g C_{p,m}^0(T_0)}{R}\left(\frac{1}{T} - \frac{1}{T_0}\right) + \frac{\Delta_l^g C_{p,m}^0}{R} ln\left(\frac{T}{T_0}\right) \tag{2.2}$$

with a constant A' which is essentially unknown including all empirical parameters which are specific for the apparatus and the substance under study. T_0 appearing in eq. 2.2 is an arbitrarily chosen reference temperature. In our study T_0 was set equal to 380 K, 542 K, or 298 K. The value $\Delta_l^g C_{p,m}^0 = C_{p,m}^0(g) - C_{p,m}^0(l)$ is the difference of the molar heat capacities of the gaseous $C_{p,m}^0(g)$ and the liquid phase $C_{p,m}^0(l)$ respectively. The temperature dependent vaporization enthalpy $\Delta_l^g H_m^0(T)$ is given by

$$\Delta_l^g H_m^0(T) = \Delta_l^g H_m^0(T_0) + \Delta_l^g C_{p,m}^0(T - T_0) \quad (2.3)$$

The frequency change rate d*f*/d*t* was measured in a few consecutive series with increasing and decreasing temperature steps. The background noise can impact the QCM signal. As a rule it depends on the vacuum conditions and possible deposits on the internal parts of the vacuum chamber. In order to reduce the impact of the background noise on the QCM it was kept at a constant temperature of 30 K higher than the temperature of walls of the vacuum system. Preliminary experiments have revealed that the background noise was less than 0.5-1% of the frequency change rate at the lowest temperature of determination. After each run the sample of IL was cooled down and the effect of background noise was checked. The QCM method provided very reproducible temperature dependences of the frequency change rate d*f*/d*t*. The experimental uncertainties assessed for the vaporization enthalpy from the d*f*/d*t* temperature dependences were always lower than ± 1.0 kJ·mol^{-1} (calculated as the twice standard deviation). In order to detect a possible decomposition of IL under the experimental conditions, the residual IL in the cavity and the IL-deposit on the QCM were analyzed by ATR-IR spectroscopy. No changes in the spectra were detected with the ILs under study in this work. For further information see QCM description in Chapter 6.

2.3 Thermogravimetrical method (TGA)

The TGA procedure was carefully developed for very low volatility compounds [30]. We used a carefully calibrated Perkin Elmer Pyris 6 TGA in this work. An IL sample of about 50-70 mg was placed in a plain platinum crucible inside of the measuring head of the TGA. The sample was stepwise heated and a mass loss of 0.1-0.8 mg from the crucible was recorded at each isothermal step. Isothermal mass loss rate d*m*/d*t* was monitored in the temperature range 480-620 K at a nitrogen flow rate of 140 ml·min^{-1}. Isothermal mass loss rate d*m*/d*t* was measured in a several consecutive series with increasing and decreasing temperature steps. In order to confirm the absence of decomposition of IL under the experimental conditions, the residual IL in the crucible was analyzed by ATR-IR spectroscopy. No changes in the spectra before and after the experiment were detected for the ILs under study.

The relationship between the mass loss d*m*/d*t* and the vaporization enthalpy was derived according to eq. 2.2 but by using the mass loss rate d*m*/d*t* measured by the TGA (instead of the frequency change d*f*/d*t* by QCM). Total experimental uncertainties of the determination of vaporization enthalpy with the TGA were assessed [30] to be at the level of ±3.0 kJ·mol^{-1}

(calculated as the twice standard deviation). For further information see TGA description in Chapter 6.

2.4 Vaporization enthalpies of [$C_n$mim][NTf_2] ILs family studied with QCM and TGA.

Enthalpies of vaporization of the even and odd ILs were measured using the QCM and TGA technique. The combination of high-vacuum conditions with the extremely sensitive QCM allows measurements of mass loss rates for ILs at temperatures down to 363 K. In contrast to the conventional Knudsen method, the Langmuir vaporization was significantly more sensitive since the total open surface is exposed to the QCM under vacuum conditions.

Vaporization Enthalpies, $\Delta_l^g H_m^0(T_{av})$, referred to average temperatures of the experimental temperature ranges obtained from temperature dependent measurements of the frequency change *df*/*dt* by the QCM and the mass loss rate *dm*/*dt* by TGA for the odd members of the homologous series [$C_n$mim][NTf_2] with the alkyl chain length n = 1, 3, 5, and 7 are given in Table 2.1 (the primary experimental data are listed in Table S1 in Supporting Information).

It is apparent from Table 2.1 that T_{av}-values for ILs under study are significantly different depending on the chain length n, as well as on the method used: long-chained species were studied at much higher temperatures in comparison to shorter one, as well as the TGA studies were performed at temperatures of 30-150 K higher than in QCM. As a matter of fact, enthalpies of vaporization $\Delta_l^g H_m^0(T_{av})$ derived from both methods (see column 3, Table 2.1) could not be compared because they referred to different T_{av}-values. For the sake of comparison, enthalpies of vaporization $\Delta_l^g H_m^0(T_{av})$ (column 3, Table 2.1) have to be adjusted to any arbitrary but reasonable common temperature, which ideally is close to the average temperatures T_{av} of the individual measurements. For the QCM studies the suitable temperature was 380 K, while for the TGA results we chose 572 K for comparison (see Figure 2.3). For comparison as well as in order to keep consistency with our previous work we *first* used in the current work the commonly acknowledged value [38] $\Delta_l^g C_{p,m}^0$= -100 J·K^{-1}·mol^{-1} in eq. 2.3. Comparison of the vaporization enthalpies at the selected temperatures 380 K for QCM and at 572 K for TGA should be least affected by an ambiguity of the $\Delta_l^g C_{p,m}^0$-value because of the deliberately short extrapolations from T_{av} of the individual measurements.

Figure 2.3 shows an impeccable linear dependence of the vaporization enthalpies for the [$C_n$mim][NTf_2] family (omitting n = 1) on the number of C-atoms in the alkyl chain of the imidazolium cation, n, when measured by using the QCM. The scatter of the results obtained by the TGA is somewhat larger, but within the experimental uncertainties the linear correlation (omitting n = 1) is also apparent for the TGA data.

Table 2.1 Experimental Vaporization Enthalpies, $\Delta_l^g H_m^0$, of [$C_n$mim][NTf_2] at T_{av} and at 298 K

T-range / K	T_{av} / K	$\Delta_l^g H^o_m$ (T_{av}) kJ·mol^{-1}	$\Delta_l^g H^o_m$ (298 K) kJ·mol^{-1}	Method
		[C_1mim][NTf_2]		
345 - 400	381.6	119.9 ± 1.0	128.2±1.0 [a]	QCM
543 - 623	590.0	104.3 ± 1.6	133.5±1.6 [a]	TGA
			126.0 ± 1.8	QCM+TGA
		[C_2mim][NTf_2]		
362 - 395	378	118.6 ± 1.0	126.9±1.0 [a]	QCM
480 - 570	520.2	110.5 ± 1.5	132.7±1.5 [a]	TGA
			123.1 ± 2.0	QCM+TGA
		[C_3mim][NTf_2]		
362 - 395	380.3	121.4 ± 1.0	129.6±1.0 [a]	QCM
480 - 570	546.2	108.8 ± 2.6	133.6±2.6 [a]	TGA
			127.6 ± 2.4	QCM+TGA
		[C_4mim][NTf_2]		
362 - 395	378	124.4 ± 1.0	132.4±1.0 [a]	QCM
513 - 572	541.8	113.5 ± 1.5	137.8±1.5 [a]	TGA
			129.7 ± 1.9	QCM+TGA
		[C_5mim][NTf_2]		
362 - 404	381.7	127.8 ± 1.0	136.2±1.0 [a]	QCM
523 - 603	560.8	110.5 ± 1.9	136.8±1.9 [a]	TGA
			135.8 ± 2.0	QCM+TGA
		[C_6mim][NTf_2]		
362 - 405	383	131.6 ± 1.0	140.1±1.0 [a]	QCM
513 - 571	541.8	118.0 ± 1.8	142.3±1.8 [a]	TGA
			138.9 ± 2.1	QCM+TGA
		[C_7mim][NTf_2]		
364 - 406	385.3	133.5 ± 1.0	142.2±1.0 [a]	QCM
503 - 603	553.7	114.3 ± 1.9	139.9±1.9 [a]	TGA
			143.4 ± 2.1	QCM+TGA
		[C_8mim][NTf_2]		
372 - 402	387	136.8 ± 1.0	145.7±1.0 [a]	QCM
513 - 571	541.8	122.6 ± 1.0	147.0±1.0 [a]	TGA
			145.0 ± 1.8	QCM+TGA
		[C_{10}mim][NTf_2]		
380 - 410	394.6	142.5 ± 1.0	152.1±1.0 [a]	QCM
493 - 552	522	125.2 ± 1.0	147.5±1.0 [a]	TGA
			155.6 ± 2.1	QCM+TGA
		[C_{12}mim][NTf_2]		
392 - 425	408.4	147.0 ± 1.0	158.0±1.0 [a]	QCM
503 - 562	533.5	126.0 ± 1.1	149.5±1.1 [a]	TGA
			165.4 ± 2.3	QCM+TGA
		[C_{14}mim][NTf_2]		
400 - 432	416.2	152.5 ± 1.0	164.3±1.0 [a]	QCM
513 - 571	541.8	132.7 ± 1.0	157.1±1.0 [a]	TGA
			171.5 ± 2.3	QCM+TGA
		[C_{16}mim][NTf_2]		
405 - 445	424.8	156.3 ± 1.0	169.0±1.0 [a]	QCM
513 - 571	541.8	136.4 ± 1.4	160.8±1.4 [a]	TGA
			177.8 ± 2.9	QCM+TGA
		[C_{18}mim][NTf_2]		
410 - 452	430.3	162.4 ± 1.0	175.6±1.0 [a]	QCM
546 - 621	582.5	138.5 ± 1.4	166.8±1.4 [a]	TGA
			183.1 ± 2.5	QCM+TGA

[a] Enthalpies of vaporization for ILs were adjusted to 298 K with $\Delta_l^g C^0_{p,m}$ = - 100 J·K^{-1}·mol^{-1}, uncertainties in the heat capacity differences were not taken into account; **in bold** – Enthalpies of vaporization for ILs adjusted with $\Delta_l^g C^0_{p,m}$ derived from TGA and QCM data (explanation below in chapter)

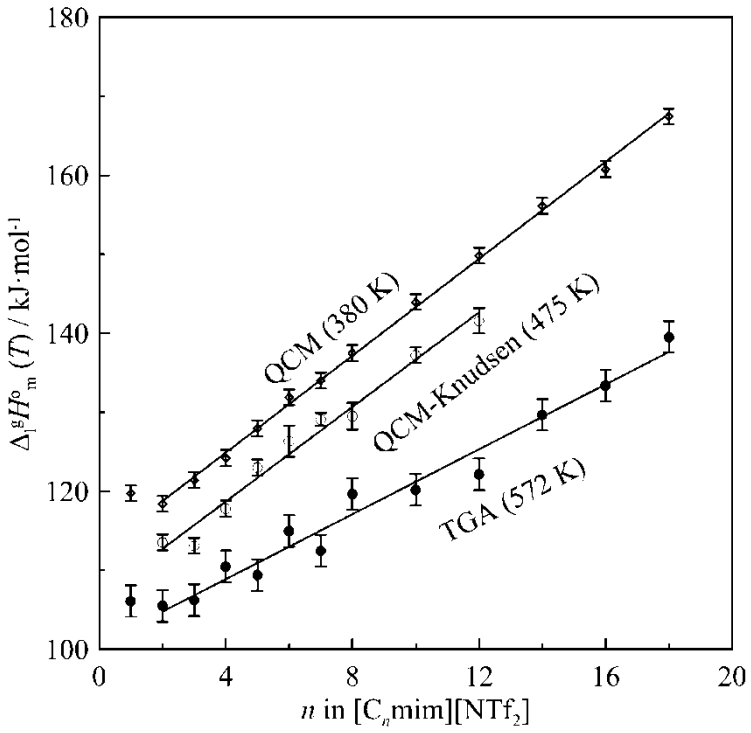

Figure 2.3 Dependence of the enthalpy of vaporization, $\Delta_l^g H_m^0(T_{av})$ for 1-alkyl-3-methylimidazolium bis(trifluoromethanesulfonyl)imides on the length of the cation alkyl chain (n). QCM-Knudsen values are taken from [31]

For comparison with our own vaporization enthalpies measured by TGA and QCM, we added to Figure 2.3 the most recent literature data measured by the combined QCM-Knudsen method [31]. We selected for comparison with their data the temperature 475 K and in this case we again used the value $\Delta_l^g C_{p,m}^0$= -100 J·K^{-1}·mol^{-1} for adjustment of vaporization enthalpies from T_{av} to the selected T = 475 K. Experimental uncertainties of our measurements as well as of the literature data are presented in Figure 2.3 as the error bars. In our opinion, the experimental vaporization enthalpies from the combined Knudsen-QCM method [31] also fit very well (within the error bars) the linear dependence on the chain length *n,* similar to our own finding. This conclusion disagrees with the interpretation given in ref. [31] where the authors consider their Knudsen-QCM results as an unusual evidence for "structural percolation phenomenon". It is also clear from Figure 2.3 that, in order for one to observe a change in slope of the enthalpy of vaporization in Rocha *et al.*'s data [31], one must throw out the *n*=2 data point, despite the fact that Rocha et al. state in their paper that the enthalpy of vaporization "results for [C$_2$mim][NTf$_2$] and [C$_4$mim][NTf$_2$] from Santos *et al* [27] are in reasonable agreement with the present set of results or most of the results found in the literature. Thus we were unsure what the justification is to exclude the *n*=2 data from the fitting. We showed that if one uses *all* of Rocha *et al*'s data and consider the associated uncertainties, there is no change in slope. Or, if one chooses to take the *n*=3 point as an outlier (for example), there is also no break in slope. This is clearly seen in Figure 2.3 of the present work. In addition to pointing this out, we provide our own experimental

data for even and odd [$C_n$mim][NTf_2] with n=1 to n=18 (see Table 2.1) and show that from n=2 to n=18 there is no change in slope. We do see an "outlier" at n=1, but then also confirm both observations with simulations [39] (see Figure 2.4), which shows why one should see an outlier at n=1 (due to Coulombic and van der Waals trends). The data presented in Figure 2.3 doesn't reveal any in the linear trend on enthalpy of vaporization with chain length (except for n = 1) within the error bars for all three data sets. In our opinion the "structural percolation phenomenon" or nano-scale aggregation of alkyl chains, which is thought to occur in ILs [31], does not result in two distinct trends in the enthalpy of vaporization with chain length, as it has been claimed recently [31]. It rather seems that this is an artifact which was over-interpreted by the authors within the boundaries of their experimental uncertainties. Simulation results performed by Maginn and Liu [39] give further support for this conclusion (see Figure 2.4).

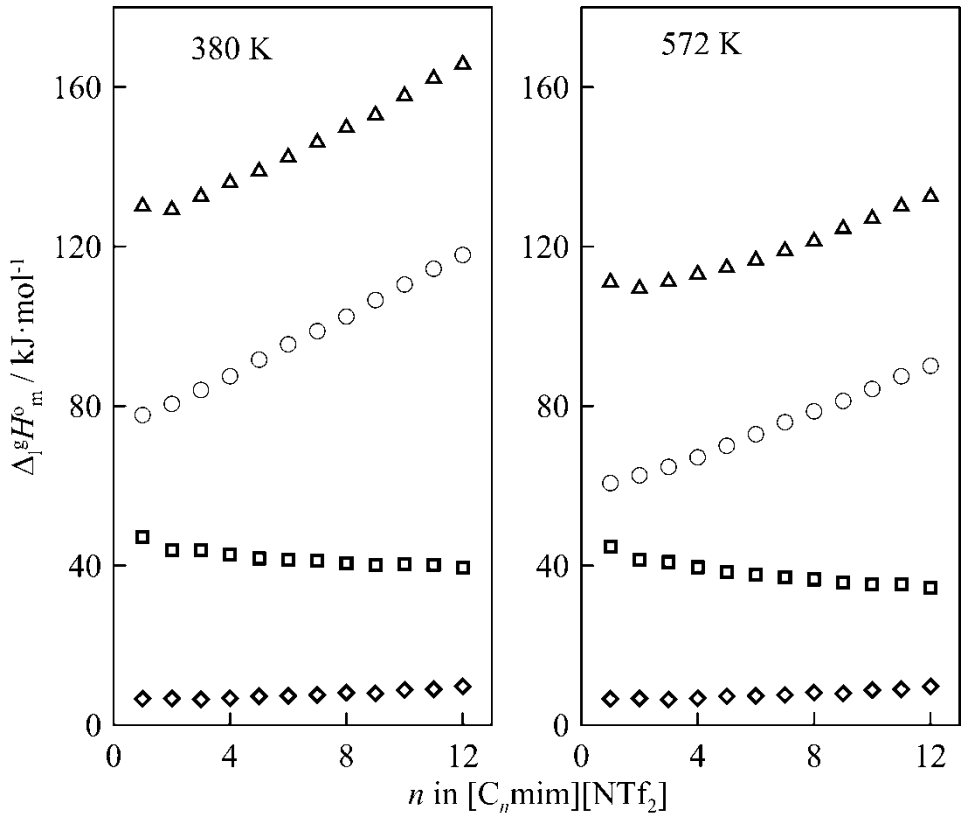

Figure 2.4 Effect of alkyl chain length on the total enthalpy of vaporization and the various components at 380K and 572K studied using MD simulations. △ (total enthalpy); ○ (van der Waals contribution); □ (Coulombic contribution); ◇ (intramolecular contribution).

The Coulomb energy decreases monotonically from [C_2mim][NTf_2] to [C_{12}mim][NTf_2] by 4 kJ·mol^{-1} for 380 K (7 kJ·mol^{-1} at 572 K) for all ILs, and shows a slightly larger drop per CH_2 in going from [C_1mim][NTf_2] to [C_2mim][NTf_2]. This latter feature is similar to the calculations by

Köddermann *et al* [40] where the Coulomb energy drops by 4.5 kJ·mol^{-1} (at 298 K) from [C_1mim][NTf_2] to [C_2mim][NTf_2], and is consistent with the physical argument presented above. In contrast to the present study, however, the results of Köddermann *et al* [40] suggest that the Coulombic energy contribution remains unchanged as the length of the alkyl chains increases beyond n = 2. Consistent with the findings of Köddermann *et al* [40], however, we also find that the increase in enthalpy of vaporization for [$C_n$mim][NTf_2] with increasing chain length arises completely from van der Waals interactions, which are dominating the vaporization process.

In order to reveal reliable structure-property relationships for the [$C_n$mim][NTf_2] family, the experimental values $\Delta_l^g H_m^0(T_{\mathrm{av}})$ (column 3, Table 2.1) were adjusted using eq 3 to 380 K (for QCM) and 572 K (for TGA), which were reasonably close to the T_{av} of the individual experiments. That is why the values of vaporization enthalpies were hardly affected by uncertainty in the $\Delta_l^g C_{p,m}^0$ value used for extrapolation. Such a procedure allowed a proper interpretation of the chain-length trends at the selected temperatures. However, it is very common to adjust the vaporization enthalpies also to the reference temperature 298 K, because the $\Delta_l^g H_m^0$ (298 K) data are required for validation of the high-level first principle calculations [41], as well as for development of the reliable force fields for MD simulations [42]. An adjustment to T = 298 K is usually done by using eq. 2.3, but it is essential to realize that over large differences (over 100 K) between T_{av} and the reference temperature, the value of $\Delta_l^g C_{p,m}^0$ used in the adjustment is crucial. Small differences in $\Delta_l^g C_{p,m}^0$ result in large differences in $\Delta_l^g H_m^0$ (298 K).

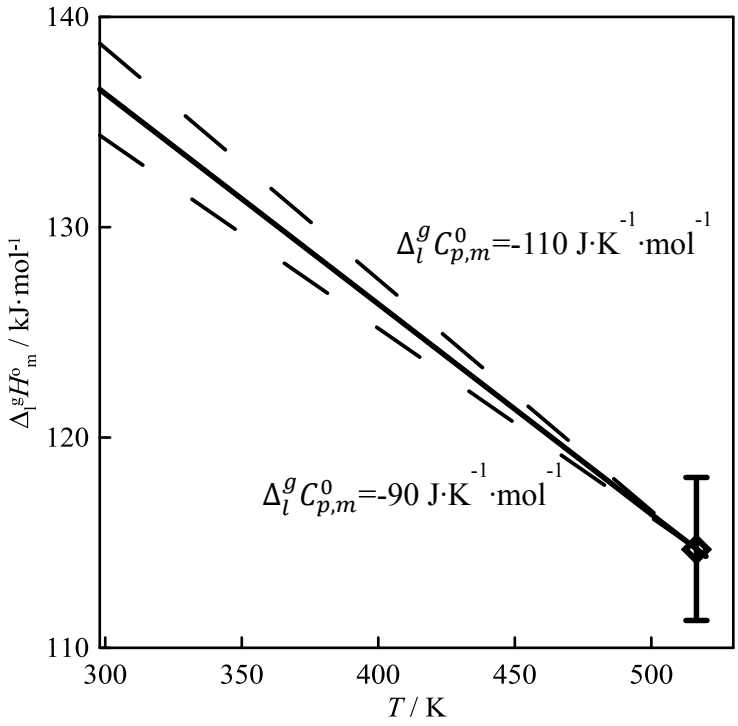

Figure 2.5 The illustration of error in the adjusted $\Delta_l^g H_m^0$ value to 298 K, due to error in $\Delta_l^g C_{p,m}^0$

On the Figure 2.5 such adjustment procedure form T_{av} to 298 K is shown. In this case the deviations of ± 10 J·mol^{-1}·K^{-1} in $\Delta_l^g C_{p,m}^0$ cause a spread of $\Delta_l^g H_m^0$ (298 K) value more than ± 4 kJ·mol^{-}1. The ambiguity of the $\Delta_l^g C_{p,m}^0$ values required for the extrapolation of experimental vaporization enthalpies to the reference temperature 298 K has been discussed recently [28], [30], [43].

Thus the determination of $\Delta_l^g C_{p,m}^0$ values is required for proper comparison and adjustment of $\Delta_l^g H_m^0$ values at 298 K.

2.5 Vaporization heat capacity difference of ILs $\Delta_l^g C_{p,m}^0 = C_{p,m}^0(g) - C_{p,m}^0(l)$

As a matter of fact the conventional value $\Delta_l^g C_{p,m}^0$ = -100 J·K^{-1}·mol^{-1} (regardless on the structure of the IL) was systematically used in the literature for the temperature adjustments according to eq. 2.3. This $\Delta_l^g C_{p,m}^0$ value was based on the calorimetric liquid heat capacity $C_{p,m}^0(l)$ measurements and statistical thermodynamic calculations $C_{p,m}^0(g)$ for a single ionic liquid [C$_4$mim][PF$_6$] [41]. A similar value of $\Delta_l^g C_{p,m}^0$= -105.4 J·K^{-1}·mol^{-1} was also derived, according to a procedure developed by Chickos and Acree [44] using the experimental isobaric molar heat capacity for [C$_4$mim][N(CN)$_2$] [15]. However, it should be mentioned that the estimation procedure by Chickos and Acree [44] was parameterized only for molecular liquids and not for ionic liquids. Thus, the current $\Delta_l^g C_{p,m}^0$ value broadly applied for temperature adjustments for ILs is a rough estimate used without regard to the structure of an IL.

Formally, $\Delta_l^g C_{p,m}^0$is the difference of molar heat capacities of the liquid and the gaseous samples: $\Delta_l^g C_{p,m}^0 = C_{p,m}^0(g) - C_{p,m}^0(l)$. As a rule, for ILs the values of $C_{p,m}^0(l)$ can be reliably measured by calorimetry or can be calculated by simple additivity rules [45]. In contrast, the experimental determination of the heat capacity of a gaseous ionic liquid is not possible. Therefore the heat capacity $C_{p,m}^0(g)$ is usually derived using the fundamental frequencies calculated with quantum chemistry, which are then used to estimate $C_{p,m}^0(g)$ using well known statistical thermodynamics procedures [46]. But it has turned out that using of this procedures in the case of the [C$_n$mim][NTf$_2$] family causes significant overestimation of the $\Delta_l^g C_{p,m}^0$ values. For [C$_2$mim][NTf$_2$] this procedure results the value $\Delta_l^g C_{p,m}^0$ (298 K) = -137.7 J·K^{-1}·mol^{-1}, using the experimental $C_{p,m}^0(l)$ [45] and $C_{p,m}^0(g)$ calculated [39] with density functional theory (DFT). The obtained $\Delta_l^g C_{p,m}^0$ estimate is not consistent with recent experimental results $\Delta_l^g C_{p,m}^0$= -56 J·K^{-1}·mol^{-1} [28]. The available in the literature and measured in our laboratory enthalpy of vaporization data for [C$_2$mim][NTf$_2$] were shown [28] to be in agreement at 298 K only with adjustment using the $\Delta_l^g C_{p,m}^0$ not higher than -50 J·K^{-1}·mol^{-1} (see Figure 2.6).

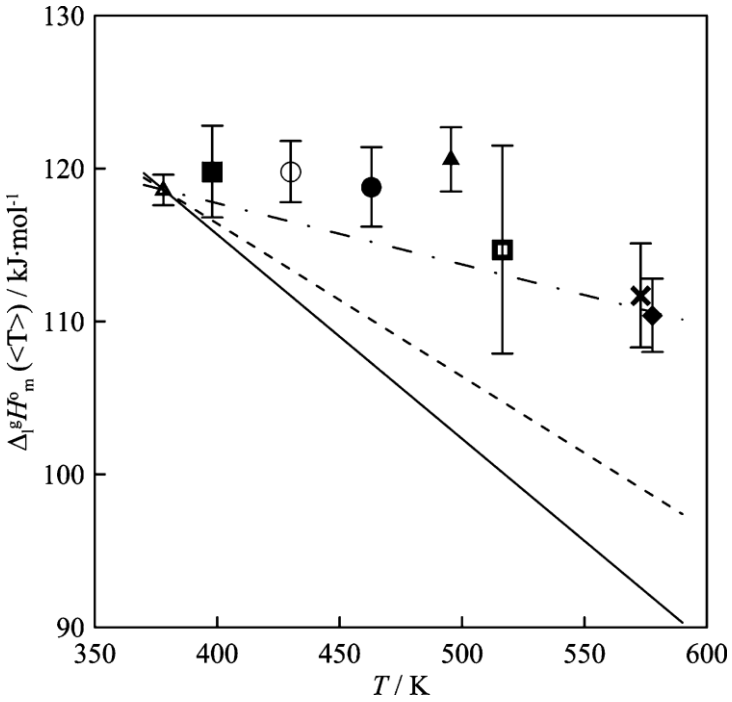

Figure 2.6 (taken from ref [28]**)** Experimental enthalpies of vaporization of [C_2mim][NTf_2] obtained by different methods. (Dot-dashed line) Temperature dependence of vaporization enthalpy was treated with $\Delta_l^g C_{p,m}^0$= -40 J·K^{-1}·mol^{-1}. (Dashed line) Temperature dependence of vaporization enthalpy was treated with $\Delta_l^g C_{p,m}^0$= -100 J·K^{-1}·mol^{-1}. (Solid line) Temperature dependence of vaporization enthalpy was treated with $\Delta_l^g C_{p,m}^0$= -134 J·K^{-1}·mol^{-1}

How to resolve this disagreement between the theoretical predictions and experimental data? As a matter of fact, in the literature there are no ideas how to obtain of $\Delta_l^g C_{p,m}^0$ values for ILs. Consequently, by using the value of $\Delta_l^g C_{p,m}^0$= - 100 J·K^{-1}·mol^{-1} the $\Delta_l^g H_m^0$ (298 K) data are generously overestimated and this fact has heavily aggravated the comparison of vaporization enthalpies measured by different methods [1], [6], [19], [26]–[28], [30]–[37], [43]. The common use of $\Delta_l^g C_{p,m}^0$ = - 100 J·K^{-1}·mol^{-1} as a constant for all ILs regardless of the structure is obviously an oversimplification since $\Delta_l^g C_{p,m}^0$ will differ for ILs with different cations and anions, as well as it should also vary as a function of alkyl chain length *n*. A significant amount of the discrepancies between the literature vaporization enthalpies for the [$C_n$mim][NTf_2] series at 298 K as measured by different methods is most likely due to the large temperature range (80 to 270 K) over which extrapolation of the measured $\Delta_l^g H_m^0$ at T_{av} to the 298 K is performed. Thus, accurate $\Delta_l^g H_m^0$ (298 K) data will not be available until reliable values of $\Delta_l^g C_{p,m}^0$ or $C_{p,m}^0(g)$ for ILs have been obtained [43].

2.6 Calculation of heat capacity difference $\Delta_l^g C_{p,m}^0$ from combined TGA + QCM experimental data (T_{av} procedure)

In this work we provide a simple and elegant procedure for properly assessing the correct $\Delta_l^g C_{p,m}^0$ values to use for the [C$_n$mim][NTf$_2$] series. This procedure is based on the experimental measurements of vaporization enthalpies $\Delta_l^g H_m^0$ (T_{av}) with two different methods at two different T_{av}. In the current work we deliberately measured the enthalpies of vaporization $\Delta_l^g H_m^0$ (T_{av}) (column 3, Table 2.1) for each IL under study using QCM and TGA at two significantly different average temperatures T_{av}. Hence, we need only to re-write eq. 2.3 as follows:

$$\Delta_l^g C_{p\,m}^0 = \frac{\Delta_l^g H_m^0(T_{av(TGA)}) - \Delta_l^g H_m^0(T_{av(QCM)})}{T_{av(TGA)} - T_{av(QCM)}} \quad (2.4)$$

in order to obtain the experimental differences between heat capacities $\Delta_l^g C_{p,m}^0$ indirectly. These values for [C$_n$mim][NTf$_2$] series calculated with eq. 2.4 are presented in Table 2.2.

Table 2.2 Heat capacity differences between liquid and gas phases for [C$_n$mim][NTf$_2$] and heat capacities for liquid [C$_n$mim][NTf$_2$] in J·K^{-1}·mol^{-1}.

[C$_n$mim][NTf$_2$]	$C_{p\,m}^o(l)$ (298 K) [a]	$\Delta_l^g C_{p\,m}^o$ (T_{av}) [b]	$\Delta_l^g C_{p\,m}^o$ (298 K) [c]	$C_{p\,m}^o(g)$ (298 K) [d]	$\Delta_l^g C_{p\,m}^o$ (298 K) [e]
1	2	3	4	5	6
[C$_1$mim][NTf$_2$]	473.9	-73 ± 9	-	348.1	-125.8
[C$_2$mim][NTf$_2$]	506.3	-56 ± 13	-85	368.6	-137.7
[C$_3$mim][NTf$_2$]	536.4	-76 ± 17	-73	389.2	-147.2
[C$_4$mim][NTf$_2$]	565.4	-67 ± 11	-88	409.6	-155.8
[C$_5$mim][NTf$_2$]	598.9	-96 ± 12	-89	429.8	-169.1
[C$_6$mim][NTf$_2$]	631.4	-86 ± 13	-95	450.2	-181.2
[C$_7$mim][NTf$_2$]	661.4	-114 ± 13	-113	470.6	-190.8
[C$_8$mim][NTf$_2$]	692.6	-92 ± 9	-124	491.2	-201.4
[C$_{10}$mim][NTf$_2$]	755.2	-136 ± 11		511.6	-243.6
[C$_{12}$mim][NTf$_2$]	817.6	-167 ± 12		532.0	-285.6
[C$_{14}$mim][NTf$_2$]	885.9	-161 ± 11		552.4	-333.5
[C$_{16}$mim][NTf$_2$]	942.6	-170 ± 15		572.8	-369.8
[C$_{18}$mim][NTf$_2$]	1005.1	-157 ± 11		593.2	-411.9

[a] The evaluated experimental data were approximated with the linear regression: $C_{p,m}^0(l, 298\,K) = 31.7\,n + 440.5$ (with $r^2 = 0.999$) and the missing $C_{p,m}^0(l, 298\,K)$ were estimated by interpolation and extrapolation. [b] Calculated using eq. 2.4 from QCM and TGA data measured in this work , uncertainty is estimated according to to the following equation $\Delta\Delta_l^g C_{p\,m}^0 = \frac{\sqrt{\left(\Delta_l^g H_m^0(T_{av(TGA)})\right)^2 - \left(\Delta_l^g H_m^0(T_{av(QCM)})\right)^2}}{T_{av(TGA)} - T_{av(QCM)}}$. [c] Estimated using volumetric properties according to Chapter 2.7. [d] Calculated in ref. 45 using DFT at the B3LYP/6-311+G(d,p) level. Values of $C_{p,m}^0(g, 298\,K)$ were estimated in ref.[31] with B3LYP/6-311+G(d,p) and these values were approximated in this work with the linear regression: $C_{p,m}^0(g, 298\,K) = 20.4\,n + 327.8$ (with $r^2 = 0.9999$) and the missing $C_{p,m}^0(g, 298\,K)$ for n = 10-18 were estimated by interpolation and extrapolation. [e] Difference (column 5 – column 2).

Table 2.2 (column 3) display distinct chain length dependence of $\Delta_l^g C_{p,m}^0$ values estimated with eq. 2.4. They are also quite different from the currently "acknowledged" in the community constant value [38] $\Delta_l^g C_{p,m}^0$= - 100 J·K^{-1}·mol^{-1}. For the calculation according to eq. 2.4, we have deliberately used only our own $\Delta_l^g H_m^0$ (T_{av}) data, however the $\Delta_l^g C_{p,m}^0$ values derived according to eq. 2.4 using all available data collected for [C$_n$mim][NTf$_2$] are indistinguishable within the boundaries of their uncertainties. The latter fact serves as good evidence that the simple $\Delta_l^g C_{p,m}^0$ procedure designed in the current study is correct, because the assessed resulting $\Delta_l^g C_{p,m}^0$ values are independent on the experimental method. It is quite surprising that the level of absolute $\Delta_l^g C_{p,m}^0$ values for the initial representatives of the [C$_n$mim][NTf$_2$] family was significantly lower (see Table 2.2) than the commonly used value of $\Delta_l^g C_{p,m}^0$ = - 100 J·K^{-1}·mol^{-1}.

2.7 Calculation of heat capacity difference $\Delta_l^g C_{p,m}^0$ based on volumetric properties of ILs

Being simultaneously surprised and confused with the lower level of the heat capacity difference $\Delta_l^g C_{p,m}^0$ for ILs, we realized that at least one additional approach was required to assess this difference independently from the experimental procedure designed above. For this purpose we decided to use the basics of statistical thermodynamics where the heat capacities of liquid and gaseous phases can be assessed as a sum of translational, rotational, and vibrational contributions. The isobaric and the isochoric heat capacities of both phases are usually expressed with the following equations:

$$C_{p\,m}^0(l) = C_{v\,m}^0(transl, l) + C_{v\,m}^0(rot, l) + C_{v\,m}^0(vib\,, l) + C_{v\,m}^0(conf, l) + \left(C_{p\,m}^0 - C_{v\,m}^0\right)_l \tag{2.5}$$

$$C_{p\,m}^0(g) = C_{v\,m}^0(transl, g) + C_{v\,m}^0(rot, g) + C_{v\,m}^0(vib\,, g) + C_{v\,m}^0(conf, g) + \left(C_{p\,m}^0 - C_{v\,m}^0\right)_g \tag{2.6}$$

where the contribution $C_{v,m}^0(conf)$ is responsible for the equilibrium mixture of conformers. Assuming the equality of the vibrational contributions into the heat capacity of the liquid and the gaseous phase, as well as the similarity for mixtures of conformers at equilibrium in these phases, the heat capacity difference can be expressed as follows:

$$\Delta_l^g C_{p\,m}^0 = C_{v\,m}^0(transl, g) + C_{v\,m}^0(rot, g) + \left(C_{p\,m}^0 - C_{v\,m}^0\right)_g$$
$$- C_{v\,m}^0(transl, l) - C_{v\,m}^0(rot, l) - \left(C_{p\,m}^0 - C_{v\,m}^0\right)_l \tag{2.7}$$

From common rules of statistical thermodynamics, a sum of contributions for the free rotation and the free translational motion of a molecule into the ideal gas heat capacity can be assigned to be equal to 3 *R*. From the oscillation theory [47] the free rotation or linear motion of a molecule

in the condensed state is converted into the low frequency vibrations. The contribution of vibrations at low frequencies into the heat capacity is equal to R for each degree of freedom: total $6R$ for the sum of rotational and translational contributions. Assuming that for the ideal gas the relation $\left(C_{p\,m}^0 - C_{v\,m}^0\right)_g = R$ is valid, we can simplify eq. 2.7 to:

$$\Delta_l^g C_{p\,m}^0 = -2R - \left(C_{p\,m}^0 - C_{V\,m}^0\right)_l \tag{2.8}$$

It is obvious from eq.2.8 that the contribution $\left(C_{p\,m}^0 - C_{V\,m}^0\right)_l$ is the main part of the heat capacity $\Delta_l^g C_{p\,m}^0$difference. It turned out that this contribution could be easily estimated from the volumetric properties according to following equation [48]:

$$\left(C_{p\,m}^0 - C_{V\,m}^0\right)_l = \frac{\alpha_p^2}{\kappa_T} V_m T \tag{2.9}$$

where $\alpha_p = -\frac{1}{\rho}\left(\frac{d\rho}{dT}\right)_p$ is the thermal expansion coefficient, K^{-1}; $\kappa_T = -\frac{1}{V}\left(\frac{dV}{dp}\right)_T$ is the isothermal compressibility, Pa^{-1}. The molar volume V_m as well as the thermal expansion coefficient α_p are usually determined from the temperature dependence of the density of liquid. The compressibilities κ_T can be calculated from the pressure dependence of density in the isothermal conditions. But κ_T are more often derived from the speed of sound $W(T,P)$ measurements as follows:

$$\kappa_T = \frac{1}{\rho}\left(\frac{1}{W^2} + \frac{T\alpha_p^2 M}{C_p}\right) \tag{2.10}$$

where ρ is the density of an IL ($kg \cdot m^{-3}$) and M is the molar mass ($kg \cdot mol^{-1}$).

We can summarize equations 2.8-2.10 in one:

$$\Delta_l^g C_{p\,m}^0 = -2R - \frac{Td^2}{M\left(\frac{1}{W^2} + \frac{MTd^2}{C_p\rho^2}\right)} \tag{2.11}$$

where $d = \left(\frac{d\rho}{dT}\right)_p$, density dependence on temperature.

It follows from eq. 2.11 that estimation of the $\Delta_l^g C_{p\,m}^0$ values requires three experimental parameters:

- density temperature dependence (frequently available)
- isobaric heat capacity of liquid (usually available or predictable)
- speed of sound in liquid phase (not often available)

In this context we investigated how the quality of the initial data $\rho(T)$, Cp, and W, could influence the resulting $\Delta_l^g C_{p\,m}^0$ values. For example, for the common IL $[C_n\text{mim}][NTf_2]$ the required data:

ρ= 1520 kg·m^{-3}, $d\rho/dT$ = -1.009 kg·m^{-3} K^{-1}, $C^0_{p\,m}(l)$ = 506.3 J·mol^{-1}·K^{-1}, W = 1240 m·s^{-1}

were available from the literature (see SI Table S1). Using this input we calculated with eq. 2.11 the value $\Delta^g_l C^0_{p\,m}$ (298 K) = -85 J·mol^{-1}·K^{-1}.(see Table 2.2. column 4). In order to trace the impact of the parameters we enlarged the input values of $\rho(T)$, *C*p, and *W* by 10% and estimated $\Delta^g_l C^0_{p\,m}$ (298 K) = -98.3 J·mol^{-1}·K^{-1}. In the case if input values of $\rho(T)$, *C*p, and *W* were reduced by 10% we estimated $\Delta^g_l C^0_{p\,m}$ (298 K) = -72.8 J·mol^{-1}·K^{-1}. This example demonstrated that in the case of the ± 10% scaling the resulting $\Delta^g_l C^0_{p\,m}$ value will be changed within ± 13 J·mol^{-1}·K^{-1} and this result is acceptable within the experimental uncertainties from *T*av method (Table 2.2 column 3). However taking into account that in the reality the accuracy of the density measurements is typically within ± 0.001- 0.002 kg·m^{-3}, for the heat capacity measurements within ± 20 J·mol^{-1}·K^{-1}(from DSC), and for the speed of sound measurements within ± 1 - 2 m·s^{-1}, the possible influence of these uncertainties on the $\Delta^g_l C^0_{p\,m}$ will not exceed ± 2 – 3 J·mol^{-1}·K^{-1}.

Unfortunately, the full set of the required for eq. 2.11 properties ($\rho(T)$, *C*p, and *W*) for a particular ILs under study is available only occasionally. In this case we have to use different empirical correlations in order to assess the volumetric properties $\rho(T)$, *C*p, and *W*. In order to evaluate the contributions and importance of each of three properties to the $\Delta^g_l C^0_{p\,m}$ we calculated the derivatives of eq. 2.11 according to the following equations:

$$\frac{d(\Delta^g_l C^0_{p\,m})}{d\rho} = -\frac{2T^2d^4}{C_p\rho^3\left(\frac{1}{W^2}+\frac{MTd^2}{C_p\rho^2}\right)^2} \tag{2.12}$$

$$\frac{d(\Delta^g_l C^0_{p\,m})}{dW} = -\frac{2Td^2}{MW^3\left(\frac{1}{W^2}+\frac{MTd^2}{C_p\rho^2}\right)^2} \tag{2.13}$$

$$\frac{d(\Delta^g_l C^0_{p\,m})}{dC_p} = -\frac{T^2d^4}{C_p^2\rho^2\left(\frac{1}{W^2}+\frac{MTd^2}{C_p\rho^2}\right)^2} \tag{2.14}$$

$$\frac{d(\Delta^g_l C^0_{p\,m})}{dd} = -\frac{2Td}{M\left(\frac{1}{W^2}+\frac{MTd^2}{C_p\rho^2}\right)} + \frac{2T^2d^3}{C_p\rho^2\left(\frac{1}{W^2}+\frac{MTd^2}{C_p\rho^2}\right)^2} \tag{2.15}$$

Results of calculations with eqs. 2.12 - 2.15 for the [C_2mim][NTf_2] are illustrated in Figure 2.7. From slopes of the approximating lines we have concluded that the $\Delta^g_l C^0_{p\,m}$ estimate is not especially sensitive for the quality of the density and the heat capacity $C^0_{p,m}(l)$ data. However, the uncertain speed of sound (*W*) data and especially the density temperature slope $\left(\frac{d\rho}{dT}\right)$ data could distort the $\Delta^g_l C^0_{p\,m}$ result. Such a simple analysis makes it easier to apply eq. 2.11 for temperature adjustment of vaporization enthalpies to the reference temperature 298 K. Fortunately, the density $\rho(T)$values are very often available in the literature or they can be easily

measured. The $C^0_{p,m}(l)$ data can be calculated by any additive procedure, or easily measured by DSC.

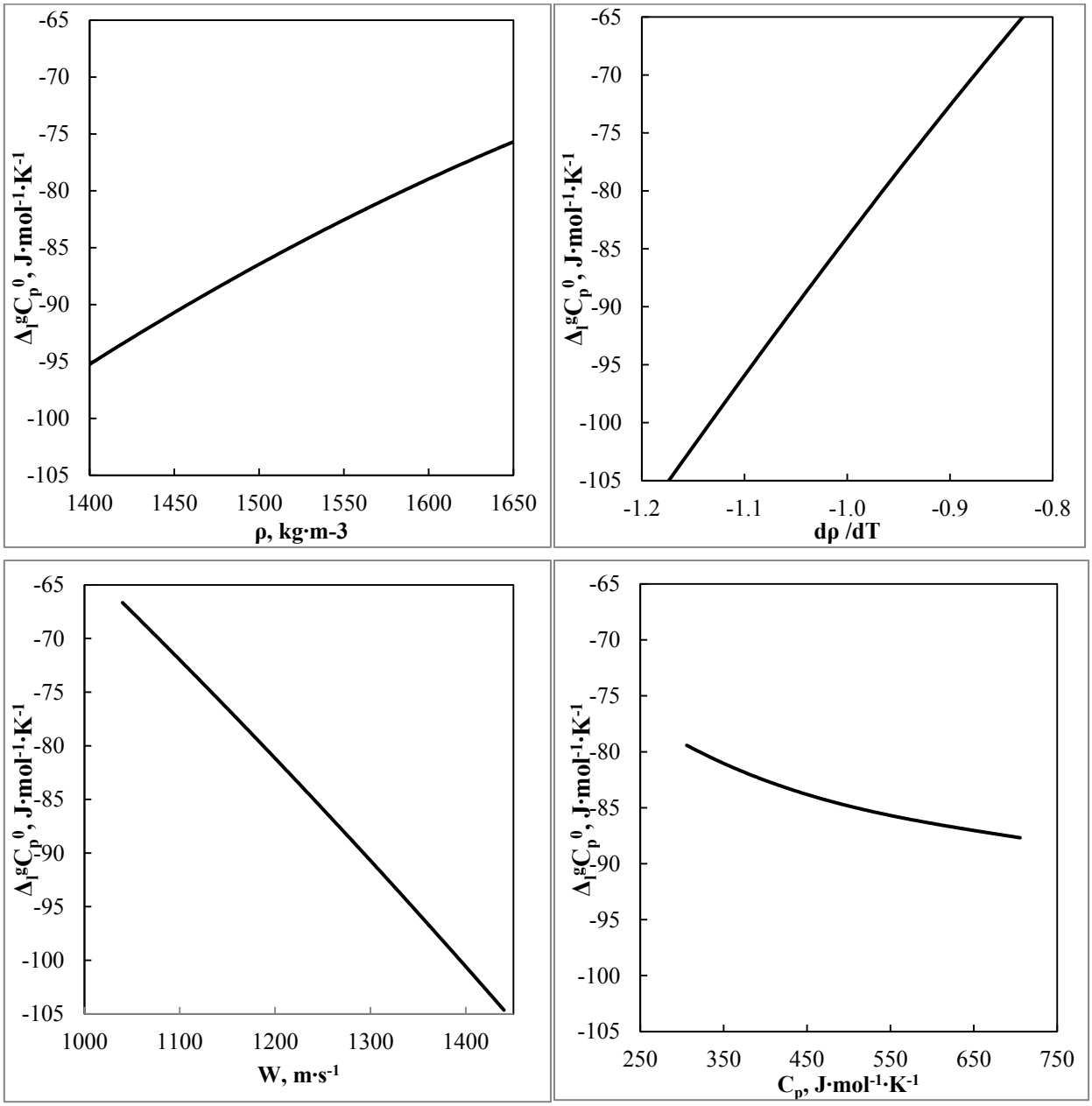

Figure 2.7 The impact of inaccuracies in the initial *W*, *C*p and $\rho(T)$ data on the $\Delta_l^g C^0_{p\,m}$. On each graph one parameter varies, other are set constant.

There is also a simple relationship between the speed of sound *W* in the liquid and the surface tension, σ, suggested Auerbach [49].

$$W = \left(\frac{\sigma}{6.33 \cdot 10^{-10} \cdot \rho}\right)^a \tag{2.16}$$

where $a = 2/3$, σ - surface tension N·m^{-1}.

This equation was recently adapted to imidazolium based ionic liquids with different anions by tuning *a* parameter by Gardas and Coutinho [50]. Their fit with the new value *a*=0.6714 was very close to original *a* = 2/3. The surface tension required for eq. 2.16 can be taken from experimental data, or can be easy calculated with eq. 2.17.

$$\sigma = \left(\frac{P_{ch} \cdot \rho}{M}\right)^4 \tag{2.17}$$

where P_{ch} – parachor is an additive property usually calculated using the Knott scheme [51]:

$$P_{ch} = \Sigma(n_i \cdot \Delta P_i) + \Sigma(n_j \cdot \Delta P_j) \tag{2.18}$$

where ΔP_i is a contribution of the *i*-th element; n_i is the number of elements of the *i*-th type in the structure; ΔP_j is a contribution of the *j*-th structural correction; n_j is the number of structural corrections of the *i*-th type in the ionic liquid.

Table 2.3 Comparison of the speed of sound *W* calculated from Parachor using Auerbach equation and experimental data.

$[C_nmim][NTf_2]$	M_w, g·mol^{-1}	P_{ch}	ρ_{exp}, kg·m^3	σ_{calc}, N m^{-1}	W_{calc}, m s^{-1}	W_{exp}, m s^{-1}
$[C_2mim][NTf_2]$	391.32	632	1519.7	0.0363	1182	1240
$[C_3mim][NTf_2]$	405.34	672	1475.6	0.0358	1194	1235
$[C_4mim][NTf_2]$	419.37	712	1436.7	0.0353	1206	1229
$[C_5mim][NTf_2]$	433.40	752	1404.5	0.0352	1221	1231
$[C_6mim][NTf_2]$	447.42	791	1371.6	0.0347	1228	1227
$[C_8mim][NTf_2]$	475.48	871	1321.5	0.0344	1252	1232

Densities are taken from SI Table S1

In order to verify the quality of the prediction with eq. 2.16 we calculated the speeds of sound, W, for the $[C_nmim][NTf_2]$ series (see Table 2.3, column 6) and compared these values with the experiment [52] (see Table 2.3, column 7). It should be mentioned that for this test we decided to make the "worst case" calculations and only density (see SI Table S1) values were used in eq. 2.16 and 2.17 as the experimental input. The surface tensions have been deliberately assessed from the P_{ch} estimated by additivity scheme (eq. 2.18) with Knott parameters taken from [51]. Comparison of columns 6 and 7 in Table 2.3 has revealed that the calculated speeds of sound are quite reliable within of 3-5%. It has turned out that calculations of the $\Delta_l^g C_{p\,m}^0$ calculated according to eq. 2.11 with the experimental speeds of sound (see Table 2.3, column 7) and with the assessed values (see Table 2.3, column 6) were in agreement within ± 10 J·mol^{-1}·K^{-1}. Such agreement was good enough within the experimental uncertainties obtained for $\Delta_l^g C_{p\,m}^0$ from T_{av} procedure (see Table 2.2). Thus, simple calculations with eqs. 2.16-2.18 seems to be enough reliable to estimate speed of sound of an ILs and apply it in eq. 2.11. Critical analysis of the data on speed of sound in ILs available in the literature has revealed, that the experimental *W*-values are barely dependent on the alkyl chain length for $[C_nmim][NTf_2]$ family, (see Table 2.3). The

same conclusion has been drawn for the [C_nPy][NTf_2] series (see SI Table S4). This observation can significantly simplify estimations of *W* for the unknown members of the ILs family.

It is important now to compare results for $\Delta_l^g C_{p\,m}^0$estimations dereived from both suggested methods: the volumetric values based procedure and the T_{av} procedure. We collected volumetric properties and the speed of sound data for the [$C_n$mim][NTf_2] series from the IL-thermo database [53] (see SI Table S1). The resulting heat capacity differences $\Delta_l^g C_{p\,m}^0$ derived from the volumetric properties are given in Table 2.2 column 4 and shown on the Figure 2.8. Comparison of the $\Delta_l^g C_{p\,m}^0$ values derived from the QCM and TGA experiments (Table 2.2 column 3) with those from the volumetric properties (Table 2.2 column 4) have shown that these results are very similar for the homologous series of [$C_n$mim][NTf_2] ILs. Thus, two independent procedures have ascertained the level of the $\Delta_l^g C_{p\,m}^0$ differences for the ILs under study and both procedures can be recommended for the practical estimations required for temperature adjustment of experimental vaporization enthalpies. Importantly, both procedures suggest that $\Delta_l^g C_{p\,m}^0$ is dependent on the chain length of the cation.

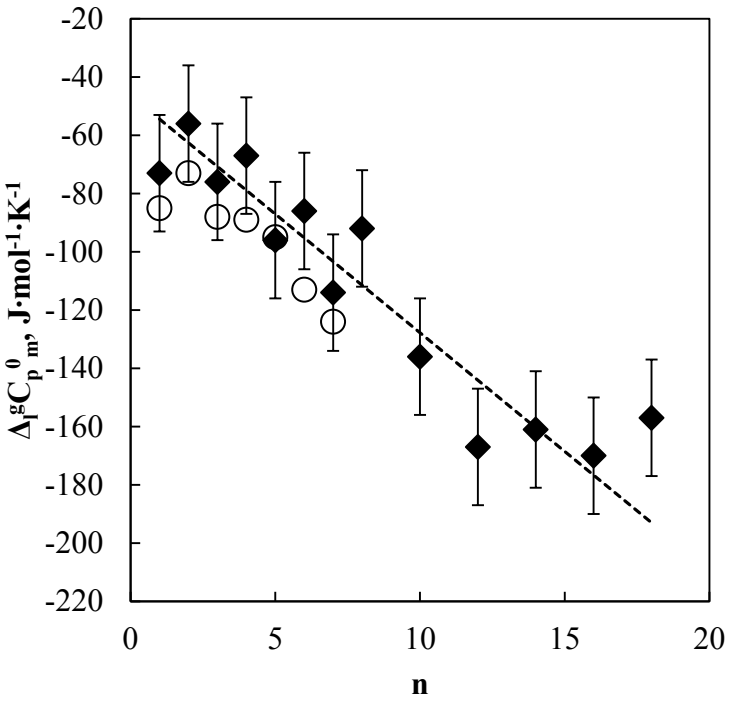

Figure 2.8 Heat capacity differences between liquid and gas phases for [$C_n$mim][NTf_2]. ○ - estimated from $(C_{p\,m}^0 - C_{v\,m}^0)$ difference. ♦ - calculated using equation $\Delta_l^g C_{p\,m}^0$ = ($\Delta_l^g H_m^0$ $(T_{av})_{QCM}$ - $\Delta_l^g H_m^0$ $(T_{av})_{TGA}$) / [$(T_{av})_{QCM}$ - $(T_{av})_{TGA}$] from QCM and TGA data. Eq. 4.1 is plotted with dotted line.

Finally, we have demonstrated that the statistical thermodynamics approach based on the volumetric properties of ILs provides a reliable and independent method for the $\Delta_l^g C_{p\,m}^0$ estimation. It requires fitting with three experimental parameters: density ρ , speed of sound W, and isobaric liquid heat capacity C_p. Lack of the available experimental data can be partly covered by reliable estimations. The volumetric properties based method provides $\Delta_l^g C_{p\,m}^0$ results in close agreement with the T_{av} procedure (see Table 2.1). For the thermally labile ILs where T_{av} procedure can fail this approach remains the only working method to assess $\Delta_l^g C_{p\,m}^0$ for ILs under study.

2.8 Analysis of heat capacities of gas phase $C_{p\,m}^0(g)$ and liquid phase $C_{p\,m}^0(l)$ of ILs

In order to get more insight in the $\Delta_l^g C_{p\,m}^0$ disagreement between values obtained from experiment and volumetric data on one hand, and from quantum chemical calculations on other hand, we analyzed separately the heat capacities $C_{p\,m}^0(g)$ and $C_{p\,m}^0(l)$ for the [C$_n$mim][NTf$_2$] series. The experimental values for $C_{p\,m}^0(l, 298\,K)$ have been critically evaluated just recently [45]. In this work we used the recommended values in Table 2.2, column 2. It turns out that the evaluated experimental data [45] (for n = 2, 4, 6, 8, and 14) fit very well to the linear chain length dependence. They were approximated with a linear regression (see Table 2.2, footnote a) and the missing $C_{p\,m}^0(l, 298\,K)$ for the [C$_n$mim][NTf$_2$] were estimated by interpolation and extrapolation (see Table 2.2, column 2). As has been already pointed out, available experimental methods are unable to measure $C_{p\,m}^0(g, 298\,K)$ for ILs. Therefore we calculated [39] these values for the [C$_n$mim][NTf$_2$] family using DFT at the B3LYP/6-311+G(d,p) level (see Table 2.2, column 5). The differences between the gaseous heat capacities (from DFT) and the liquid heat capacities (from experiment) are given in Table 2.2 (column 6). These differences follow the already expected increasing trend with the increasing chain length, but the absolute values are about twice as large as those obtained from our experimental findings from TGA and QCM methods (Table 2.2, column 3).

We are reticent now to give any reasonable explanation for the significant difference between experimental and theoretical $\Delta_l^g C_{p\,m}^0$values. For the DFT calculations, the disagreement could be attributed to the simple rigid rotor-harmonic oscillator approximation used in the first principles calculations of the $C_{p\,m}^0(g, 298\,K)$. Unfortunately, the size of the ILs under study in the current work is too large to perform calculations without this approximation. The currently observed disagreement of the absolute experimental and theoretical $\Delta_l^g C_{p\,m}^0$values merits further extended investigation. In spite of this fact, two independent approaches of $\Delta_l^g C_{p\,m}^0$ determination from the experiment and statistical thermodynamics show very similar results and they allow one to make recommendations on how to adjust vaporization enthalpies to the reference temperature properly.

2.9 Quick appraisal of the heat capacity difference $\Delta_l^g C_{p,m}^0$ using liquid heat capacities $C_{p,m}^0(l)$

Taking into account that the experimental data on $C_{p\,m}^0(l, 298\,K)$ for the [C$_n$mim][NTf$_2$] are quite reliable, it seems to be reasonable to develop an empirical correlation between the experimental $C_{p\,m}^0(l, 298\,K)$ and the experimental $\Delta_l^g C_{p\,m}^0$. It turns out that a simple linear correlation (plotted in Figure 2.8 with dotted line):

$$\Delta_l^g C_{p\,m}^0 = C_{p\,m}^0(l, 298\,K) \cdot (-0.26 \pm 0.05) + (68.7 \pm 37.0) \text{ with r2 = 0.950} \quad (2.19)$$

can be derived using our own QCM and TGA data (except for *n*= 1, 12, and 18) and the literature $C_{p\,m}^0(l, 298\,K)$ data which are given in Table 2.2 which will be very useful for quick appraisal of $\Delta_l^g C_{p\,m}^0$ for the [C$_n$mim][NTf$_2$] series with any chain length.

The correlation according to eq. 2.19 is adjusted now for the [C$_n$mim][NTf$_2$] series, but we recommend to apply this simple correlation for another ILs instead of using the conventional constant $\Delta_l^g C_{p\,m}^0$= - 100 J·K^{-1}·mol^{-1}. We are aware that eq. 2.19 could get other coefficients by adjusting to other types of ILs (e.g. pyridinium, pyrrolidinium), but we expect the fluctuations of these coefficients not to be too large. At the current state of our knowledge, eq. 2.19 seems to be of crucial importance because it helps to avoid ambiguity of the $\Delta_l^g C_{p\,m}^0$ values commonly used nowadays in the literature, taking into account at least the chain-length dependence. Eq. 2.19 should be considered as the third option to assess the $\Delta_l^g C_{p\,m}^0$ values. For short this method will be named as the "experimental $C_{p\,m}^0(l)$ based method".

2.10 Test of the "experimental $C_{p\,m}^0(l)$ based method" estimation of heat capacity difference $\Delta_l^g C_{p,m}^0$ on the [C$_{n1}$Pyrr][NTf$_2$] and [C$_{n1}$Py][NTf$_2$] families

As a matter of fact the volumetric properties based method and also T_{av} method for estimation of the $\Delta_l^g C_{p\,m}^0$ are often very demanding. In contrast the third option "the $C_{p\,m}^0(l)$ method" seems to be the simplest procedure. In spite of the fact, that coefficients in eq 2.19 were adjusted only for [C$_n$mim][NTf$_2$] it was interesting to test, whether these coefficients were also valid for other series with [NTf$_2$]$^-$ anion.

We tested this approach for the [C$_n$Py][NTf$_2$] with n = 2-6. For this family of IL it was not possible to calculate $\Delta_l^g C_{p\,m}^0$ from T_{av}-procedure, because these ILs are decomposing under TGA experimental conditions. Table 2.4 lists the estimated values of $\Delta_l^g C_{p\,m}^0$ from available volumetric data for [C$_n$Py][NTf$_2$] (see SI Table S4). For comparison we also applied the eq. 2.19. The resulting $\Delta_l^g C_{p\,m}^0$ values show acceptable agreement within ± 20 J·K^{-1}·mol^{-1}. Such agreement has been a good sign that eq. 2.19 can be applied for IL families with [NTf$_2$]$^-$ anion regardless of the cation structure.

Table 2.4 Heat capacity differences between liquid and gas phases for alkyl-pyridinium bis(trifluoro-methanesulfonyl)imides $[C_nPy][NTf_2]$ and heat capacities for liquid state.

Compound	$C^0_{p\,m}(l)$, $J\cdot K^{-1}\cdot mol^{-1}$	$\Delta^g_l C^0_{p\,m}$, [a] $J\cdot K^{-1}\cdot mol^{-1}$	$\Delta^g_l C^0_{p\,m}$, [b] $J\cdot K^{-1}\cdot mol^{-1}$
$[C_2Py][NTf_2]$	518	-61	-66
$[C_3Py][NTf_2]$	550	-66	-74
$[C_4Py][NTf_2]$	582	-70	-83
$[C_5Py][NTf_2]$	614	-73	-91
$[C_6Py][NTf_2]$	646	-77	-99

a - estimated from $(C^0_{p\,m} - C^0_{v\,m})$ difference. b - calculated using equation 2.19 developed for $[C_nmim][NTf_2]$.

In order to test this suggestion we used the experimental results for pyrrolidinium based ILs We made similar calculations for $\Delta^g_l C^0_{p\,m}$ for $[C_{n1}Pyrr][NTf_2]$ family. The results are listed in the Table 2.5. In contrast to $[C_nmim][NTf_2]$ and $[C_nPy][NTf_2]$ families, neither T_{av} procedure, nor $(C^0_{p\,m} - C^0_{v\,m})_l$ could generate the $\Delta^g_l C^0_{p\,m}$ data for the whole range of $[C_{n1}Pyrr][NTf_2]$. TGA results with the pyrrolidinium based ILs with n = 7,8,10 were less accurate than it is required for the sensitive $\Delta^g_l C^0_{p\,m}$ calculations. In order to check the trend of the $\Delta^g_l C^0_{p\,m}$– values with the chain length n we approximated data for $[C_{41}Pyrr][NTf_2]$ and $[C_{61}Pyrr][NTf_2]$ given in column 4 (Table 2.5) with the linear regression: $\Delta^g_l C^0_{p\,m}$ /($J\cdot K^{-1}\cdot mol^{-1}$) = -23 – 11.5·$n$. We used this regression to estimate the $\Delta^g_l C^0_{p\,m}$– values for $[C_{n1}Pyrr][NTf_2]$ family with n = 5,7,8,10 (column 5, Table 2.5).

Table 2.5 Heat capacity differences between liquid and gas phases for $[C_{n1}Pyrr][NTf_2]$ and heat capacities for liquid $[C_{n1}Pyrr][NTf_2]$ in $J\cdot K^{-1}\cdot mol^{-1}$.

$[C_{n1}Pyrr][NTf_2]$	$C^0_{p\,m}(l)$ (298 K) [a]	$\Delta^g_l C^0_{p\,m}$ (T_{av})[c]	$\Delta^g_l C^0_{p\,m}$ (298 K)[d]	$\Delta^g_l C^0_{p\,m}$ (298 K)[e]	$\Delta^g_l C^0_{p\,m}$ (298 K)[b]
1	2	4	5	6	3
$[C_{31}Pyrr][NTf_2]$	554.0 [26]	-40±20	-	-	-75
$[C_{41}Pyrr][NTf_2]$	589.3 [27]	-69±20	-	-89	-85
$[C_{51}Pyrr][NTf_2]$	622.6	-	-80	-	-93
$[C_{61}Pyrr][NTf_2]$	655.1	-92±13	-	-	-102
$[C_{71}Pyrr][NTf_2]$	685.1	-	-104	-	-109
$[C_{81}Pyrr][NTf_2]$	716.3	-	-115	-	-118
$[C_{10,1}Pyrr][NTf_2]$	778.9	-	-138	-	-134

[a] Calculated from experimental data for $[C_nmim][NTf_2]$ with equation (in $J\cdot K^{-1}\cdot mol^{-1}$): $C^0_{p\,m}$ (l, $[C_{n1}Pyrr][NTf_2]$)/($J\cdot K^{-1}\cdot mol^{-1}$) = $C^0_{p\,m}$ (l, $[C_nmim][NTf_2]$) + 23.7. [b] calculated using equation 2.19 developed for $[C_nmim][NTf_2]$. [c] calculated using equation 2.4 [d] Estimated using the linear regression $\Delta^g_l C^0_{p\,m}$/($J\cdot K^{-1}\cdot mol^{-1}$) = -23 – 11.5·$n$ derived from the experimental $\Delta^g_l C^0_{p\,m}$ data for $[C_{41}Pyrr][NTf_2]$ and $[C_{61}Pyrr][NTf_2]$ given in the column 4 in this table. [e] Estimated from volumetric properties . [f] Very close result $[C_{41}Pyrr][NTf_2]$ = 589.3 $J\cdot K^{-1}\cdot mol^{-1}$ was also reported in [54]

Unfortunately the volumetric properties and the speed of sound data required for calculation $(C_{p\,m}^0 - C_{v\,m}^0)_l$ are scarce. We found experimental data only for the $[C_{41}mim][NTf_2]$ (see SI Table S4). The resulting heat capacity difference $\Delta_l^g C_{p\,m}^0$ is given in Table 2.5 column 6.

Finally we have applied the eq. 2.19 to $[C_nmim][NTf_2]$ family. In order to do this we collected $C_{p\,m}^0(l)$ (298 K) for the $[C_{n1}Pyrr][NTf_2]$ series. We have found experimental results only for $[C_{31}Pyrr][NTf_2]$ and $[C_{41}Pyrr][NTf_2]$ (see Table 2.5). However, in the ref. [55] heat capacities of $[C_{41}Pyrr][NTf_2]$ = 589.3 $J{\cdot}K^{-1}{\cdot}mol^{-1}$ and of $[C_4mim][NTf_2]$ = 565.3 $J{\cdot}K^{-1}{\cdot}mol^{-1}$ were measured by high-precision adiabatic calorimetry. We assumed the difference between these two values of 23.7 $J{\cdot}K^{-1}{\cdot}mol^{-1}$ to be constant and heat capacities at 298 K of the pyrrolidinium based ILs can be estimated with the equation:

$$C_{p\,m}^0(l)\ ([C_{n1}Pyrr][NTf_2])/(J{\cdot}K^{-1}{\cdot}mol^{-1}) = C_{p\,m}^0(l)\ ([C_nmim][NTf_2]) + 23.7 \qquad (2.20)$$

provided that heat capacities for imidazolium based ILs are known (see SI Table S1). We checked the validity of the assumption used for eq 2.20 with the experimental heat capacity of $[C_{31}Pyrr][NTf_2]$. The data calculated according to eq. 2.20 $C_{p\,m}^0(l)$ $[C_{3l}Pyrr][NTf_2]$ = 560 $J{\cdot}K^{-1}{\cdot}mol^{-1}$ was in good agreement with the experimental value 554 $J{\cdot}K^{-1}{\cdot}mol^{-1}$ [56]. Heat capacities at 298 K of the $[C_{n1}Pyrr][NTf_2]$ family calculated with eq. 2.19 are presented in Table 2.5 (column 2). We used these values as input for eq. 2.19 and estimated $\Delta_l^g C_{p\,m}^0$ for this family (see Table 2.5, column 3). A monotonic increase in the $\Delta_l^g C_{p\,m}^0$ values with the increasing chain length was observed in accord with the data for $[C_nmim][NTf_2]$. The absolute $\Delta_l^g C_{p\,m}^0$ values are similar in magnitude to the corresponding ILs from the $[C_nmim][NTf_2]$ family (see SI Table S1). The further comparison of the column 3 and 4 in Table 2.5 shows the acceptable agreement of the $\Delta_l^g C_{p\,m}^0$–values for the $[C_{n1}Pyrr][NTf_2]$ family. Comparison of the $\Delta_l^g C_{p\,m}^0$ values derived from eq 2.19 (see Table 2.5 column 3), from the QCM and TGA experiments (Table 2.5 column 4) with those from the volumetric properties (Table 2.5 column 6) have shown that these results are hardly distinguishable for the $[C_4mim][NTf_2]$. Importantly, all procedures suggest that $\Delta_l^g C_{p\,m}^0$ is dependent on the chain length of the cation. Thus three independent procedures have ascertained the level of the $\Delta_l^g C_{p\,m}^0$ differences for the ILs under study and all three procedures could be recommended for the practical estimations required for temperature adjustment of experimental vaporization enthalpies.

2.11 Final remark on heat capacity difference $\Delta_l^g C_{p\,m}^0$ of ILs

In the frame of the current work we suggested three independent procedures to assess the $\Delta_l^g C_{p\,m}^0$ values:

1. T_{av} procedure
2. volumetric properties based
3. experimental $C_{p\,m}^0(l)$ based method

At the current state of our knowledge, eq. 2.19 seems to be the simplest but reliable option because it helps to avoid ambiguity of the $\Delta_l^g C_{p\,m}^0$ values commonly used nowadays in the literature, taking into account at least the chain-length dependence. We tested it on 3 ILs families and found out that this equation was capable to produce satisfactory results for the $\Delta_l^g C_{p\,m}^0$ of ILs. Eq. 2.19 is easy to apply because the $C_{p\,m}^0(l)$ (298 K) of ILs are available [53] or easily measured with the commercially available DSC, which are commonly used in modern IL labs. Moreover, the $C_{p\,m}^0(l)$ (298 K)-values required for eq 2.19 could also be predicted with a reasonable accuracy [57] as a function $C_{p\,m}^0(l)$ (298 K) = $f(V_m)$ of the molar volume V_m. This simple empirical correlation was shown to be reliable within 3% (or ± 16 J·K^{-1}·mol^{-1}) [57]. The molar volume V_m values are usually obtained from the densities of ILs, which are routinely determined as a part of a physical-chemical attestation of new ILs. Thus, use of eq 2.19 for temperature adjustment of vapor pressure measurements provides a convenient option for comparison and validation of experimental results measured by different techniques.

2.12. Adjustment of vaporization enthalpies of ILs to the 298 K using heat capacity differences $\Delta_l^g C_{p\,m}^0$ determined in this work

In order to demonstrate the advantage of using $\Delta_l^g C_{p\,m}^0$ values derived in this work instead of -100 J·K^{-1}·mol^{-1}, we adjusted experimental results from T_{av} to the reference temperature 298 K for the [C$_n$mim][NTf$_2$] family, measured in this work and collected from the literature. We used $\Delta_l^g C_{p\,m}^0$values obtained using the T_{av} procedure with $\Delta_l^g H_m^0$ from QCM and TGA measurements. The resulting plot is given in Fig. 2.9.

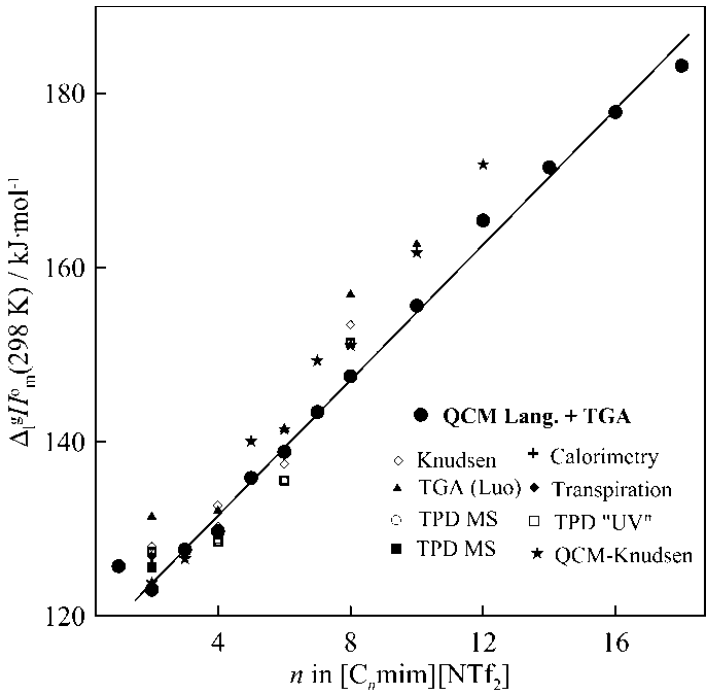

Figure 2.9 The experimental $\Delta_l^g H_m^0$ (298 K) adjusted with $\Delta_l^g C_{p\,m}^0$ from Table 3, column 3.

In contrast to the disorder in literature data, adjusted to 298 K with $\Delta_l^g C_{p\,m}^0$= -100 J·K^{-1}·mol^{-1}, which were discussed in the Chapter 2.1 and shown in the Figure 2.1, it is now quite obvious that there is a simple linear dependence of the vaporization enthalpy on the chain length. Certainly, some scatter of the $\Delta_l^g H_m^0$ (298 K) data still remains, but in our opinion this scatter is rather the evidence of the challenging task to measure the vapor pressure and the vaporization enthalpy of extremely heavy, low volatile ionic liquids. The outlying values of $\Delta_l^g H_m^0$ (298 K) obtained from thermogravimetry [19] and a high-temperature spectroscopic technique [26] could be an indicator that these methods still require further development. We also deliberately omitted the calorimetric data measured by drop microcalorimetry [27] for [C$_n$mim][NTf$_2$] from Fig. 2.9, because of a systematic error discussed in [30]. It is very discouraging that the data for C$_{10}$ and C$_{12}$ measured [31] with the very good QCM-Knudsen method are significantly out of the linear correlation apparent on Fig. 2.9. However, a careful analysis of the primary experimental data of this work has revealed that both ILs were measured in a very narrow (about 15 K) temperature range. From our experiences, a larger range of about 30-50 K is necessary to provide a reliable slope and $\Delta_l^g H_m^0$ (T_{av}). Thus, the proper adjustment of vaporization enthalpies to 298 K using simple empirical rules developed in the current study has converted the mess of experimental points available in the literature (see Fig. 2.1) into a logical structure-property dependence presented in Fig. 2.9.

2.13 The limitations of the QCM and TGA methods

In this work we have developed and successfully applied two "direct" methods the QCM and the TGA for $\Delta_l^g H_m^0$ measurements of thermally stable imidazolium, pyridinium and pyrrolidinium based ILs with [NTf$_2$]$^-$ anion. However, for many ILs (e.g. with anions [Cl]$^-$, [Br]$^-$, [SCN]$^-$, [C(CN)$_3$]$^-$, etc.) the operating temperature range of TGA was significantly higher than the decomposition temperature of ILs under study and the vaporization enthalpy measurements failed. This fact makes the QCM method the only available experimental method for the $\Delta_l^g H_m^0$ determination for these ILs. From our experience every experimental method has a potential for a systematic error. Consequently, only a combination of a few methods applied to study the same sample could reveal the consistency of the result. In our earlier works [16], [58] we developed two additional "indirect" options to assess vaporization enthalpies of ILs based on experimental measurements of enthalpies of formation of liquid $\Delta_f H_m^0(l)$ by using combustion calorimetry, as well as reaction calorimetry by DSC. Combined with quantum-chemical (QC) calculations of the ideal gas enthalpy of formation, $\Delta_f H_m^0(g)$, the required enthalpy of vaporization can be obtained indirectly and compared with the result from the direct method (QCM or TGA). In this work we also developed and tested the solution calorimetry method for estimation of vaporization enthalpies of ILs in indirect way in combination with the combustion and QC methods.

An additional advantage of the indirect methods to derive vaporization enthalpies is that the $\Delta_l^g H_m^0$ values for ILs are already ascribed to the reference temperature 298 K. Consequently, the combination of combustion, reaction, and solution calorimetry can be used for validation of the $\Delta_l^g C_{p\,m}^0$ procedures described above. Next Chapter will describe contributions from the indirect calorimetric methods for evaluation of the consistency of the vaporization enthalpies data set.

3. Vaporization enthalpies of ionic liquids at 298 K from indirect methods.

ILs are claimed to be environmentally benign predominantly owing to their negligible vapor pressures. Due to this fact, most of the chemical and technical applications of ILs are indeed based on this remarkable property and the scientific community has been faced with the continuously increasing challenge to measure the vapor pressure and the vaporization enthalpies. However, thermal stability of ILs is often restricted and the direct experimental methods (e.g. Knudsen, TGA or QCM) fail to provide reliable data. Apart from the direct methods for determination of $\Delta_l^g H_m^0$, there are some other valuable options to estimate vaporization enthalpies of ILs indirectly. The following thermodynamic relationship exhibits the basic idea to obtain the $\Delta_l^g H_m^0$ at 298 K for any IL:

$$\Delta_f H_m^0(g)(298\ K) = \Delta_f H_m^0(l)(298\ K) + \Delta_l^g H_m^0(298\ K) \qquad (3.1)$$

where $\Delta_f H_m^0(g)$, is the molar gaseous enthalpy of formation, $\Delta_f H_m^0(l)$ is the molar enthalpy of formation in the liquid state, and $\Delta_l^g H_m^0$ is the molar enthalpy of vaporization. The desired $\Delta_l^g H_m^0$-value is estimated according to equation.

$$\Delta_l^g H_m^0(298\ K) = \Delta_f H_m^0(g)(298\ K) - \Delta_f H_m^0(l)(298\ K) \qquad (3.2)$$

Enthalpy of formation $\Delta_f H_m^0(g)$ can be calculated by using suitable quantum-chemical (QC) methods. As a rule, these calculations are performed after careful conformational analysis for the cation, the anion, and the neutral IL molecule, in order to determine the stability of gaseous ion pairs and to calculate $\Delta_f H_m^0(g)$ by an independent, theoretical method, which allows to perform a thermodynamic consistency test of both methods, the experimental and the theoretical one. The choice of the suitable QC methods is the challenging task. The G3MP2 and the CBS-QB3 [59] methods have been tested successfully. In this work we used these both methods for the QC calculations. Details on QC calculations used in this work are given in the Chapter 6. Enthalpy of formation $\Delta_f H_m^0(l)$ required for using of eq. 3.2 can be derived by high precision combustion calorimetry [15] or with help of the reaction calorimetry by using the DSC [52].

3.1 Enthalpies of formation $\Delta_f H_m^0(l)$ from combustion calorimetry

ILs are claimed to be environmentally benign due to their nonflammability. However, a series of special designed energetic ionic liquids have been shown to be combustible due to their high nitrogen content and decomposition products [60]. Bomb calorimetry is the well-established and precise experimental technique to measure energies of combustion of organic compounds in oxygen [61]. However, the pre-requisite of a reliable calorimetric experiment is a completeness of combustion and well defined final products of reaction (in ideal CO_2 and H_2O). It is apparent, that these requirements were hardly applicable to the first-generation ionic liquids (imidazolium-

aluminate systems). With the discovery of second-generation and third-generation ionic liquids, the selection of the available structures has become more acceptable for the purpose of using combustion calorimetry. However, due to presence of combinations of F, Cl, P, and S-elements in the common anions (e.g. $[PF_6]$ or $[NTf_2]$) the problem of defining the final degree of oxidation of hetero-elements still remains challenging. At the same time, the current variety of available ammonium-, imidazolium-, pyridinium-, or pyrrolidinium-based cations with the anions, such as $[NO_3]^-$, $[CH_3CO_2]^-$, $[N(CN)_2]^-$, $[C(CN)_3]^-$, or $[SCN]^-$ builds a promising collection of C,H,N,O,S-containing ILs, where combustion reaction occurs with very well established final states, provided that completeness of combustion will be achieved. To realize the idea given by eqs 3.1 and 3.2, we have measured combustion enthalpies of ILs systematically.

The general combustion process can be described by the next reaction:

$$C_nH_mN_pO_q + \left(n + \frac{m}{4}\right) O_2 = nCO_2 + \frac{m}{2} H_2O + \frac{p}{2} N_2 \qquad (3.3)$$

Application of the Hess law to the reaction 3.3 in order to calculate the $\Delta_f H_m^0(l)$ of compound results into the equation 3.4:

$$\Delta_f H_m^0(l) = n \cdot \Delta_f H_m^0(g, CO_2) + \frac{m}{2} \cdot \Delta_f H_m^0(l, H_2O) - \Delta_{comb} H_m^0 \qquad (3.4)$$

where molar combustion enthalpy $\Delta_{comb} H_m^0$ was measured during combustion experiment. Molar enthalpies of formation of CO_2 $\Delta_f H_m^0(g)$ and H_2O $\Delta_f H_m^0(l)$ were taken as recommended by CODATA [62]. The more detailed description of the method find in ref. [61].

The bomb calorimetry was successfully applied to the ammonium, imidazolium, pyridinium, pyrrolidinium ILs with such anions as nitrate $[NO_3]^-$ [63], dicyanamide $[N(CN)_2]^-$ [23], acetate $[CH_3CO_2]^-$, tricyanomethanide $[C(CN)_3]^-$ [59]. However, there are two restrictions of the bomb calorimetry towards ILs. The first one is that the method requires about 10 g of the highly pure IL. Keeping in mind a pricelist for the commercially available ILs, the systematic studies of ILs could turn out to be very expensive. The second restriction is the highest level of 99.9% purity. As a rule, synthesis of ILs is designed to obtain the desired IL already on the level of 98-99%. However, the residual (1-2%) impurities (e.g precursors) in the combustion are inacceptable for the combustion calorimetry. The subsequent purification of the sample is very demanding, because the traditional for molecular compounds methods such as distillation or recrystallization fail for ILs. For example ILs readily form glass instead of crystallization[64], , thus making the recrystallization purification procedure ineffective. Another restriction is the purity control of the sample for combustion calorimetry. The traditional for molecular compounds gas-chromatography failed. Sensitivity of the ion-chromatography is good only for the ionic species. The NMR spectra are also insensitive for impurities on the level smaller than 3-5%. Scope of these restrictions has made the combustion calorimetry unfeasible for the broad systematic studies on ILs. This frustration has enforced development of an alternative method – reaction calorimetry by using DSC, where aforementioned restrictions could be overcome.

3.2 Enthalpies of formation $\Delta_f H_m^0(l)$ and vaporization $\Delta_l^g H_m^0$ from reaction calorimetry with DSC

Experimental enthalpy of any ILs synthesis reactions (e.g. 3.5):

$$\text{1,2-diMe-Imidazole } (l) + \text{C}_n\text{Br } (l) = [\text{C}_n\text{mmim}][\text{Br}]\ (l) \qquad (3.5)$$

measured by DSC opens the direct way to derive enthalpies of formation of ILs and in combination with quantum chemical calculations to determine vaporization enthalpies according to eq. 3.2. For the experiment precursors of ILs (1,2-diMe-Imidazole *and* C_nBr *(l)*) were mixed in the aluminium pans and sealed hermetically. Enthalpies of the ILs synthesis reactions, $\Delta_r H_m^0(l)$, were determined in a series of several consequent DSC runs under optimized conditions elaborated in [58]: in excess of alkylimidazole, dilution with the solvent $[C_4mim][NTf_2]$, and temperature scanning with 50 K/min in the range 298-523 K. A sharp reaction peak with well-defined baseline was achieved, providing reproducible results under these conditions.

In comparison with the combustion calorimetry, the DSC reaction calorimetry for the determination of $\Delta_r H_m^0(l)$ was significantly less demanding. As a rule the IL is produced from precursors according to eq. 3.5 and the selectivity of the reaction is responsible for the purity of the IL under study. Moreover, purity of the fresh distilled precursors at the level of 99% was already sufficient for the reaction calorimetry experiments. These advantages are of crucial importance for systematic investigation of ILs where research samples are expensive and often available only in small quantities.

In our recent work we developed and tested the DSC method [58]. Experimental results on $\Delta_r H_m^0(l)$ and $\Delta_l^g H_m^0$ for the $[C_n mim][Hal]$ family with the [Cl] and the [Br] anions were obtained [58]. In this work we extended our structure-property relations studies of the imidazolium based ILs. There were at least two attractive ideas how to modify the imidazolium structural unity. The first idea was to study ILs with the methylated 2nd position on the imidazolium cation (see Fig. 3.1). It is well recognized that Ils with the methylation of the 2-nd position on the imidazolium ring possess significantly different physical-chemical properties in comparison with the 1,3-alkylated imidazolium cation. The reason is that in the ILs with the $[C_n mim]^+$ cation the presence of hydrogen in 2-nd position gives the possibility to form hydrogen bond network among cations and anions in the liquid phase. In ILs with the methylated 2nd position of the cation $[C_n mmim]^+$ (see Fig. 3.1) this strong hydrogen bonding is absent and only weaker hydrogen bonded networking over the 4th and 5th hydrogens on the imidazolium ring are still effective.

Consequences of the methylation of the second position on the imidazolium ring for density, viscosity, surface tension, etc. were already reported in the literature. Systematic study of vaporization enthalpies for ILs with this pattern of substitution ($[C_n mmim]^+$) has been performed in this work for the first time.

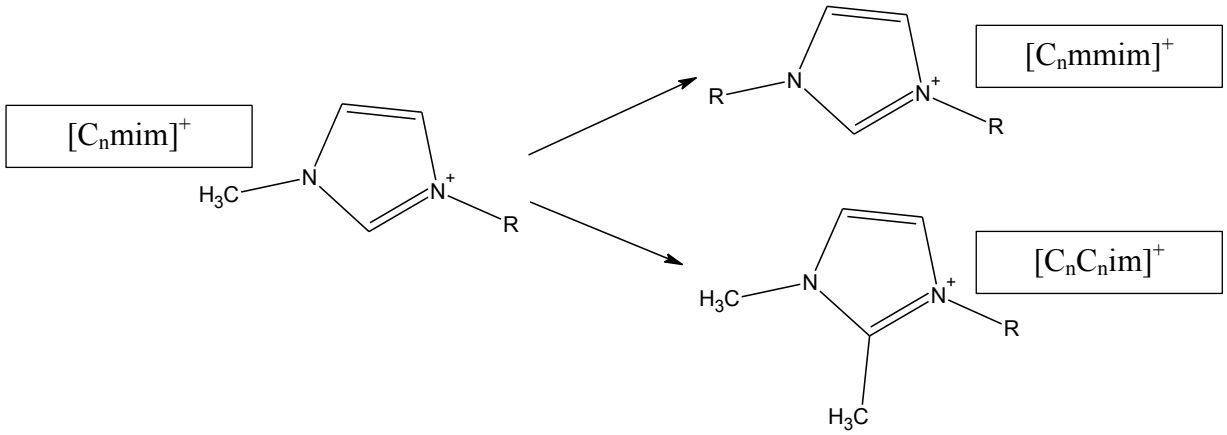

Figure 3.1 Modification of well-studied $[C_nmim]^+$ cation to symmetrical $[C_nC_nim]^+$ cation and 2-nd position methylated $[C_nmmim]^+$ cation.

The second idea was to study ILs with the symmetric alkylated in 1 and 3 positions imidazolium cation $[C_nC_nim]^+$ (see Fig 3.1). Rocha et al. [65] reported that the $[C_nC_nim][NTf_2]$ IL family, have the trend in the $\Delta_l^g H_m^0$- alkyl-chain (n) dependence different from those for the asymmetric series $[C_nmim][NTf_2]$. Such difference could be an evidence for unusual interplay between van der Waals and Coulomb interactions in such type of the symmetric Ils. In this context we decided to extend our studies to the symmetric imidazolium based ILs but with [Br] and [I] anions.

The reaction enthalpies of the ILs synthesis reaction according to eq. 3.5 and vaporization enthalpies (according to eq. 3.2) for the 2nd methylated $[C_nmmim][Hal]$, and the symmetric $[C_nC_nim][Hal]$, where Hal = Br, I derived in this work are listed in the Table 3.1.

Table 3.1 Vaporization enthalpies of ILs at 298 K, derived from combination of DSC measurement and quantum chemical calculations.

IL	$\Delta_r H_m^0(g)$,kJ·mol^{-1}			$\Delta_r H_m^0(l)_{exp}$, kJ·mol^{-1}	$\Delta_l^g H_m^0$, kJ·mol^{-1}
	CBS-QB3	b3lyp/ 6-311G**	corrected[a]		
$[C_4mmim][Br]$	-39.75	-8.41	-39.8 ± 4.0	-96.7 ± 2.7	152.5 ± 4.8
$[C_5mmim][Br]$	-39.82	-8.34	-39.7 ± 4.0	-96.3 ± 1.9	156.6 ± 4.4
$[C_8mmim][Br]$		-8.38	-39.8 ± 4.0	-96.2 ± 1.7	171.1 ± 4.3
$[C_4mmim][I]$		-23.46	-48.5 ± 4.0	-107.1 ± 2.7	158.2 ± 4.8
$[C_5mmim][I]$		-23.39	-48.4 ± 4.0	-106.7 ± 1.3	162.5 ± 4.2
$[C_8mmim][I]$		-23.06	-48.1 ± 4.0	-107.6 ± 2.6	176.7 ± 4.8
$[C_4C_4im][Br]$		-19.60	-51 ± 4.0	-98.9 ± 1.8	149.7 ± 4.4
$[C_5C_5im][Br]$		-19.80	-51.2 ± 4.0	-102.4 ± 2.3	161.4 ± 4.6
$[C_8C_8im][Br]$		-20.53	-51.9 ± 4.0	-100.2 ± 2.3	185.3 ± 4.6
$[C_4C_4im][I]$		-31.49	-56.5 ± 4.0	-105.4 ± 3.4	154.7 ± 5.2
$[C_5C_5im][I]$		-31.71	-56.7 ± 4.0	-103.8 ± 2.4	161.5 ± 4.7
$[C_8C_8im][I]$		-31.70	-56.7 ± 4.0	-103.2 ± 3.5	186.0 ± 5.3

[a] all DFT values were corrected on -25 kJ·mol-1, b3lyp/6-311G values on -31.4 kJ·mol-1, see explanation in text.

Table 3.1 shows that all reactions were strongly exothermic. Strictly speaking, enthalpies of reaction, $\Delta_r H_m^0(l)$, derived by integration of the DSC-peak are referred to the temperature of the peak maximum, T_{max} (see Figure 6.3). However, from our experiences [58], a correction estimated for adjustment of the measured enthalpies to the reference temperature 298 K (using heat capacities of the reaction participants) does not exceed 0.3-0.4 kJ·mol^{-1} and this correction is well negligible within the boundaries of the DSC experimental uncertainties of 1-3 kJ·mol^{-1}. We set in this work the experimental DSC-values of $\Delta_r H_m^0(l)$ to be equal those at the reference temperature 298 K.

It is apparent from Table 3.1 that enthalpies of ILs synthesis reactions (Table 3.1, column 5) seem to be independent on the alkyl chain length within the group of the common anion. The same behaviour were already observed for homologous series of [$C_n$mim][Br] [58], as well as for pyridinium based [C_nPy][Cl], [C_nPy][Br] and pyrrolidinium based [C_{n1}Pyrr][Cl], [C_{n1}Pyrr][Br] ionic liquid families ionic liquid families [66].

There are two possibilities [58] to derive enthalpies of vaporization by using eq. 3.2. The first one is based on eq. 3.2 using the difference between theoretical gas phase enthalpies of formation, $\Delta_f H_m^0(g)$ (298 K) calculated with the composite CBS-QB3 method and the experimental molar enthalpies of formation in the liquid state, $\Delta_f H_m^0(l)$ (298 K) measured by DSC (e.g eqs. 3.6).

$$\Delta_l^g H_m^0 \text{ (IL, 298 K)} = \Delta_f H_m^0(g)\text{(IL)} - \Delta_r H_m^0(l)\text{(IL)} - \Delta_f H_m^0(l)\text{(1,2-diMeIm)} - \Delta_f H_m^0(l)(C_4\text{Br}) \quad (3.6)$$

However, this way is not optimal, because in this case $\Delta_l^g H_m^0$ suffers from ambiguity of value of the theoretical enthalpy of formation, $\Delta_f H_m^0(g)$ used in eq. 3.6 [58]. The second way is to calculate the enthalpy of the reaction in a gas phase $\Delta_r H_m^0(g)$ with the first-principles methods directly, shown in eq. 3.7 ([$C_n$mmim][Br] family is taken as example):

$$\text{1,2-diMeIm } \textit{(g)} + C_n\text{Br } \textit{(g)} = [C_n\text{mmim}][\text{Br}] \textit{ (g)} \quad (3.7)$$

As a rule, the value of $\Delta_r H_m^0(g)$ is calculated from the enthalpies H_{298} at T = 298 K for all reaction participants of reaction 3.7 by the CBS-QB3 (or any suitable quantum chemical method) approach and using the Hess' Law, for example. the enthalpy of reaction for [C_4mmim][Br]) was calculated as follows:

$$\Delta_r H_m^0(g) = H_{298}([C_4\text{mmim}][\text{Br}], \text{g}) - H_{298}(\text{1,2-diMeIm, g}) - H_{298}(C_4\text{Br, g}) = -(39.75\pm5.0) \text{ kJ·mol}^{-1} \quad (3.8)$$

It is important to underline that the value $\Delta_r H_m^0(g)$ was obtained using quantum chemical methods *directly* from the calculated H_{298} bypassing the conventional calculation of the enthalpies of formation with help of atomization or isodesmic procedures [67]. This $\Delta_r H_m^0(g)$

value is not affected by the choice of atomization or bond separation procedure required for the first way.

Unfortunately we were able to perform CBS-QB3 calculations only for [C_4mmim][Br] and [C_5mmim][Br]. Other ILs listed in Table 3.1 have been too large to complete calculations with this method in reasonable time. As a compromise, all bromine containing compounds $\Delta_r H_m^0(g)$ were additionally calculated using B3LYP/6-311G** method. Comparison of reaction enthalpy values, $\Delta_r H_m^0(g)$, for [C4mmim][Br] and [C5mmim][Br] calculated by CBS-QB3 and B3LYP /6-311G** has revealed (see Table 3.1) that the difference between two methods is of -31.4 kJ·mol^{-1} constant. We used this shift of -31.4 kJ·mol^{-1} for correction of $\Delta_r H_m^0(g)$ values obtained by B3LYP/6-311G** method for the [Br] containing ILs with the long alkyl chains.

As an example for the $\Delta_l^g H_m^0$ calculations listed in Table 3.1 let us consider the result for [C_4mmim][Br]. Having the value of $\Delta_r H_m^0(l)$ measured by using the DSC and $\Delta_r H_m^0(g)$ from quantum chemistry, we have estimated the vaporization enthalpy of [C_4mmim][Br] as follows:

$$\Delta_l^g H_m^0 \text{ (IL, 298 K)} = -\Delta_r H_m^0(l)_{exp} + \Delta_r H_m^0(g) + \Delta_l^g H_m^0 \text{ (1,2-diMeIm)} + \Delta_l^g H_m^0 \text{ (C}_4\text{Br)}] =$$
$$= -(-96.7) + (-39.8) + (58.9) + (36.7) = 152.5 \pm 4.8 \text{ kJ·mol}^{-1} \quad (3.9)$$

Using the theoretical value $\Delta_r H_m^0(g)$ in the gas phase and enthalpies of vaporization at 298 K of precursors $\Delta_l^g H_m^0$ (1,2-diMeIm) = 58.9 ± 0.2 kJ·mol^{-1}, $\Delta_l^g H_m^0$ (C_4Br) = 36.7 ± 0.1 kJ·mol^{-1} and the enthalpy of reaction $\Delta_r H_m^0(l)_{exp}$ measured using the DSC in the liquid phase, we calculated the enthalpy of vaporization of [C_4mmim][Br]. In the same way, enthalpies of vaporization of other ILs were calculated with help of eq. 3.9 and listed in the Table 3.1. The additional vaporization enthalpies of precursors were taken from the literature [68] and they are listed in SI (Table S6 & S7).

Reaction enthalpies according to eq. 3.5 for the iodine containing ILs are listed in the Table 3.1. However, in order to derive the vaporization enthalpies according to eq. 3.2, the $\Delta_r H_m^0(g)$ values calculated by QC are required. It has turned out that the available precise composite methods do not possess the parameterization for the iodine element. Such parameterisation was available only in the less precise DFT methods. The correction of $\Delta_r H_m^0(g)$ calculated at B3LYP/6-311G** level of theory for $[I]^-$ containing ILs was evaluated taking into account the trends in the $\Delta_l^g H_m^0$ found for [C4mim][Hal] (Hal = Cl, Br, I) by using QCM technique [unpublished]. Thus the results of B3LYP/6-311G** calculations for $[I]^-$ containing ILs were shifted by approximately -25 kJ·mol^{-1} in order to get at least reasonable level of vaporization for these ionic liquids. In this context, the absolute values of $\Delta_l^g H_m^0$ for the iodine containing should be considered as the tentative, but the general trends, e.g for the vaporization enthalpy chain length dependence are expected to be not affected.

Using the DSC reaction calorimetry has allowed the express excess to the systematic study of the thermochemical properties of ILs and the resulting vaporization enthalpies $\Delta_l^g H_m^0$ (298 K).

However, the DSC method also has its own limitations. For example the DSC method is not optimal for very fast synthesis reactions were the reaction heat could be evolved already outside the measuring unity during the sample preparation. Also the ILs, which are synthesizes by the anion exchange (e.g. $[BF_4]^-$, $[PF_6]^-$, etc.) reactions cannot be studied by this method. In order to get thermochemical information we applied the solution calorimetry method described below.

3.3 Indirect way to obtain vaporization enthalpy $\Delta_l^g H_m^0$ from solution calorimetry

In addition to the combustion calorimety and the DSC applied in this work to calculate vaporization enthalpy, $\Delta_l^g H_m^0$, indirectly we have established and tested the solution calorimetry in our lab. The idea to use solution calorimetry to get the $\Delta_l^g H_m^0$ is the same as expressed by eq. 3.2, but the value of the molar enthalpy of formation in the liquid state, $\Delta_f H_m^0(l)$ in this case is derived from data measured by solution calorimetry. The main argument to develop the solution calorimetry method for this work is that it operates directly at 298 K and the resulting $\Delta_l^g H_m^0$ - values, are valuable to test the temperature adjustment procedures presented earlier.

Solution calorimetry is a well-established experimental method with a long history and well-developed theory. It is based on measuring the heat of the dissolution process of the solid or the liquid samples in the liquid solvent. In the calorimetric experiment the sample under study is quickly introduced into the solvent and the temperature change is measured. This temperature difference multiplied by the heat capacity of the calorimetric system equals to the heat of the dissolution process. The dissolution process (e.g. for $[C_4mim][BF_4]$) is usually ascribed to the following reaction:

$$[C_4mim][BF_4]_{liq} + aq \xrightarrow{solution} [C_4mim]^+_{aq} + [BF_4]^-_{aq} \qquad (3.10)$$

where $[C_4mim]^+_{aq}$ and $[BF_4]^-_{aq}$ are the cation and anion in aqueous state respectively. The reaction enthalpy of 3.10 is defined as solution enthalpy $\Delta_{sol}H_m^0$. According to the Hess Law:

$$\Delta_f H_m^0\left([C_4mim][BF_4]_{liq}\right) = \Delta_f H_m^0\left([C_4mim]^+_{aq}\right) + \Delta_f H_m^0\left([BF_4]^-_{aq}\right) - \Delta_{sol}H_m^0 \qquad (3.11)$$

where $\Delta_f H_m^0\left([C_4mim]^+_{aq}\right)$ and $\Delta_f H_m^0\left([BF_4]^-_{aq}\right)$ are enthalpies of formation of ions dissolved in water and referred to the infinite dilution. The enthalpy $\Delta_{sol}H_m^0$ is measured with the solution calorimeter. Values of $\Delta_f H_m^0(aq)$ for anions and cations relevant to ILs studied in this work are available in the literature [62] and collected in Table 3.2. Thus, from the combination of the experimentally measured $\Delta_{sol}H_m^0$ with the available in the literature enthalpies of formation of the aqueous ions $\Delta_f H_m^0(aq)$ the desired enthalpy of formation of an IL can be calculated according to eq. 3.11.

Table 3.2 $\Delta_f H_m^0(aq)$ available from the literature

Ion	$\Delta_f H_m^0(aq)$, kJ·mol^{-1}
NO_3^-	-206.85 ± 0.40 [62]
Cl^-	-167.08 ± 0.10 [62]
Br^-	-121.41 ± 0.15 [62]
I^-	-56.78 ± 0.05 [62]
SCN^-	74.3 ± 0.5 [69]
$CH_3CO_2^-$	-485.6 ± 0.5 [69]
HSO_4^-	-886.9 ± 1.0 [62]
BF_4^-	-1571.5 ± 5.0 [69]
$N(CH_3)_4^+$	-103.9 ± 1.0 [63]
$N(n\text{-}C_4H_9)_4^+$	-422.0 ± 2.2 [63]

Having enthalpy of formation $\Delta_f H_m^0(g)$ for this IL from a suitable QC methods, the vaporization enthalpy $\Delta_l^g H_m^0$, can be calculated with eq. 3.2 for the IL under study.

However, such a successful application of the solution calorimetry for $\Delta_l^g H_m^0$ calculations is thwarted with the simple fact that the most $\Delta_f H_m^0(aq)$ - values collected in Table 3.2 refer to the ions specific for classical salts, but not for ionic liquids. Values of $\Delta_f H_m^0(aq)$ for anions and cations specific for imidazolium, pyridinium, pyrrollidinium based ILs are absent in the literature. Thus in order to encompass these types of ILs we need to measure solution enthalpies of the typical representatives of the IL series and to derive the ionic liquid specific $\Delta_f H_m^0(aq)$ - values. In this study we restricted the extension of the available $\Delta_f H_m^0(aq)$ database (see Table 3.2) with some new ions: $[C_n\text{mim}]^+$ with n = 0 (Hmim), 2, 4, $[N(CN)_2]^-$, $[C(CN)_3]^-$, $[C_4C_1\text{Pyrr}]^+$, $[3\text{-Me-}C_4\text{Py}]^+$. In order to reduce experimental efforts and obtain a maximum amount of data our work has been performed in the following steps:

- Select an ionic compound, where $\Delta_f H_m^0(aq)$ for one ion is already known, but the $\Delta_f H_m^0(aq)$ for the second ion is unknown
- Determine the formation enthalpy $\Delta_f H_m^0\ (l)$ of this compound by any available method. (combustion calorimetry, reaction calorimetry, or the combination of quantum chemical calculations and vaporization calorimetry using eq. 3.1)
- Measure the solution enthalpy $\Delta_{sol} H_m^0$ of this compound using the solution calorimeter
- Use eq 3.11 to calculate the $\Delta_f H_m^0(aq)$ of the unknown ion

An example of determination of $\Delta_f H_m^0(aq)$ is given below. As a matter of fact the value of the enthalpy of formation of $\Delta_f H_m^0\left([NO_3]_{aq}^-\right)$ is known from the literature (see Table 3.2). Enthalpy of formation, $\Delta_f H_m^0\ (l)$, for this IL is one of the most reliable in the current literature, because the enthalpy of combustion for $[C_4\text{mim}][NO_3]$ was measured twice in different thermochemical labs [70] and the results were indistinguishable within experimental uncertainties. Thus, to obtain the aqueous enthalpy of formation of the $[C_4\text{mim}]^+$ cation we used the following equation:

$$\Delta_f H_m^0\left([C_4mim]_{aq}^+\right) = \Delta_f H_m^0\left([C_4mim][NO_3]_{liq}\right) + \Delta_{sol} H_m^0 - \Delta_f H_m^0\left([NO_3]_{aq}^-\right) =$$

(-261.4 ± 2.9) + (0.2 ± 0.2) - (-206.85 ± 0.4) = -54.4 ± 2.9 kJ·mol^{-1} (3.12)

From this calculations the value of -54.4 ± 2.9 kJ·mol^{-1} can be now quantified for the aqueous enthalpy of formation of the $[C_4mim]^+$ cation. Similar calculations were performed for other ILs. The initial data and the results are presented in Table 3.3.

Table 3.3 Enthalpies of formation of the aqueous ions at $\Delta_f H_m^0(aq)$ 298 K derived in this work. All values are in kJ·mol^{-1}.

		state	$\Delta_f H_m^0$, kJ·mol^{-1}	$\Delta_{sol} H_m^0$, kJ·mol^{-1}	$\Delta_f H_m^0(aq)$ ion
$[C_4mim]$	$[NO_3]$	l	-261.4 ± 2.9[70]	0.2 ± 0.2	-54.4 ± 2.9
	[Cl]	cr	-214.7 ± 1.9 [71]	-5.0 ± 1.0[c] [72]	-52.6 ± 2.1
	[Br]	cr	-182.1 ± 1.9 [58]	10.1 ± 0.9	-50.6 ± 2.1
				weighted avg	**-52.2 ± 1.3**
$[C_2mim]$	$[NO_3]$	cr	-235.7 ± 2.0 [70]	17.1 ± 1.0	-11.8 ± 2.3
	[SCN]	l	52.8 ± 2.3[73]	7.8 ± 0.1	-13.7 ± 2.4
				weighted avg	**-12.7 ± 1.6**
[Hmim]	$[CH_3CO_2]$	l	-425.7 ± 1.2 [74]	-28.1 ± 0.1[74]	**31.8 ± 1.3**
$[N(CN)_2]$	$[C_2mim]$	l	235.3 ± 3.1[16]	3.3 ± 0.3	251.3 ± 3.5
	$[C_4mim]$	l	195.0 ± 2.7 [16]	3.0 ± 1.0	250.2 ± 3.2
				weighted avg	**250.7 ± 2.4**
$[C(CN)_3]$	$[C_2mim]$	l	342.2 ± 2.5 [59]	12.6 ± 1.0	367.5 ± 3.2
	$[C_4mim]$	l	279.2 ± 2.6 [59]	12 ± 0.7	343.4 ± 3.0
				weighted avg	**354.9 ± 2.2**
$[C_{41}Pyrr]$	$[N(CN)_2]$	l	57.9 ± 2.8 [23]	-1.3 ± 0.7	**-194.1 ± 3.7**
[3Me-C_4Py]	$[N(CN)_2]$	l	181.3 ± 3 [75]	-0.4 ± 0.2	**-69.8 ± 3.8**

c- recalculated using initial data

The analysis of the $\Delta_f H_m^0(aq)$ –values derived in the Table 3.3 revealed some interesting structure-property relations. We observed very good linear correlation (see Figure 3.2) of the aqueous enthalpy of formation $\Delta_f H_m^0(aq)$ of $[C_nmim]^+_{(aq)}$ cations with the number of the C-atoms (n) in the alkyl chain:

$$\Delta_f H_m^0(aq)\ [C_nmim]^+ = -21.0\ n + 31.0\ (r = 0.998) \quad (3.13)$$

Such linear dependence was also observed earlier for quaternary ammonium cations $[N(R)_4]^+$ with different chains R [63].

$$\Delta_f H_m^0(aq)\ [N(C_n)_4]^+ = -104.7\ n + 2.4\ (r = 0.998) \quad (3.14)$$

These simple linear correlations are very useful to reduce the amount of experimental work and they allow predicting the desired $\Delta_f H_m^0(aq)$ for the imidazolium and ammonium based cations for arbitrary number of C-atoms (n) in the cation alkyl chains. It is also reasonable to assume the similar regularities for other families of pyrrolidinium, pyridinium, or phosphonium based ILs.

Thus, these simple structure-property relations open an express way for assessment of the unknown $\Delta_f H_m^0(aq)$ of ions.

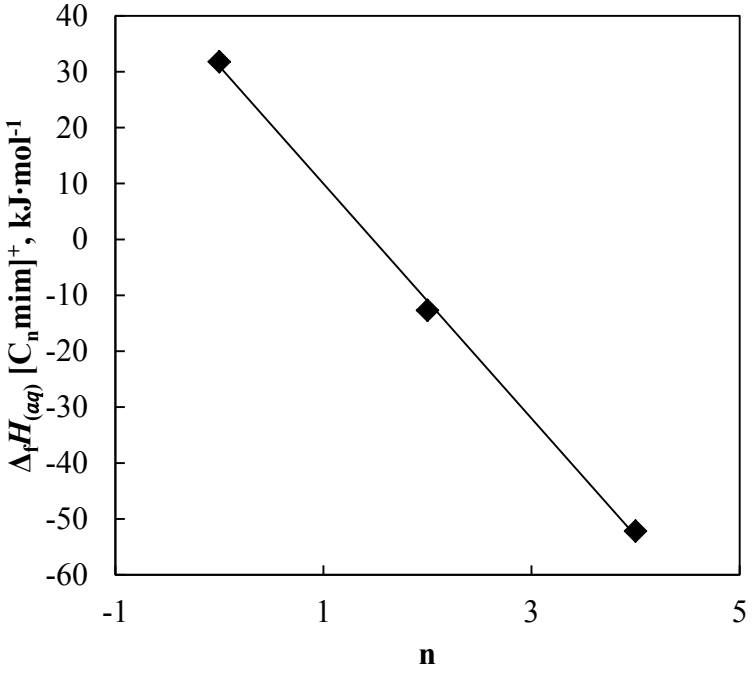

Figure 3.2 Standard enthalpies of formation of the aqueous $[C_n mim]^+$ cations dependence on the number of carbon atoms (n) in the alkyl chain.

Having established the values of enthalpies of formation $\Delta_f H_m^0(aq)$ of the aqueous cations, and anions, it became possible to predict enthalpies of vaporization, $\Delta_l^g H_m^0$, of different ILs by using eq. 3.2. For example for $[C_4mim][BF_4]$:

$$\Delta_l^g H_m^0([C_4mim][BF_4]) = \Delta_f H_m^0\left([C_4mim][BF_4]_g\right) -$$

$$-\Delta_f H_m^0\left([C_4mim]_{aq}^+\right) - \Delta_f H_m^0\left([BF_4]_{aq}^-\right) + \Delta_{sol} H_m^0 \qquad (3.15)$$

where, $\Delta_f H_m^0\left([C_4mim]_{aq}^+\right)$ was derived in this work, $\Delta_f H_m^0\left([BF_4]_{aq}^-\right)$ was taken from Table 3.2, $\Delta_{sol} H_m^0$ was measured with solution calorimetry, and $\Delta_f H_m^0\left([C_4mim][BF_4]_g\right)$ was calculated with the G3MP2 level of theory. Some other results for ILs with $[BF_4]^-$ anion are presented in Table 3.4.

Enthalpies of vaporization derived with help of the solution calorimetry have been in acceptable agreement with those measured by QCM (see Table 3.4). Moreover for $[N_{1111}][BF_4]$ had such low vapor pressure that cannot be measured even using QCM, thus leaving solution calorimetry as the only available option for its $\Delta_{cr}^g H_m^0$ prediction.

Table 3.4 Enthalpies of vaporization (or sublimation) for ILs with $[BF_4]^-$ anion, calculated from $\Delta_f H_m^0(aq)$ of ions, solution calorimetry data, and quantum chemical (G3MP2) calculations. All values are in kJ·mol^{-1}.

	$\Delta_f H_m^0$ (g)	$\Delta_{sol} H_m^0$	$\Delta_l^g H_m^0(calc)$	$\Delta_l^g H_m^0(exp)$
$[C_2mim][BF_4]$(l)	-1456.6 ± 5.0	18.2 ± 0.2	145.8 ± 7.3	135.5[u]
$[C_4mim][BF_4]$(l)	-1503.8 ± 5.0	17.2 ± 0.6	137.1 ± 7.2	142.6[u]
$[N_{1111}][BF_4]$(cr)	-1554.8 ± 5.0	43.1 ± 0.5	163.7 ± 7.2[s]	-
$[N_{4444}][BF_4]$(cr)	-1828.2 ± 5.0	6.6 ± 0.5	171.9 ± 7.2[s]	175.9[u]

[u] – unpublished QCM data adjusted to 298 K with $\Delta_l^g C_{p\,m}^0$ calculated using eq. 2.19, [s] - sublimation

Finally, direct methods to measure vaporization enthalpy together with three calorimetric indirect options: combustion calorimetry, differential scanning calorimetry, and solution calorimetry in combination with the quantum chemical calculations have allowed obtaining of the broad scope of the thermodynamic data required for analysis of the structure-property relations in ILs, discussed in Chapter 4.

4. Results and Discussion

"Structure Determines Properties" is a powerful concept in chemistry and in all fields in which chemistry is important. Ionic structures of ILs offer at least two initial patterns to study structure-property relationships: to keep the cation constant and change the anion systematically and vice versa. In this work we followed these two patterns and looked for some general qualitative and quantitative regularities between the structure of ILs and their thermodynamic properties with the focus on the vaporization enthalpy.

4.1 Vaporization enthalpy alkyl chain dependence

Cations of typical ILs contain as a rule alkyl chains of different length. It is well established for the molecular compounds, that thermodynamic properties usually obey group additivity rules. The most simple manifestation of additive rules is the correlation of any property, with the number of C-atoms. The increasing experimental data for ILs raise a question, whether the general additivity rules can be also applied to the ILs. The answer to this question could simplify reliable predictions for ILs, provided that a general transfer of the group contributions established for the molecular compounds to the *ionic liquids* is valid. Earlier reported experimental results (see Figure 2.1, 2.2) showed non-linear trends.

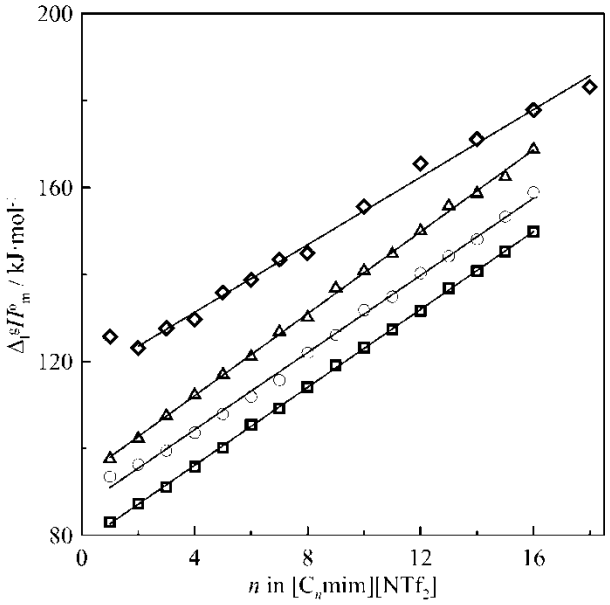

Figure 4.1 The enthalpies of vaporization for 1-alkyl-3-methylimidazolium bis(trifluoromethanesulfonyl)imides, alkyl benzenes, alkyl nitriles and alcohols at 298 K. ◊ - [C$_n$mim][NTf$_2$] (joined treatment of the QCM and TGA results from this work). Δ - n-alcohols (for comparison with ILs the data were shifted by 60 kJ·mol^{-1}). ○ - n- alkyl nitriles (for comparison with ILs the data were shifted by 60 kJ·mol^{-1}). □ - n-alkyl benzenes (for comparison with ILs the data were shifted by 45 kJ·mol^{-1})

Nevertheless, the careful analysis of the $\Delta_l^g C_{p\,m}^0$ discussed in Chapter 2 revealed the linear alkyl chain length dependence for [C$_n$mim][NTf$_2$] family, adjusted to 298 K. In Figure 4.1 we plotted for comparison the $\Delta_l^g H_m^0$ (298 K) chain length dependence for some molecular homologous series together with the results for the ionic liquids [C$_n$mim][NTf$_2$]. It is apparent from this figure that the intercepts for the different families are totally different and we have even scaled them in order to fit them on the same plot. But all the slopes presented in Fig. 4.1 seem to be similar and they generally represents the contribution of the CH_2-group to the vaporization enthalpy $\Delta_l^g H_m^0$ (298 K).

Is the linearity of $\Delta_l^g H_m^0$ specific only for [C$_n$mim][NTf$_2$] family? To answer this question we also studied other families of ILs with different cations and anions: [C$_{n1}$Pyrr][NTf$_2$], [C$_n$Py][NTf$_2$], [C$_{n1}$Py][Hal], [C$_n$mmim][Hal], and [C$_n$C$_n$im][Hal]. Enthalpies of vaporization for the [C$_{n1}$Pyrr][NTf$_2$] family were measured with QCM and TGA. Results are shown in the table 4.1.

Study of the [C$_n$Py][NTf$_2$] family with the TGA failed because of the rapid decomposition of ILs under experimental conditions. However, study of this series by the QCM has been successful, because of significantly lower temperature range specific for this method. Our experimental results together with some data available from the literature are collected in Table 4.2.

Experimental vaporization enthalpies given in Tables 2.1, 4.1 and 4.2 were approximated with the following linear equations:

$$[C_n\text{mim}][NTf_2]:\ \Delta_l^g H_m^0\ (298\ \text{K})/\text{kJ·mol}^{-1} = (115.7\pm1.8)+(3.9\pm0.2)\ n\ (r = 0.995) \qquad (4.1)$$

$$[C_{n1}\text{Pyrr}][NTf_2]:\ \Delta_l^g H_m^0\ (298\ \text{K})/\ \text{kJ·mol}^{-1} = (129.1 \pm 2.3) + (3.6 \pm 0.4)\ n\ (r= 0.988) \qquad (4.2)$$

$$[C_n\text{Py}][NTf_2]:\ \Delta_l^g H_m^0\ (298\ \text{K})/\text{kJ·mol}^{-1} = (123.8\pm0.9) + (3.6\pm0.2)\ n\ (r= 0.997) \qquad (4.3)$$

Very high correlation coefficient r = 0.99 for all three series is the clear evidence that for ILs with $[NTf_2]^-$ anion and different cations exists very simple linear dependence of the vaporization enthalpy on the chain length, similar to the those for the molecular compounds (see Fig. 4.1). The slopes in eqs 4.1-4.3 for the different homologous series exhibit CH_2 group contribution to the vaporization enthalpy of around 4.0 kJ·mol^{-1}. This value was somewhat lower than contribution of 4.5-5.0 kJ·mol^{-1} typically observed in *molecular liquids* (for n-alkylbenzenes, n-alkyl-nitriles, n-alkanes [39]). This lower contribution seems to be a consequence of the intensive Coulomb forces specific for *ionic liquids*. The close agreement for the CH_2 contribution in different ILs families is the clear evidence of the consistency of the measured vaporization enthalpies as well as the good validation of the procedures applied for the assessing of the $\Delta_l^g C_{p\,m}^0$- values described in this work.

Table 4.1 Experimental Vaporization Enthalpies, $\Delta_l^g H_m^0$, of [C_{n1}Pyrr][NTf_2] at T_{av} and at 298 K.

T-range / K	T_{av} / K	$\Delta_l^g H_m^0$ (T_{av}) kJ·mol^{-1}	$\Delta_l^g H_m^0$ (298 K)[a] kJ·mol^{-1}	Method
		[C_{31}Pyrr][NTf_2]		
395-437	415.7	131.3±1.0	140.1±1.0	QCM
532-577	554.2	125.8±2.6	145.0±2.6	TGA
			140.7±0.9 [b]	average
		[C_{41}Pyrr][NTf_2]		
395-437	415.8	133.7±1.0	143.7±1.0	QCM
532-577	554.3	124.2±2.8	146.0±2.8	TGA
412-519	470	134.0±3.0 [24]	148.6±3.0	TPD-LOSMS
583-613	598	167±19 [76]	(192±19) [c]	TPD-UV
			144.4±0.9 [b]	average
		[C_{51}Pyrr][NTf_2]		
375-432	405.7	135.4±1.0	145.4±1.0	QCM
		[C_{61}Pyrr][NTf_2]		
378-435	405.9	138.0±1.0	149.0±1.0	QCM
532-577	554.7	124.3±1.6	150.5±1.6	TGA
412-519	460	139.0±2.0 [24]	155.5±2.0	TPD-LOSMS
			150.3±0.8 [b]	average
		[C_{71}Pyrr][NTf_2]		
380-438	408.3	141.5±1.0	153.5±1.0	QCM
532-577	554.9	130.9±2.2	158.9±2.2	TGA
			154.4±0.9 [b]	average
		[C_{81}Pyrr][NTf_2]		
383-440	410.9	144.3±1.0	157.6±1.0	QCM
539-586	562.1	130.1±3.2	169.6±2.4	TGA
412-519	470	143.0±2.0 [24]	163.3±2.0	TPD-LOSMS
			158.9±0.9 [b]	average
		[$C_{10,1}$Pyrr][NTf_2]		
390-448	418.4	148.7±1.0	164.8±1.0	QCM
540-586	562.3	135.1±3.0	170.5±3.0	TGA
			165.4±1.0 [b]	average

[a] - enthalpies of vaporization for ILs were adjusted to 298 K with $\Delta_l^g C_{p\,m}^0$ values from column 3 in Table 2.5 (uncertainties in the heat capacity differences were not taken into account). [b] - Average values were calculated using the experimental uncertainty as the weighing factor. Values in bold are recommended for further thermochemical calculations. [c] - this value was not considered for the average calculation.

Table 4.2 The enthalpies of vaporization $\Delta_l^g H_m^0$ of [C_nPy][NTf_2] at T_{av} and at 298 K.

Compound	T_{av}/K	$\Delta_l^g H_m^0$ (T_{av}), kJ·mol^{-1}	$\Delta_l^g H_m^0$ (298 K)[a] kJ·mol^{-1}
[C_2Py][NTf_2]	400.6	125.3 ± 1	131.4
[C_3Py][NTf_2]	398.2	128.0 ± 1	134.5
[C_4Py][NTf_2]	399.5	131.1 ± 1	138.1
[C_4Py][NTf_2]	553	117.5 ± 1.1[24]	135.3
[C_5Py][NTf_2]	400.6	134.2 ± 1	141.7
[C_6Py][NTf_2]	405.7	137.3 ± 1	145.9
[C_6Py][NTf_2]	440	137.0 ± 1[77]	147.9

[a] adjusted to the 298 K using $\Delta_l^g C_{p\,m}^0$ from column 3 Table 2.4

It is also important to point out that enthalpies of vaporization for the [C$_n$mim][NTf$_2$] family with *odd* and *even* chain length of the alkyl-imidazolium cation fit into the same straight line and it is obvious that $\Delta_l^g H_m^0$ (298 K) of ILs follows the same pattern as that of the molecular liquids, where the *odd* and *even* effect was observed for such thermodynamic properties as melting point, fusion or sublimation enthalpy but not for vaporization enthalpy [78].

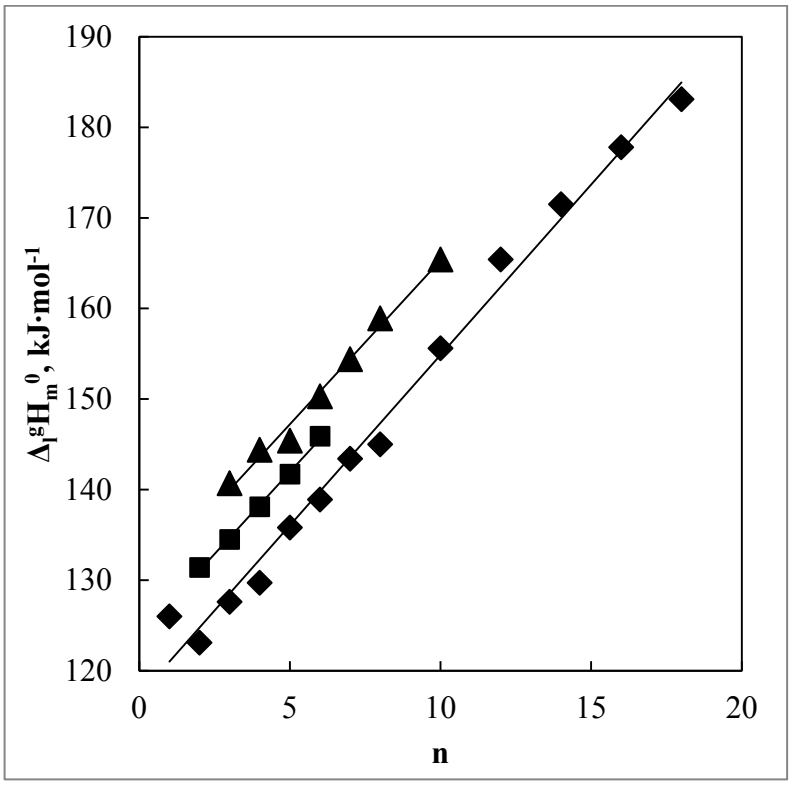

Figure 4.2 The enthalpies of vaporization of [C$_n$mim][NTf$_2$] (♦), [C$_n$Py][NTf$_2$] (■) and [C$_{n1}$Pyrr][NTf$_2$] (▲) at 298 K.

Another interesting observation was then apparent from the comparison of enthalpies of vaporization for [C$_n$Py][NTf$_2$], [C$_{n1}$Pyrr][NTf$_2$]and [C$_n$mim][NTf$_2$] (see Table 4.3). It is obvious from Table 4.3 that enthalpies of vaporization of species with the comparable chain length are different by a constant contribution of about 12 kJ·mol^{-1} between [C$_n$mim][NTf$_2$] and [C$_{n1}$Pyrr][NTf$_2$], and about 7 kJ·mol^{-1} between [C$_n$mim][NTf$_2$] and [C$_n$Py][NTf$_2$]. This observation could be used as a simple "rule of thumb" for a quick assessment of $\Delta_l^g H_m^0$ (298 K) values for ILs with the same anion.

Table 4.3 Comparison of enthalpies of vaporization $\Delta_l^g H_m^0$ (298 K) (in kJ mol^{-1}) for [C$_n$Py][NTf$_2$], [C$_{n1}$Pyrr][NTf$_2$] and [C$_n$mim][NTf$_2$].

	n=2	n=3	n=4	n=5	n=6
[C$_n$mim][NTf$_2$]	123.1	127.6	129.7	135.8	138.9
[C$_n$Py][NTf$_2$]	131.4	134.5	138.1	141.7	145.9
[C$_{n1}$Pyrr][NTf$_2$]	-	140.7	144.4	145.4	150.3
Δ(C$_n$mim →C$_n$Py)	8.4	6.9	8.4	5.7	7.0
Δ(C$_n$mim →C$_{n1}$Pyrr)		13.1	14.7	9.6	11.4

Equations 4.1-4.3 clearly demonstrated linear chain length dependence of $\Delta_l^g H_m^0$ for the families [X][NTf_2] with the same anion r [NTf_2]. What happens if we change the common anion, e.g. with $[Cl]^-$ or $[Br]^-$? To answer this question we studied the structure-property relation for [$C_n$mim][Hal] [58] and [C_nPy][Hal] [66], where Hal = Cl, in order to understand, whether ILs with different anions would still show linearity in the alkyl chain length dependence. The results for $\Delta_l^g H_m^0$ (298 K) were obtained by using DSC reaction calorimetry and quantum chemical calculations [52] and they are presented for [$C_n$mim][Br] and [$C_n$mim][Cl] in Figure 4.3. It is apparent that in contrast with the [$C_n$mim][NTf_2] series, the halogen-containing ILs have the significantly higher vaporization enthalpies , but the linear chain length dependence keeps also for these series [$C_n$mim][Br] and [$C_n$mim][Cl] true.

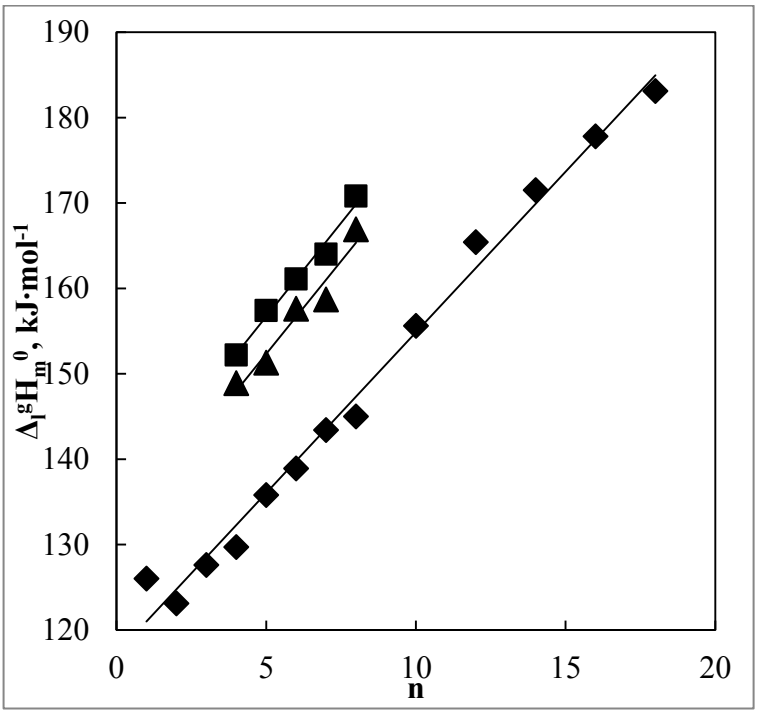

Figure 4.3 The comparison of the enthalpies of vaporization of [$C_n$mim][NTf_2] (♦) (from Chapter 2), [$C_n$mim][Br] (■) and [$C_n$mim][Cl] (▲) at 298 K.

The results of $\Delta_l^g H_m^0$ (298 K) for [C_nPy][Br] and [C_nPy][Cl] were obtained by using DSC reaction calorimetry and quantum chemical calculations [66] and they are presented in Figure 4.4 as the chain length dependence.

As it apparent from Figures 4.3 and 4.4, the linearity of vaporization enthalpy with the growing chain length on the cation seems to be a general feature for ionic liquids, independent of the cation and anion structures. The dependence of vaporization enthalpy on the total number of C-atoms for $n \geq 2$ is expressed by the following equations:

$$[C_n\text{mim}][\text{Cl}]: \quad \Delta_l^g H_m^0 \text{ (298 K)/ kJ·mol}^{-1} = 133.1 + 4.2\,n \quad (r = 0.980) \qquad (4.4)$$

$$[C_n\text{mim}][\text{Br}]: \quad \Delta_l^g H_m^0 \text{ (298 K)/ kJ·mol}^{-1} = 136.6 + 4.1\,n \quad (r = 0.988) \qquad (4.5)$$

$$[C_n\text{Py}][\text{Cl}]: \quad \Delta_l^g H_m^0 \text{ (298 K)/ kJ·mol}^{-1} = 157.1 + 3.6\,n \quad (r = 0.941) \qquad (4.6)$$

$$[C_n\text{Py}][\text{Br}]: \quad \Delta_l^g H_m^0 \text{ (298 K)/ kJ·mol}^{-1} = 155.7 + 4.4\,n \quad (r = 0.985) \qquad (4.7)$$

These eqs. can be used to calculate the enthalpy of vaporization $\Delta_l^g H_m^0$ (298 K) for other longer chained representatives of these series.

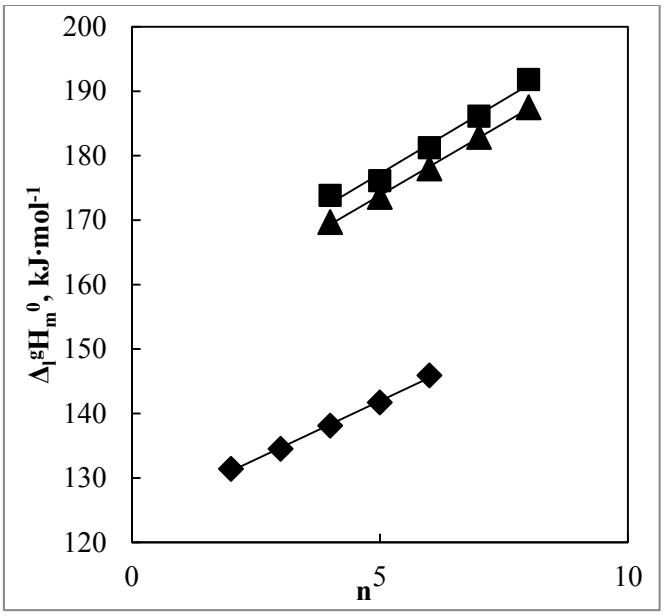

Figure 4.4 The comparison of the enthalpies of vaporization of [C$_n$Py][NTf$_2$] (♦), [C$_n$Py][Br] (■) and [C$_n$Py][Cl] (▲) at 298 K.

Similar to the ILs with $[NTf_2]^-$ anion, the contribution to vaporization enthalpy of about 4 kJ.mol^{-1} per each CH_2 group is apparently constant. This contribution is slightly lower in comparison with those of 4.95 kJ·mol^{-1} per each CH_2 group typical for the n-alkane family [34]. As additional important prove for consistency of the new $\Delta_l^g H_m^0$ (298 K) data sets for chlorine and bromine based ILs could serve the direct comparison of the differences in vaporization enthalpies for [Cl] and [Br] containing species. Such a comparison was performed for imidazolium (Table 4.4) and pyridinium (Table 4.5) based ILs.

Table 4.4. Comparison of the vaporization enthalpies $\Delta_l^g H_m^0$ (298 K)/ kJ.mol^{-1} for alkyl halides and for imidazolium based ionic liquids.

	C_n-halide					[$C_n$mim][halide]				
	C_4	C_5	C_6	C_7	C_8	C_4	C_5	C_6	C_7	C_8
Br	36.7	41.1	46.1	50.8	55.8	152.2	157.4	161.1	164.0	170.8
Cl	33.5	38.2	42.8	47.7	52.4	152.0	154.5	159.9	161.7	166.1
Δ	3.2	2.9	3.3	3.1	3.4	0.0	2.9	0.2	2.3	3.7

Table 4.5. Comparison of the vaporization enthalpies$\Delta_l^g H_m^0$ (298 K)/ kJ.mol^{-1}, for pyridinium and based ionic liquids.

	[C_nPy][halide]				
	C_4	C_5	C_6	C_7	C_8
Br	173.8	176.1	181.2	186.1	191.8
Cl	169.7	173.6	178.0	182.9	187.5
Δ	4.1	2.5	3.2	3.2	4.3

As it follows from Tables 4.4 and 4.5, the differences for the molecular liquids $\Delta_l^g H_m^0$ (C_nBr) - $\Delta_l^g H_m^0$ (C_nCl) are at the average level of about 3 kJ·mol^{-1}. For the ionic liquids the differences between [Cl] and [Br] also showed similar spread close to the average level of 3-4 kJ·mol^{-1}. Somewhat large spread of the differences for ILs in comparison to the molecular compounds is quite explainable taking into account the uncertainties of ±1-3 kJ·mol^{-1} typical for the DSC measured reaction enthalpies and uncertainties in the QC calculations (see Table 3.1).

The linear chain length dependence for the series with asymmetric imidazolium cation [$C_n$mim][Br] in Fig. 4.3 shows the linear shape in agreement with linear trends for pyridinium and pyrrolidinium cations. The following question arises, whether such linear trend is also valid for the symmetrical imidazolium cations [$C_nC_n$im]? Using the DSC and QC methods we derived vaporization enthalpies for ILs with the symmetric cation [$C_nC_n$im][Hal] (see Chapter 3). The results are presented in the Table 4.6 and in the Figure 4.5.

Table 4.6 Comparison of $\Delta_l^g H_m^0$ in kJ·mol^{-1} of [$C_n$mim][Br], [$C_mC_m$im][I] and [$C_mC_m$im][Br] at 298 K

n	[$C_n$mim][Br] [58]	[$C_mC_m$im][Br]	[$C_mC_m$im][I]
4	152.2		
5	157.4		
6	161.1		
7	164.0		
8	170.8	149.7	154.7
10		161.4	161.5
16		185.3	186.0

m=0.5 n

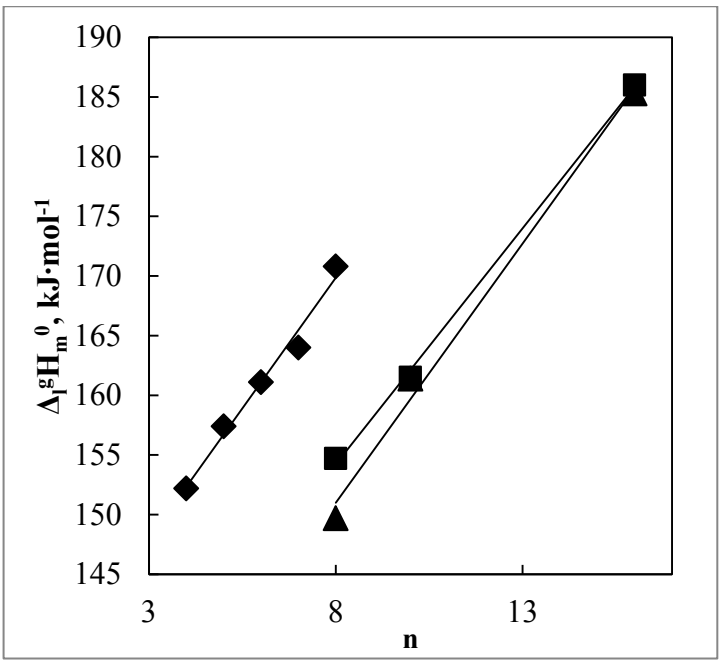

Figure 4.5 Comparison of the enthalpies of vaporization of [$C_n$mim][Br] [58] (♦), [$C_mC_m$im][I] (■) and [$C_mC_m$im][Br] (▲) at 298 K. (m= 0.5n)

As it follows, the Figure 4.5 ILs with the symmetric cations show the same trend in comparison to the asymmetric [$C_n$mim][Hal] series. The dependence of vaporization enthalpy on the total number of C-atoms in alkyl chain is expressed by the following equations:

$$[C_nC_n\text{im}][\text{Br}]: \ \Delta_l^g H_m^0 \ (298\ \text{K})/\ \text{kJ·mol}^{-1} = 116.3 + 4.3\ n{\cdot}2 \quad (r= 0.993) \qquad (4.8)$$

$$[C_nC_n\text{im}][\text{I}]: \quad \Delta_l^g H_m^0 \ (298\ \text{K})/\ \text{kJ·mol}^{-1} = 122.6 + 4.0\ n{\cdot}2 \quad (r= 0.998) \qquad (4.9)$$

The slope of the eqs 4.8 and 4.9 was close to the generally common for ILs value of 4 kJ·mol^{-1}. Thus, it seems to be reasonable to conclude that symmetry or asymmetry of the alkyl chain attached to the cation is not of importance. However this conclusion disagrees with the recent study of the symmetric series [$C_nC_n$im][NTf_2] reported by Rocha [65] (see Figure 4.6).

In our opinion the trend for the symmetric series [$C_nC_n$im][NTf_2] reported by Rocha [65] should be validated using other experimental techniques.

As we already discussed in Chapter 3 the methylation of the 2nd position of the imidazolium cation switching of the hydrogen networking of the liquid phase. In what extend this mutilation could be important for vaporization enthalpies of ILs having this structure? On Figure 4.7 vaporization enthalpies of [$C_n$mim][Br] with [$C_n$mmim][Br] and [$C_n$mmim][I] are compared. The dependence of vaporization enthalpy on the total number of C-atoms in the alkyl chain is expressed by the following equations:

[$C_n$mmim][Br]: $\Delta_l^g H_m^0$ (298 K)/ kJ·mol^{-1} = 133.5 + 4.7 n (r= 0.99) (4.10)

[$C_n$mmim][I]: $\Delta_l^g H_m^0$ (298 K)/ kJ·mol^{-1} = 139.5 + 4.7 n (r= 0.99) (4.11)

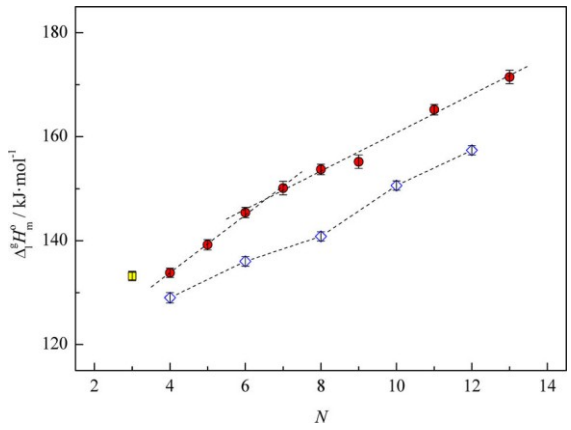

Figure 4.6 Comparison of the enthalpies of vaporization $\Delta_l^g H_m^0$ (298 K) of [$C_n$mim][NTf_2] (red dots) and [$C_nC_n$im][NTf_2] (blue diamods) reported by Rocha [65] at 298 K.

The slope of the eqs 4.10 and 4.11 was close to the generally common for ILs value of 4 kJ·mol^{-1} but it was also definitely about 0.7 kJ·mol^{-1} larger. Thus, it seems to be reasonable to conclude that methylation of the 2nd position on the imidazolium ring also reflects on the level of the vaporization enthalpy.

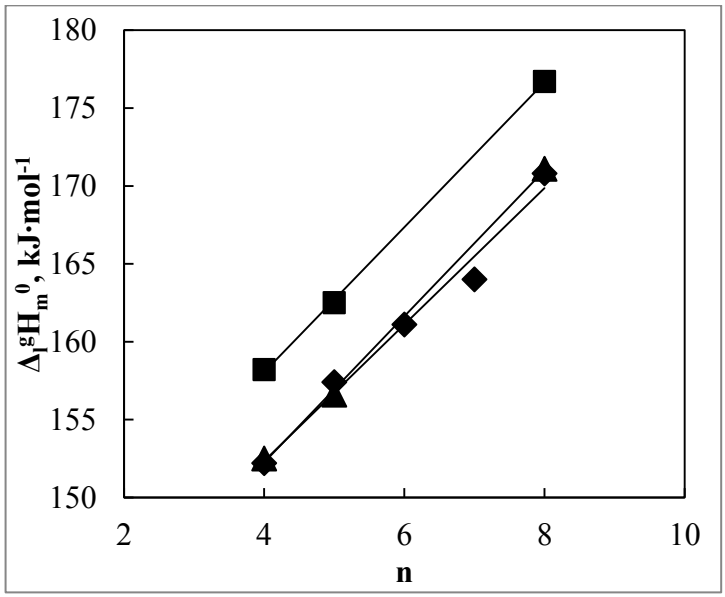

Figure 4.7 The comparison of the enthalpies of vaporization of [$C_n$mim][Br] (♦), [$C_n$mmim][I] (■) and [$C_n$mmim][Br] (▲) at 298 K.

Group-additivity procedures for prediction of thermodynamic properties of *molecular liquids* are well established [16], [78]. In this work we showed that the enthalpies of vaporization of *ionic liquids* also obey the general additivity rules. This knowledge is simplifying reliable predictions for ILs, provided that a general transfer of the group contributions established for the molecular compounds to the *ionic liquids* is valid. The simplest form of general additivity, the correlation of enthalpy of vaporization with the number of C-atoms, is reliably established for ILs with different anions and cations. This correlation in the series of homologues additionally serves as a valuable test to check the internal consistency of the experimental results. It has turned out, that the anion dependence in ILs was significantly more complex in comparison to the alkyl chain length dependence. The anion dependence of vaporization enthalpy is discussed in the Chapter 4.2

4.2 Anion dependence of vaporization enthalpy $\Delta_l^g H_m^0$ of ILs

To study of the influence of the anion on the vaporization enthalpy of ILs we measured and collected from the literature the data for ILs with the same cation $[C_2mim]^+$ but with different anions. Vaporization enthalpies of $[C_2mim][X]$ have been measured using the QCM technique. Enthalpies of vaporization $\Delta_l^g H_m^0$ (T_{av}) obtained at the average temperatures T_{av} (Table 4.7) were preliminary adjusted to the reference temperature T = 298 K using the value $\Delta_l^g C_{p\,m}^0$= - 100 J·K^{-1}·mol^{-1}, because it was not possible to apply neither of the three methods described in this work, due to the lack of the input experimental data. Our experimental results on $\Delta_l^g H_m^0$(298K) together with some data available from the literature are collected in Table 4.7

Table 4.7 the Vaporization enthalpies, $\Delta_l^g H_m^0$, and physico-chemical properties of the $[C_2mim][X]$

Substance	Method	T_{av} / K	$\Delta_l^g H_m^0$ (T_{av}) kJ·mol^{-1}	$\Delta_l^g H_m^0$ 298 K kJ·mol^{-1}	ε	E_T^N	α^-
$[C_2mim][NTf_2]$	QCM	378	118.6 ± 1.0	121.8	12.0	0.657	9.49
$[C_2mim][C_2SO_4]$	QCM	422	143.5 ± 1.0	155.9	28.0		5.67
$[C_2mim][C_2SO_4]$	LOSMS	454.0	137.0±3.0[25]	152.6	28.0		5.67
$[C_2mim][C_1SO_4]$	QCM	442	135.2 ± 1.0	149.6			4.43
$[C_2mim][SCN]$	QCM	413.2	142.2 ± 1.0	153.7	11.7		
$[C_2mim][SCN]$	LOSMS	490.0	131.0±2.0[24]	150.2	11.7		
$[C_2mim][C_4SO_4]$	QCM	437.9	144.4 ± 1.0	158.4	30.0		
$[C_2mim][C_8SO_4]$	QCM	447.8	157.0 ± 1.0	172.0			12.93
$[C_2mim][CF_3CO_2]$	QCM	384	120.7 ± 1.0	129.3		0.630	4.41
$[C_2mim][CF_3SO_3]$	QCM	412.8	126.4 ± 1.0	137.9	15.0	0.667	
$[C_2mim][(C_2H_5O)_2PO_2]$	QCM	392.9	136.6 ± 1.0	146.1	16.9		7.84
$[C_2mim][PF_6]$	QCM	435.2	129.9 ± 1.0	143.6	12.0	0.676	1.44
$[C_2mim][BF_4]$	QCM	431.6	122.2 ± 1.0	135.5	13.0	0.710	1.26
$[C_2mim][B(CN)_4]$	QCM	403.9	125.0 ± 2.2	135.6			
$[C_2mim][C(CN)_3]$	QCM	423.2	126.0 ± 1.0	138.5			
$[C_2mim][C(CN)_3]$	CC	298.15	138.8 ± 7.0	138.8			

[C_2mim][FAP]	QCM	373.4	118.3 ± 1.0	125.8			
[C_2mim][NO_3]	CC			163.7[16]		0.642	12.15
[C_2mim][$N(CN)_2$]	CC			156.4[16]	11.0	0.648	4.95
[C_2mim][beti]	TGA	503.0	115.3±1.8[19]	135.8			12.90
[C_2mim][TOS]	QCM	460.5	149.8 ± 1.0	166.1			

Table 4.7 cont.

	B^-	ρ	V_{molar}	M_w	σ	P_{ch}	δ_H	ν_σ, cm^{-1}
[C_2mim][NTf_2]	275.1	1519.2	2.58	391.3	36.1	631	8.56	84.8
[C_2mim][C_2SO_4]	348.1	1237.4	1.91	236.3	46.9	500		106.4
[C_2mim][C_2SO_4]	348.1	1237.4	1.91	236.3	46.9	500		106.4
[C_2mim][C_1SO_4]	347.8	1286.0	1.73	222.3	62.9	487	9.21	105.3
[C_2mim][SCN]				169.3	57.8		9.15	116.3
[C_2mim][SCN]				169.3	57.8			116.3
[C_2mim][C_4SO_4]		1176.2	2.25	264.3	40.8	568		105.1
[C_2mim][C_8SO_4]	332.9	1095.7	2.93	320.5		684	9.32	105.6
[C_2mim][CF_3CO_2]	338.0			224.2			9.74	107.5
[C_2mim][CF_3SO_3]		1383.6	1.88	260.2	44.4	486	8.91	89.5
[C_2mim][$(C_2H_5O)_2PO_2$]	394.5			264.3				108.0
[C_2mim][PF_6]	427.3	1468.3	1.74	256.1		455	8.38	
[C_2mim][BF_4]	513.5	1279.8	1.55	198.0	53.9	419	8.64	102.0
[C_2mim][$B(CN)_4$]				226.1	47.8			84.2
[C_2mim][$C(CN)_3$]				201.2				97.5
[C_2mim][$C(CN)_3$]				201.2				72.4
[C_2mim][FAP]				556.2	34.8		7.45	72.4
[C_2mim][NO_3]	330.3			173.2			9.57	118.9
[C_2mim][$N(CN)_2$]	332.9	1108.9	1.60	177.2	42.6	408	8.96	113.9
[C_2mim][beti]	244.8	1593.2	3.08	491.3				
[C_2mim][TOS]		1210.0	2.33	282.4				100.3

Simple structure-property correlations in the [$C_n$mim][NTf_2] family described above have prompted our efforts to find other correlations for the new vaporization enthalpies data set where the cation [C_2mim] remains constant with 17 most common counteranions (Table 4.7).

In order to reveal any possible anion dependencies in the vaporization enthalpies we have reviewed a number of physico-chemical parameters which are generally relevant to the polarity of ILs or properties which could reflect the intensity of the cation-anion interactions.

Static dielectric constant

The static relative dielectric permittivity ε of a solvent (or "static dielectric constant"), is one of key properties for understanding of solvation processes [79], [80]. However, the anion variation has shown not very pronounced effects on ε and some results were even counterintuitive [79]. For example, the dielectric constants of ILs with symmetrical anions without permanent electric dipole moments, such as [PF_6] or [BF_4], showed the ε values of the order of ε = 12 to 13 [79] and it is surprising that dielectric constants of ILs with dipolar anions, such as [NTf_2], thiocyanate, or trifluoromethanesulfonate, are of the same order of magnitude (see Table 4.7) [79]. Vaporization enthalpy dependence on the static dielectric constant ε meets the general trend: low enthalpies of

vaporization correspond to low ε–values and higher $\Delta_l^g H_m^0$ values can be referred to higher dielectric constants (see Fig. 4.8). However, the ILs with [N(CN)$_2$], [SCN], and [PF$_6$] do not meet this expectation.

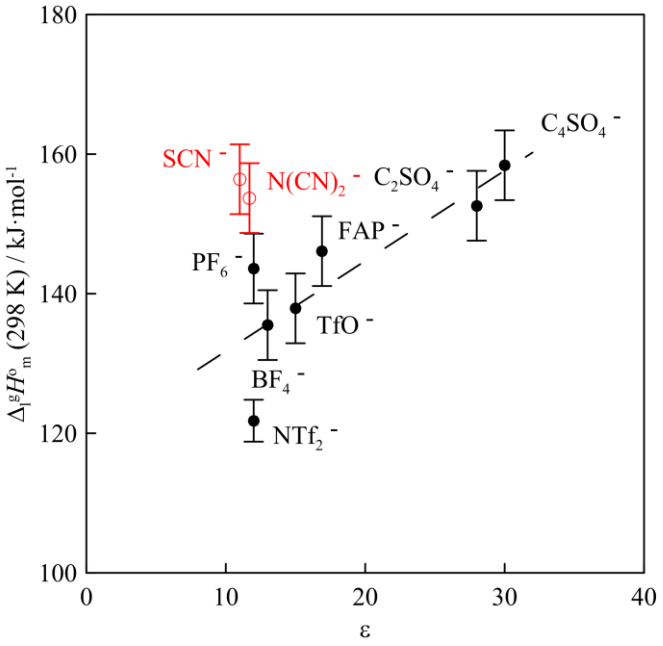

Figure 4.8 Correlation of the enthalpy of vaporization with static dielectric constant

E_T^N and Kamlet-Taft parameters

The polarity of ionic ILs is often assessed with an empirical scale of solvent polarity measured with solvatochromic dyes and expressed in terms of E_T^N and Kamlet-Taft parameters (dipolarity/polarizability (π*), hydrogen bond donor acidity (α), and hydrogen bond basicity (β) [81]. Significant variations of polarity were observed on changing the anion and cation combination [81]–[83]. Unfortunately, only few experimental values of E_T^N and Kamlet-Taft parameters were available for [C$_2$mim][Anion] ionic liquids. From this restricted data set we were not able to derive any reasonable trend for vaporization enthalpy dependence on these parameters (see Fig. 4.9).

Molecular polarisabilities

Molecular polarisabilities and special Lewis acidity and basicity descriptors could be also used for correlation with the vaporization enthalpy. We used the polarisability of the cation, α^+, the polarisability of the anion, α^-, the hydrogen bond acidity of cation, A^+, and the Lewis basicity of anion, B^-. These parameters were reported recently for the twelve ILs listed in Table 4.7 [84]. Parameters for the ionic liquid cations and anions of [C$_2$mim][Anion] were calculated at the AM1 semi-empirical level of theory [84].

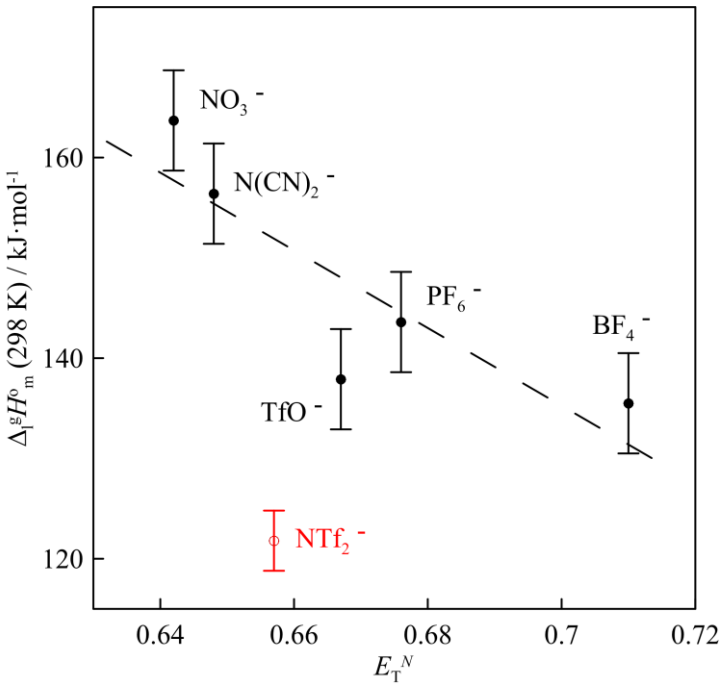

Figure 4.9 Correlation of the enthalpy of vaporization with normalized solvent polarity E_T^N.

Most of the [C_2mim] based vaporization enthalpies showed the distinct trend (see Fig. 4.10): low enthalpies of vaporization corresponded to low α-–values and higher $\Delta_l^g H_m^0$values are referred to higher α-values (see Fig. 4.10), except for apparent outliers - ILs with [NTf_2], [FAP], and [beti]. The ILs with anions [$(C_2H_5O)_2PO_2$] and [CF_3SO_3] also slightly deviated from the general trend.

Volume-Based Thermodynamics.

Volume-Based Thermodynamics (VBT) is a scope of correlation methods that rely on volume to predict thermodynamic quantities. The formula-unit volume V_m is among the most accessible of physical quantities, as it can be obtained through diffraction techniques, from density, or by a variety of estimation methods [85]. Molar volume V_{molar} is related to V_m through the equation $V_m = V_{molar}$ /Na, where Na is the Avogadro constant. In this work we looked for the correlation of vaporization enthalpies with the molar volume V_{molar}. Already the experimental densities of the [C_2mim][Anion] ionic liquids showed acceptable straight-line correlation with the vaporization enthalpies (see Fig. 4.11)

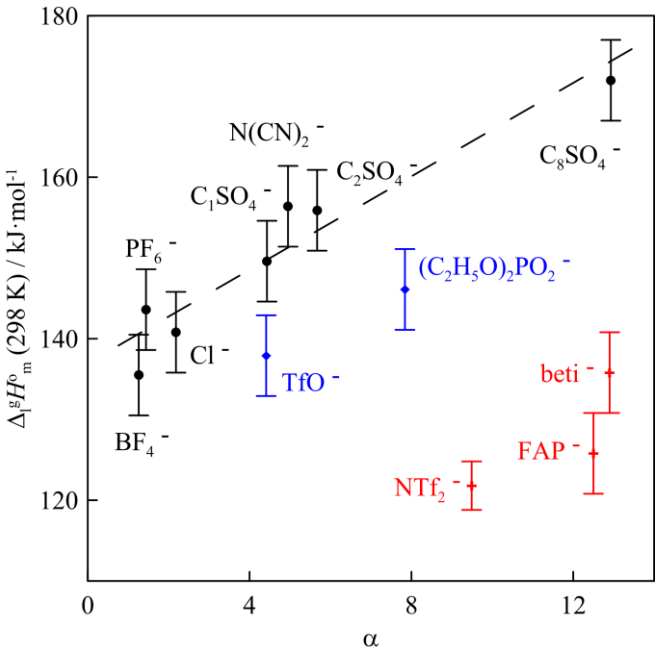

Figure 4.10 Correlation of the enthalpy of vaporization with anion polarisability α^-.

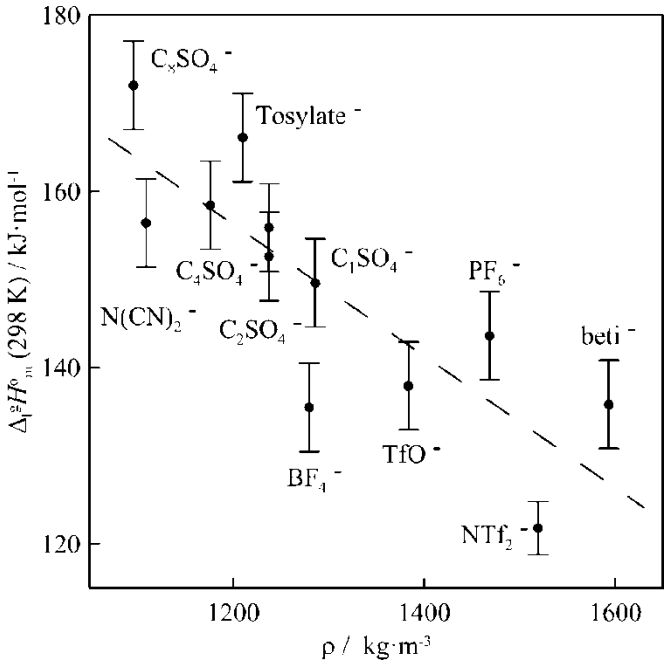

Figure 4.11 Correlation of the enthalpy of vaporization with the density

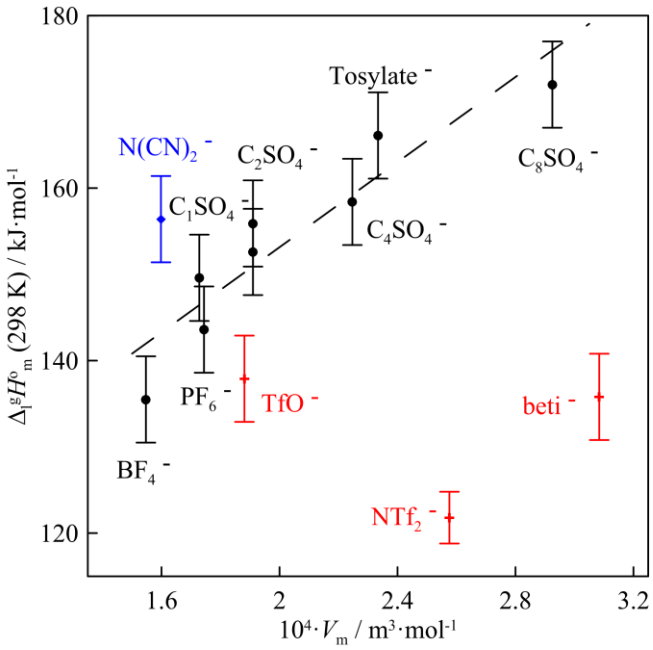

Figure 4.12 Correlation of the enthalpy of vaporization with the molar volume

However the plot of the vaporization enthalpies vs. the molar volume V_{molar} showed more sophisticated relationships (see Fig. 4.12)

Ionic liquids with fluorinated anions [beti], [NTf_2], and somewhat less [CF_3SO_3] were drastically lower in comparison to the general trend. At the same time the IL with [$N(CN)_2$] was noticeably above the trend. Very similar behaviour of the ILs with fluorinated anions [beti], [NTf_2], and additionally for [FAP] was apparent by plotting vaporization enthalpies vs. molecular mass (see Fig. 4.13). This made it conspicuous, that only evasive increasing trend was observed on molar mass dependence of vaporization enthalpies of ionic liquids (Fig. 4.13) in contrast to the molecular liquids, where linear relationships were more profound.

Surface tension and parachor

The surface tension is directly related to the cohesive energy and vaporization enthalpy [37]. We collected the available literature data for surface tension, σ, at 298 K for 13 ionic liquids (see Table 4.7) and correlated vaporization enthalpies with the σ -values (Fig. 4.14). Surprisingly, only very vague trend was observed.

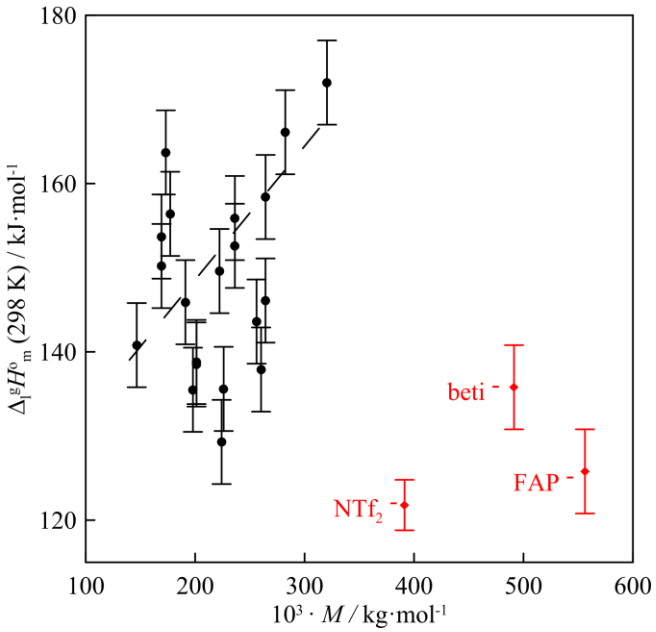

Figure 4.13 Correlation of the enthalpy of vaporization with the molar mass.

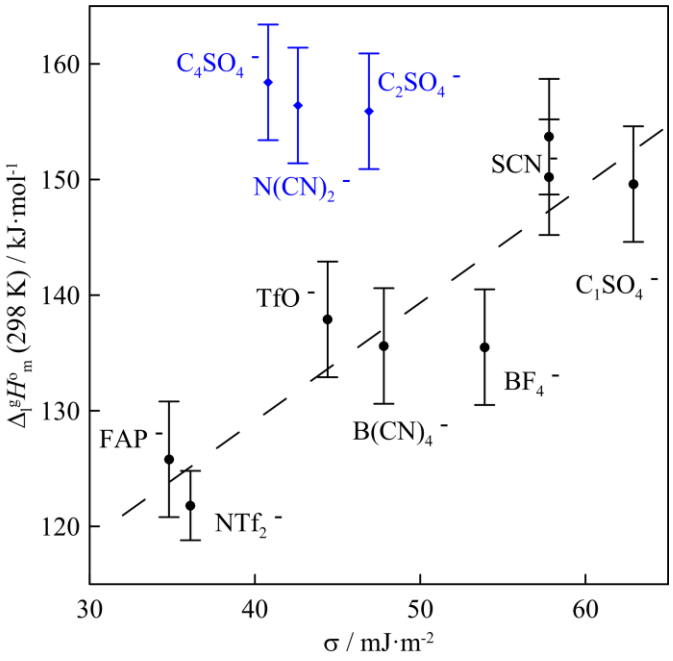

Figure 4.14 Correlation of the enthalpy of vaporization with the surface tension.

It was apparent that all ILs with the alkylsulfate anions $[C_2SO_4]^-$, $[C_4SO_4]^-$, as well as with $[N(CN)_2]^-$ were significantly above the general trend. One of the possible reasons for the pure correlation observed is that the experimental values on σ derived by different methods and different authors varied significantly [86]. The correlation of vaporization enthalpy with the surface tension could be better provided that validated σ - values are used for comparison.

In order to improve correlation and to take more sufficient details into account we additionally correlated vaporization enthalpies with the parachor.

Parachor [87] expresses (see eq. 2.17) the temperature-independent relationship between molecular weight, M_w, density, ρ, and surface tension, σ

We plotted the vaporization enthalpy vs. parachor in Fig. 4.15 and except for $[N(CN)_2]^-$, $[NTf_2]^-$ and $[CF_3SO_3]^-$ an acceptable linear correlation was obtained.

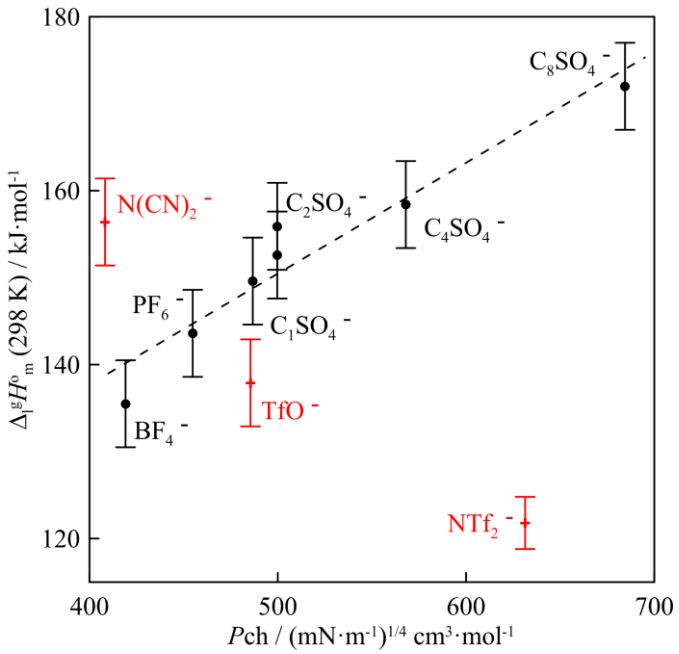

Figure 4.15 Correlation of the enthalpy of vaporization with the parachor

^{1}H NMR shifts.

The anion-dependent differential ^{1}H NMR shifts were proven to be a direct measure of the strength of hydrogen bonding in imidazolium-based ILs [88]–[90].

While ^{1}H NMR shifts were found to indicate very specifically the strongest hydrogen-bond interaction between the hydrogen attached to the C_2 position and the anion, this shift could correlate with the vaporization processes in ionic liquids.

From the ^{1}H NMR shifts (δ_H in ppm) data reported for the eleven [C_2mim][Anion] ionic liquids more or less straight dependence of the vaporization enthalpy as a function of the δ_H was observed (see Fig. 4.16) Mostly striking in this trend are the $[CF_3SO_3]$ and $[NTf_2]$ anions. In spite of this fact the anion-dependent differential 1H NMR shifts could be considered not only as the direct measure of the strength of hydrogen bonding in imidazolium-based ILs, but also could be qualitatively used for quick appraisal at least of the level of the vaporization enthalpy from the experimentally measured ^{1}H NMR shifts.

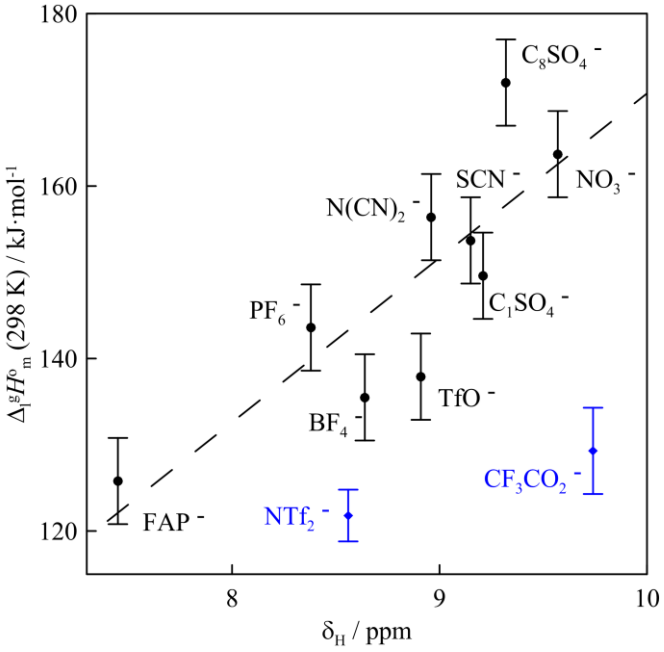

Figure 4.16 Correlation of the enthalpy of vaporization with the ^{1}H NMR shifts

FIR low frequency vibrational bans.

In our previous work we systematically measured the low frequency vibrational spectra of imidazolium based ionic liquids in the range between 30 and 300 cm^{-1} by using far-infrared spectroscopy [91]–[93]. It has turned out that the contributions below 150 cm^{-1} can be definitely assigned to the bending and stretching vibrational modes responsible for the intermolecular interactions between cations and anions. As a consequence, these infrared vibrational modes seem not only to be a reliable measure of the cation–anion interaction strength but they can serve for predicting enthalpies of vaporization of ionic liquids [94].

In addition to results reported in [94] we measured the far infrared (FIR) spectra of 11 ionic liquids including the same 1-ethyl-3-methylimidazolium cation (C_2mim) but various anions . The measured spectra are presented in Figure 4.17. The maximum values of the vibrational bands responsible for the intermolecular interactions are collected in Table 4.7. The visible maxima in the measured spectra mainly coincide with those obtained from the deconvolution procedure into Voigt functions (see Supporting Information).

The experimental enthalpies of vaporization of (C_2mim) imidazolium-based ionic liquids (from Table 4.8) are plotted versus wavenumbers of the vibrational bands (Figure 4.18) obtained from the deconvolution procedure (Figure 4.17).

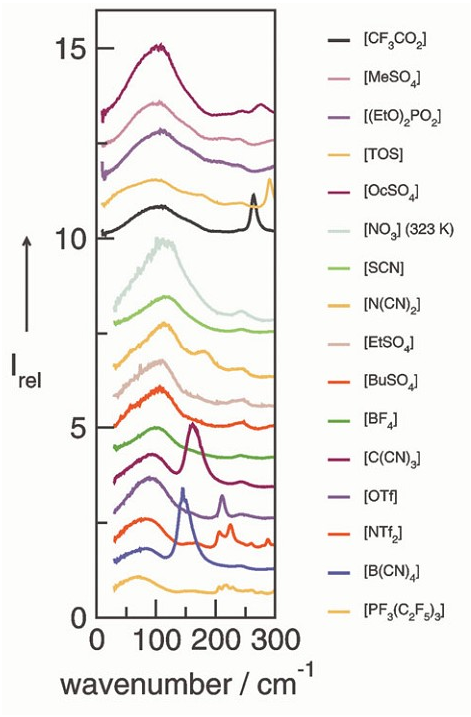

Figure 4.17 Low-frequency vibrational FIR spectra of ionic liquids

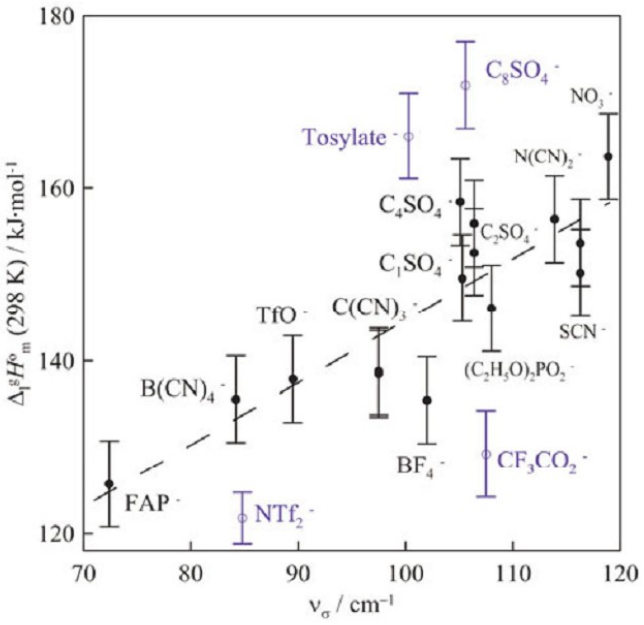

Figure 4.18 Experimental values for maxima of the low frequency vibrational bands from FIR vs experimental enthalpies of vaporization taken from Table 4.8.

Vaporization enthalpies, $\Delta_l^g H_m^0$ (298 K), showed linear dependency on the intermolecular vibrational frequencies ν_σ. The plot of $\Delta_l^g H_m^0$ (298.15 K) against the ν_σ in the imidazolium based

ILs is presented in Figure 4.18. The dependence of vaporization enthalpy on the ν_σ is described by the following equation:

$$\Delta_l^g H_m^0 \text{ (298.15 K)/ kJ·mol}^{-1} = 72.9 + 0.72\ \nu_\sigma \quad (R^2 = 0.75) \qquad (4.12)$$

from which enthalpy of vaporization $\Delta_l^g H_m^0$ (298 K) of other representatives of this series can be calculated, provided that the maximum value ν_σ is measured by FIR spectroscopy. The correlation of enthalpies of vaporization with the ν_σ -values in the series of homologues imidazolium based ILs is also a valuable test to check the internal consistency of the experimental results.

4.3 Group-additivity methods for prediction of vaporization enthalpies $\Delta_l^g H_m^0$

In spite of the success of the new experimental methods towards reliable experimental determination of vaporization enthalpies of ILs, the development of an empirical or semi-empirical method that yields a reasonable approximation of the enthalpies of vaporization, $\Delta_l^g H_m^0$, for the new ionic liquids is still necessary.

Predictive group contribution models were developed for various thermophysical properties, such as density, viscosity, surface tension, speed of sound, refractive index, heat capacity, electrical conductivity, thermal conductivity, isobaric expansivity, and isothermal compressibility, of various families of ionic liquids [87], [95], [96].

In ref [97] a simple approach using the molecular volume and the gas phase enthalpic correction to the total energy for the vaporization enthalpy is reported. Group additivity (GA) methods to make quantitative predictions of the physical properties successfully were also tested and reported [16]. For example, scarce experimental results on enthalpies of vaporization and enthalpies of formation of imidazolium based ionic liquids with the cation [C_nMIM] (where n= 2 and 4) and anions [$N(CN)_2$], [NO_3], [NTf_2], [Cl], [BF_4] and [PF_6] were collected and checked for internal consistency using a group additivity procedure. It was established that the thermodynamic properties of these ionic liquids obey the group additivity rules [16]. In this work we also established the linear dependence of the vaporization enthalpies on the chain length for a series of [$C_n$mim][NTf_2] and other ILs, as well as a constant additive contribution of about 4 kJ·mol for the CH_2 unity in the alkyl chain in the IL cation.

The assessment procedure according to the eq 4.3 for the vaporization enthalpy of an IL at 298 K with help of simple additive equation was reported in ref. [98]:

$$\Delta_l^g H_m^0\ (IL) = \Sigma(n_i \cdot \Delta H_i) + \Sigma(n_j \cdot \Delta H_j) \qquad (4.13)$$

where ΔH_i is the contribution of the *i*-th element; n_i is the number of elements of the *i*-th type in the ionic liquid; ΔH_j is the contribution of the *j*-th structural correction; n_j is the number of structural corrections of the *i*-th type in the ionic liquid. In this work we have developed more

detailed group-additivity procedure specific for predicting vaporization enthalpy of the alkyl imidazolium based ILs with the anions listed in Table 4.7 and the alkyl chain of an arbitrary length and structure. Indeed, any alkyl imidazolium based IL could be considered as the combination of the imidazolium cation and the alkyl chains attached to this cation (see Table 4.8 and Fig . 4.19).

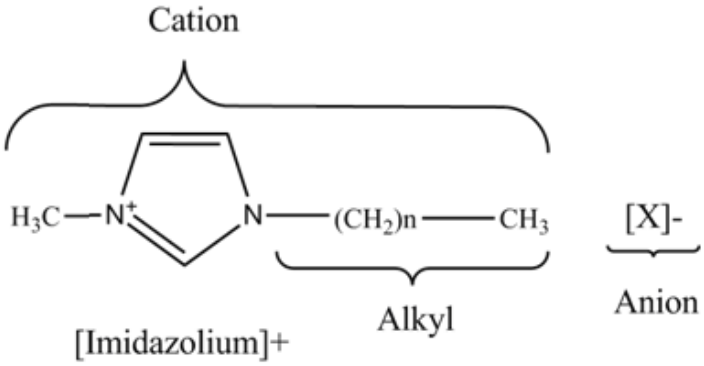

Figure 4.19 Additive calculations of vaporization enthalpies of imidazolium based ILs.

Table. 4.8. Additivity parameters for calculation of enthalpies of vaporization of ILs at 298 K (in kJ·mol^{-1}). [a] CH_3-(C) ≡ CH_3-(Imidazolium) ≡ CH_3-(SO_4). [b] CH_2-$(C)_2$ ≡ CH_2-(Imidazolium) ≡ CH_2-(SO_4). [c] Parameters were taken from ref. [99]

	Parameters
Alkane-chain	
CH_3-(C)	6.3[a,c]
CH_2-$(C)_2$	4.0[b]
CH-$(C)_3$	1.2[c]
C-$(C)_4$	-2.7[c]
Cation	
$[Imidazolium]^+$	78.5
Anions	
$[NTf_2]$	28.2
$[(SO_4)$-(C)]	52.7
[SCN]	64.8
$[CF_3CO_2]$	40.4
$[CF_3SO_2]$ or [OTf]	49.0
$[(C_2H_5O)_2PO_2]$	57.2
$[PF_6]$	54.7
$[BF_4]$	46.6
$[B(CN)_4]$	46.7
$[C(CN)_3]$	49.6
[FAP]	36.9
$[NO_3]$	74.8
$[N(CN)_2]$	67.5
[beti]	46.9
[TOS]	77.2

The additive parameters were derived by the least square treatment of the vaporization enthalpies collected Table 1 and the data set for $[C_nmim][NTf_2]$, reported recently [37]. These parameters are given in the Table 4.8. In spite of the fact that the additive parameters were derived from the limited data set of 26 ionic liquids (17 from this study and 9 from [37]), they are valid over a broad range of ILs containing the imidazolium cation and the anions studied in this work. Additionally to the ILs with the linear alkyl chains, vaporization enthalpies of ILs with the branched alkyl chains could be predicted with help of increments $CH-(C)_3$ and $C-(C)_4$ given in Table 4.8.

The same methodology could be easily adjusted for the prediction of vaporization enthalpies of any IL with the functional substituted (e.g. OH, CN, etc.) alkyl chain. In this case the appropriate additive parameters could be obtained from the molecular compounds of the similar structure.

4.4 Solution Enthalpies of ILs in Water.

4.4.1 Conductometric study of the diluted solution of ILs.

Enthalpies of formation of aqueous ions used in eq. 3.15 require the infinite dilution conditions for ions and it means that the ionic liquid has to be completely dissociated. This assumption is true for the classic salt in diluted solutions (e.g. NaCl). But for the ionic liquid a situation could be possible when the contact ion pair is solvated completely by water molecules but the ionic bond remains unbroken. We have not found in the literature clear answer, whether the ions of the IL dissociated or not. To clarify this issue, we studied the diluted water solutions of $[C_2mim][NTf_2]$ with help of conductometry. This IL is not very good soluble in water. Consequently, if $[C_2mim][NTf_2]$ exists in the solution as separated ions in the concentration range close to infinite dilution, so ILs with less hydrophobic ions (e.g. Cl^-, NO_3^-) should also do. For comparison we also studied the typical salts $[Na][NTf_2]$ and collected literature data for NaCl in the same conditions, in order to detect a possible aggregation of imidazolium based organic cations in the aqueous solution.

Prior to the experiment, samples of $[C_2mim][NTf_2]$ and $[Na][NTf_2]$ were carefully dried in vacuum at 373 K for 48 hours. The residual water content at the level of 70 ppm in samples for the conductometric studies was measured with Karl-Fischer titration method. Starting solutions of $[C_2mim][NTf_2]$ and $[Na][NTf_2]$ were prepared with the molality 0.01 - 0.02 $mol \cdot kg^{-1}$ using double distilled water. Solutions were studied at 298 K using 7-pole-cell conductivity sensor for probe systems von AMT Analysenmesstechnik GmbH conductometer. Initial solutions were stepwise diluted and the values of conductivity were measured down to the limit of the sensitivity of the device. Results of conductivity experiments are shown on the Figures 4.20 and 4.21. and listed in the SI Tables S8 and S9.

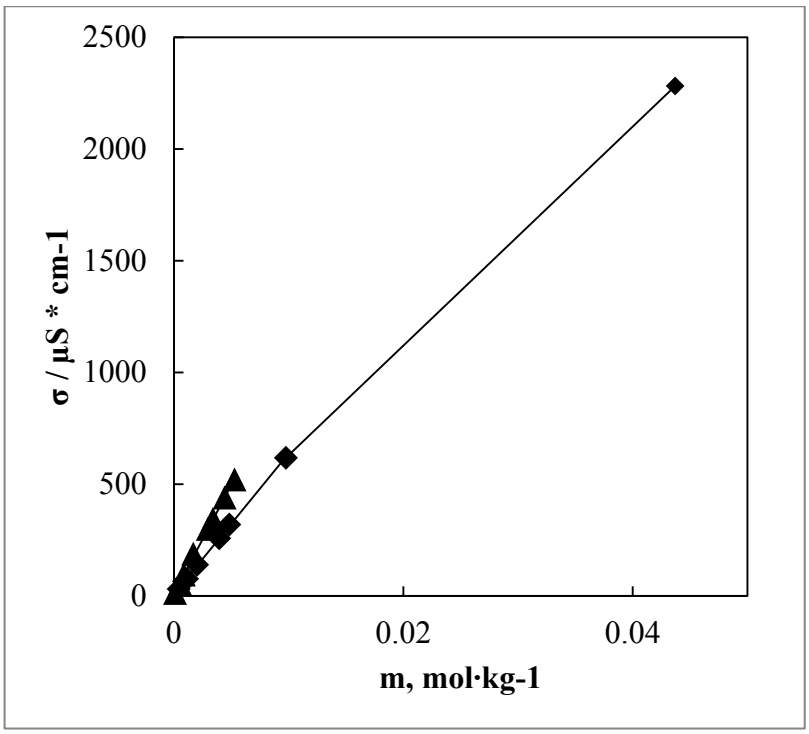

Figure 4.20 Conductivity dependence on solution molality of [EMIM][NTf_2] and Na[NTf_2] (marked as ♦ and ▲ respectively).

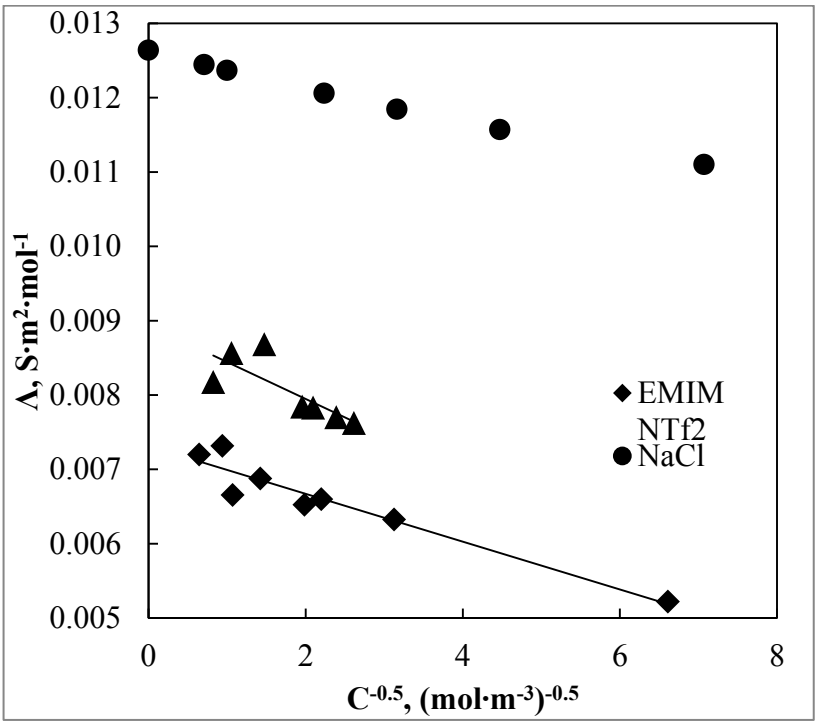

Figure 4.21 Comparison of limiting molar conductivity of [EMIM][NTf_2] (♦) and Na[NTf_2] (▲) with behavior of NaCl (●) ([100])

Figures 4.20 and 4.21 shows almost linear dependence of [C_2mim][NTf_2] and [Na][NTf_2] solutions in concentration range up to 0.05 mol·kg^{-1}. Moreover, the linear dependence of the

limiting molar conductivity on concentration has the same slope in comparison with the NaCl. This indicates that [C_2mim][NTf_2] and [Na][NTf_2] apparently obey the Kohlrausch's Law

$$\Lambda_m = \Lambda_m^0 - KC^{0.5} \tag{4.14}$$

where: Λ_m – molar conductivity, $\Lambda_m{}^0$- limiting molar conductivity, C – molar concentration, K – empirical constant. Such a behavior proves that ILs at infinite dilution conditions exist as independent ions solvated by water molecules similar to the typical salts. Thus solution enthalpies of ILs measured in this work refer to the process of complete separation of IL ions in water, making possible the application of eq 3.15

4.4.2 Solution enthalpies of ILs, experimental data

In this work we measured solution enthalpies, $\Delta_{sol}H_m^0$, at 298 K in water of imidazolium, pyridinium and pyrrolidinium based ILs. Additionally, we collected calorimetric $\Delta_{sol}H_m^0$ -values of ILs available in the literature. Moreover, there were a lot of literature data on the solubility studies of ILs in water. We also derived the solution enthalpies from the primary data on the temperature dependencies of solubility in water (see Table 4.9) using eqs 4.15. and 4.16.

$$\frac{\Delta_{sol}H_m^0}{RT^2} = \left(\frac{\partial \ln x_{IL}}{\partial T}\right)_p \tag{4.15}$$

where, x_{IL}- the mole fraction of saturated IL solution in water, and experimental x_{IL} data is smoothed using the next formula :

$$ln\, x_{IL} = C + \frac{D}{T} + E \cdot ln\, T \tag{4.16}$$

where: C, D, E – the adjusted parameters.

Solubility measurements were made by different techniques (UV-VIS [101], Karl-Fischer titration [102], cloud point [102]). In comparison to the solution enthalpies measured calorimetrically, values derived from eq. 4.15 should be considered as less reliable. Collection of solution enthalpies measured in this work together with results available from the literature is listed in the Table 4.10. In order to indicate the initial state of ILs in the solution experiments, melting temperatures T_m and enthalpies of fusion $\Delta_{cr}^{l}H_m^0$ are also collected in this table.

Table 4.9 Compilation of the solution enthalpies of ILs (in kJ·mol^{-1})

IL	$T_m/\Delta_{cr}^{l}H_m^0$	T-range	$\Delta_{sol}H_m^0$	Method
Imidazolium Based				
[C_2mim][BF_4] (l)			17.3 ± 0.3 [56]	SolCal (iso)
			13.5 (11^d) [103]	SolCal (iso)
			18.2 ± 0.2	SolCal (iso)
[C_3mim][BF_4](l)			15.1 (12^d) [104]	

$[C_4mim][BF_4](l)$	-		15.7 [105]	SolCal (iso)
			26.8± 0.3 (17^d) [106]	SolCal (iso)
			13.52 (11^d) [103]	SolCal (iso)
			15.0± 0.2 [107]	SolCal (adiab)
			16.64± 0.06 [108]	SolCal (iso)
			15.8 ± 0.3 [56]	SolCal (iso)
			15.7 ± 0.3 [109]	SolCal (iso)
			17.2 ± 0.6	SolCal (iso)
$[C_5mim][BF_4](l)$			16.5 (13^d) [104]	
$[C_6mim][BF_4](l)$		278-324	16.2/ 15.9 ± 1.8^b [110]	UV-VIS
$[C_8mim][BF_4](l)$	-		19.0 ± 0.2[107]	SolCal (adiab)
			17.7 ± 2.0	SolCal (iso)
$[C_2mim][PF_6]$ (s)	332.8/17.9 [111]			
		308-313	45.1 [102]	cloud point/KF
			46.0 ± 0.7	SolCal (iso)
$[C_3mim][PF_6]$ (s)	311.2/15.0 [112]			
		288-303	32.8±0.3 [112]	UV-VIS
$[C_3mim][PF_6]$ (l)		303-318	9.3 ± 1.5 [112]	UV-VIS
$[C_4mim][PF_6]$ (l)	-	303-323	16 [102]	
		278-353	15.2 ± 1.0^b [113]	cloud point
		288-321	12.6 ± 1.5 [101]	UV-VIS
		278-323	15.00 / 14.5 ± 1.2^b [110]	UV-VIS
			19.9 ± 0.5	SolCal (iso)
$[C_6mim][PF_6]$ (l)		278-354	14.6 ± 1.0^b [113]	cloud point
		288-322	12.7 ± 1.5 [101]	UV-VIS
		278-325	13.1 / 13.1 ± 1^b [110]	UV-VIS
$[C_8mim][PF_6]$ (l)		278-355	15.5 ± 1.0^b [113]	cloud point
		288-323	12.6 ± 1.5[101]	UV-VIS
$[C_2mim][Cl]$ (s)	360.7/15.5 [114]			
			-8.97 (-5^d) [103]	SolCal (iso)
			-19.15 (-5^d) [115]	SolCal (iso)
			-16.5 ± 2.0	SolCal (iso)
$[C_3mim][Cl]$ (s)	325.2/10.1 [116]			
$[C_4mim][Cl]$ (s)	341.9/21.7 [116]			
	342.0/14.1 [117]			
			-16.03 (-5^d) [72]	SolCal (iso)
			1.7 ± 0.2(l)	SolCal (iso)
$[C_5mim][Cl]$ (s)				
			-17.85(-6^d) [118]	SolCal (iso)
$[C_6mim][Cl]$ (s)				
			-17.3±0.2 (-9^d) [119]	SolCal (iso)
$[C_2mim][Br]$ (s)	349.9/18.3[120]			
	349.5/15.7 [116]			
			11.0 ± 1.0	SolCal (iso)
$[C_3mim][Br]$ (s)	306.0/14.3 [116]			
$[C_4mim][Br]$ (s)	351.4/22.9 [120]			
	347.5/16.3 [116]			
	350.8/23.6 [121]			
			6.3 [105]	SolCal (iso)
			10.1 ± 0.9	SolCal (iso)

$[C_2mim][NO_3]$ (s)	311.8/19.5 [70]			
			17.1 ± 0.7(s)	SolCal (iso)
			2.0 ± 1.0(l)	SolCal (iso)
$[C_4mim][NO_3]$ (s)	309.2/18.0 [57]			
			0.2 ± 0.2(l)	SolCal (iso)
$[C_2mim][SCN]$ (l)			7.8 ± 0.1	SolCal (iso)
$[C_4mim][SCN]$ (l)			7.7 ± 0.1	SolCal (iso)
$[C_2mim][C_1SO_4]$ (l)			-14.2 ± 1.0	SolCal (iso)
$[C_4mim][C_1SO_4]$ (l)			-11.0 ± 0.7	SolCal (iso)
$[C_2mim][C_2SO_4]$ (l)			-14.4 ± 0.6 (-9[d]) [122]	SolCal (iso)
			-11.0 ± 0.1 [123]	SolCal (iso)
			-10.8 ± 0.2	SolCal (iso)
$[C_2mim][C_4SO_4]$ (l)			-11.6 ± 0.3	SolCal (iso)
$[C_2mim][C_8SO_4]$ (l)			-6.1 ± 0.2	SolCal (iso)
$[C_2mim][CF_3SO_3]$ (l)			2.6 ± 0.2	SolCal (iso)
$[C_4mim][CF_3SO_3]$ (l)			1.7 ± 0.1	SolCal (iso)
$[C_2mim][N(CN)_2]$ (l)			3.3 ± 0.3	SolCal (iso)
$[C_2mim][C(CN)_3]$ (l)			12.5 ± 0.4	SolCal (iso)
$[C_4mim][C(CN)_3]$ (l)		288-320	10.1 ± 1.5[101]	UV-VIS
			12.0 ± 0.7	SolCal (iso)
$[C_4C_4im][BF4]$ (l)			21.5 ± 0.5	SolCal (iso)
Pyrrolidinium Based				
$[C_{41}Pyrr][N(CN)_2]$ (l)			-1.3 ± 0.7	SolCal (iso)
Pyridinium Based				
$[3Me\text{-}C_4Py][N(CN)_2]$ (l)			-0.4 ± 0.2	SolCal (iso)
Tetraalkylammonium Based				
$[N_{1111}][BF_4]$(s)			43.1 ± 0.5	SolCal (iso)
$[N_{4444}][BF_4]$(s)			6.6 ± 0.5	SolCal (iso)

SolCal (iso) – isoperibol solution calorimetry; SolCal (adiab) – adiabatic solution calorimetry; UV-VIS - solubility determination by UV-VIS spectroscopy; cloud point – solubility determination using cloud point method; KF – solubility determination using Karl-Fischer titration; b -calculated based on initial solubility data; d - recalculated from initial solution calorimetry data;

The analysis of $\Delta_{sol}H_m^0$ listed in Table 4.9 indicates confusing problems with measurements on ILs in contrast to measurements on salts. It is well established that calorimetric solution studies on salt as a rule provide very accurate data with uncertainties of about ± 0.1 kJ·mol^{-1} . The values reported for ILs by different authors for the same IL are different in the best case ± 2 kJ·mol^{-1} but sometimes also by ± 10 kJ·mol^{-1}. This spread of values shows systematic errors in experimental measurements. The solution enthalpy measurement for ionic liquids in comparison to typical salts exhibits following challenges:

- slow solution kinetics for some ILs
- high hygroscopycity of ILs
- phase transitions
- possible hydrolysis process in water
- volatile and non-volatile impurities in the ILs

These complications should be taken into account by choice of the experimental method. For example, ILs with long alkyl chain length in the cation and long solution time (more than 20 minutes) are hardly suitable for studies with the isoperibol solution calorimeter. Highly hygroscopic ILs with $[Br]^-$, $[Cl]^-$, and $[NO_3]^-$ anions should be dried very carefully and handled in the dry atmosphere in a glove box. Moreover, these ILs (especially with $[Cl]^-$ anion) tend to undercool readily, or form glasses instead of crystalline structure. For that reason for ILs with these anions we measured the solution enthalpies of undercooled liquid state, as the most reliable value. For the ILs $[C_n mim][Cl]$ ILs measured by Wang et al. the resulting values seemed to be in disagreement, as well as the solution enthalpy dependence on molality. We took the initial data provided in the articles and made our own recalculation (marked with letter *d* in Table 4.9).

ILs with some anions (e.g. $[BF_4]^-$) are known to hydrolyze slowly in water. The study of the literature showed that, although this anion partially hydrolyses in water, the energetic effect of the hydrolysis reaction distorts the $\Delta_{sol}H_m^0$ values no more than 1 - 1.5 %, which is totally acceptable within the scope of this work [107].

In spite of some spread of solution enthalpies given in Table 4.10, it has been possible to draw several general conclusions. First of all, the solution enthalpies of ILs in the liquid state are practically independent of the number of C atoms in the alkyl chain in cation, or in anion. This can be best illustrated with the $\Delta_{sol}H_m^0$ values for the $[C_n mim][BF_4]$ family. The $\Delta_{sol}H_m^0$ obtained in this work as well as literature data obtained with different methods localize the $\Delta_{sol}H_m^0$ on the level 17-18 kJ·mol^{-1} for the whole family. The same conclusion can be made for $[C_2 mim][C_n SO_4]$ with the alkyl chain in anion. Somewhat lower $\Delta_{sol}H_m^0$ value for $[C_2 mim][C_8 SO_4]$ in comparison to other $[C_2 mim][C_n SO_4]$, could be explained by slow kinetics of solution, during which a hydrolysis occurred. This simple observation could be used to assess consistency of the available data within the IL family.

The second important conclusion is that, $\Delta_{sol}H_m^0$ values for imidazolium, pyridinium and pyrrolydinium based ILs do not differ significantly. The comparison between $\Delta_{sol}H_m^0$ values of $[C_2 mim][N(CN)_2]$, $[C_{41} Pyrr][N(CN)_2]$ and $[3Me\text{-}C_4 Py][N(CN)_2]$ shows that the difference do not exceed 4 kJ·mol^{-1}. The same difference was observed in the comparison of $[C_n mim][BF_4]$ and IL with symmetrical cation $[C_n C_n im][BF_4]$. Thus the interaction with the water seems to be mostly determined by anion.

The analysis of the Table 4.9 shows that $\Delta_{sol}H_m^0$ depends strongly on the nature of the anion. In order to find the reasonable correlation of $\Delta_{sol}H_m^0$ with the nature of anion, we treated the $\Delta_{sol}H_m^0$ in the same manner as we did for $\Delta_l^g H_m^0$ in Chapter 4.2. We correlated the $\Delta_{sol}H_m^0$ values from the Table 4.9 and the physical-chemical properties of ILs with $[C_2 mim]^+$ cation from the Table 4.7: static dielectric constant, E_T^N and Kamlet-Taft parameters, molecular polarisabilities, density, molar volumes, surface tension, parachor, 1H NMR shifts, and IR spectrum maximum.

In contrast with correlations with $\Delta_l^g H_m^0$, we observed for $\Delta_{sol} H_m^0$ some significant correlations only with ^{1}H NMR shifts, and E_T^N. The results of correlations are shown in the Figure 4.22:

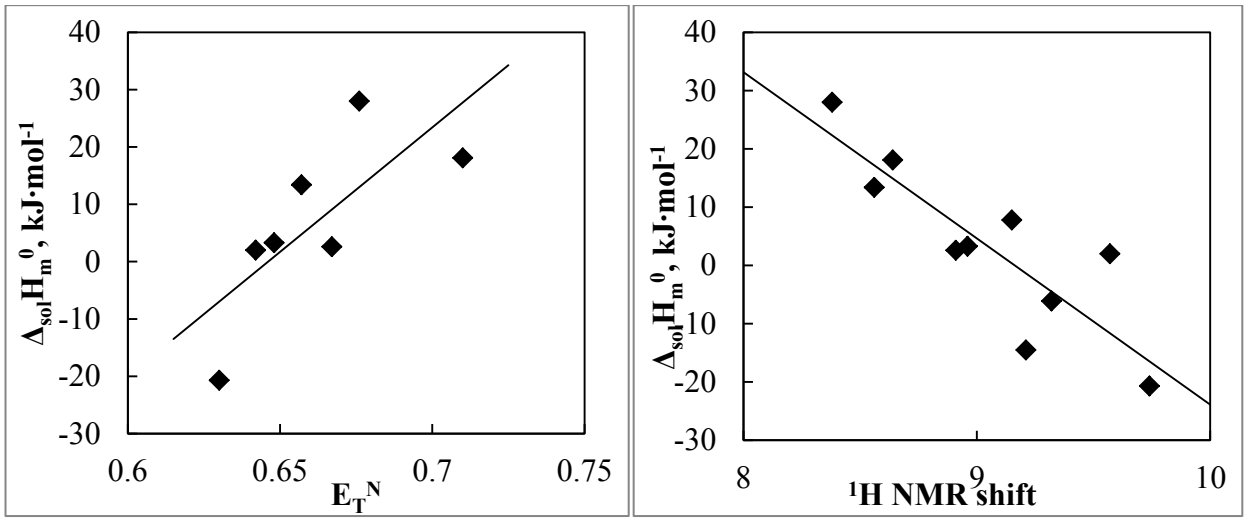

Figure 4.22 Correlation of the enthalpy of vaporization with the Kamlet-Taft parameter and ^{1}H NMR shifts

It turned out that $\Delta_{sol} H_m^0$ values for ILs in the most cases were at the level of 5-15 kJ·mol^{-1}, hardly depended on the cation ant its chain length. The $\Delta_{sol} H_m^0$- values mostly depended on the nature of anion, but they could be easily assessed using analogous data collected in Table 4.9. This simple "rule of thumb" could be used for a quick appraisal of solution enthalpies.

4.5 Prediction of the vaporization enthalpies $\Delta_l^g H_m^0$ of ILs from enthalpies of formation of aqueous ions $\Delta_f H_m^0([ion]_{aq}^n)$

Solution calorimetry allows to handle the thermodynamic properties of ions separately. Experimental data on the solution enthalpies collected in Table 4.9 have been used to extend the library of $\Delta_f H_m^0([ion]_{aq}^n)$ with ions specific for ionic liquids (see Tables 3.2 and 3.3). This library now can be used for prediction of vaporization enthalpies $\Delta_l^g H_m^0$ according to the following equation:

$$\Delta_l^g H_m^0 = \Delta_f H_m^0([Cat][An]_g) - \Delta_f H_m^0([Cat]_{aq}^+) - \Delta_f H_m^0([An]_{aq}^-) + \Delta_{sol} H_m^0 \qquad (4.17)$$

where $\Delta_f H_m^0([Cat][An]_g)$ is obtained from QC, $\Delta_f H_m^0([ion]_{aq}^n)$ is taken from library (Table 3.2, Table 3.3), $\Delta_{sol} H_m^0$ is measured or assessed as suggested in Chapter 4.4. Combination of available data with crude estimates within the eq. 4.17 provides the possibility of quick appraisal of vaporization enthalpy with reasonable accuracy for ILs, where other procedures fail, due to the lack of the input data.

5. Conclusion

ILs represent a novel class of “designer” solvents and electrolytes with a promising wide range of practical applications. These organic salts are composed solely of ions. Selection of appropriate cation-anion pairs is crucial for the design of ILs key physical and chemical properties. In this work experimental and theoretical studies have been focused on thermodynamic properties of ILs such as enthalpies of phase transitions (liquid-gas, solid-liquid, solid-gas), as well as on enthalpies of formation, and enthalpies of solution. As part of this work a series of direct and indirect methods have been developed and used to obtain the consistent data for vaporization enthalpy as one of the goal properties in this work. Two recently established direct methods: QCM and TGA have been used for accumulation of vaporization enthalpies. The indirect option to get vaporization enthalpy using the solution calorimetry has been developed and tested successfully. The comprehensive experimental and quantum chemical studies of imidazolium, pyrrolidinium, pyridinium based ILs with different counteranions have been carried out using the aforementioned method. One of the challenging tasks in this work has been the development of an approach for the temperature adjustments of IL vaporization enthalpies required for the proper comparison of the experimental data. Ambiguity of heat capacity values required for temperature adjustments of vaporization enthalpies has been resolved and three simple methods based on the different input data have been suggested and tested successfully.

The theoretical objectives of the present work were twofold: (a) to investigate structure-property relations for thermodynamic properties under study within the ILs families, and (b) to develop any kind of predictive schemes based on the structure property relations. As to objective (a), dependences of vaporization enthalpies on physical-chemical parameters specific for cation and anion interactions have been revealed. A linear relation between enthalpies of vaporization and the chain length, as well as the intermolecular vibrational frequencies have been observed and suggested for calculation of unknown ILs. As to objective (b), it has been shown that enthalpies of vaporization generally obey group additivity rules. However, the values of the additivity parameters for ionic liquids are somewhat different from those for molecular compounds. A simple group-contribution method has been developed for prediction of vaporization enthalpies of alkyl imidazolium based ILs.

6. Experimental and computational methods used in this work.

6.1 Langmuir method in combination with quartz micro balance (QCM)

We used the self-made computer controlled apparatus for the $\Delta_l^g H_m^0$ measurements. The basic principle of the method is the combination of the evaporation from the open surface in vacuum and condensation on the quartz-micro balance. The detailed development history and installation itself is described in [28]. The experimental installation is shown on the Figure 6.1.

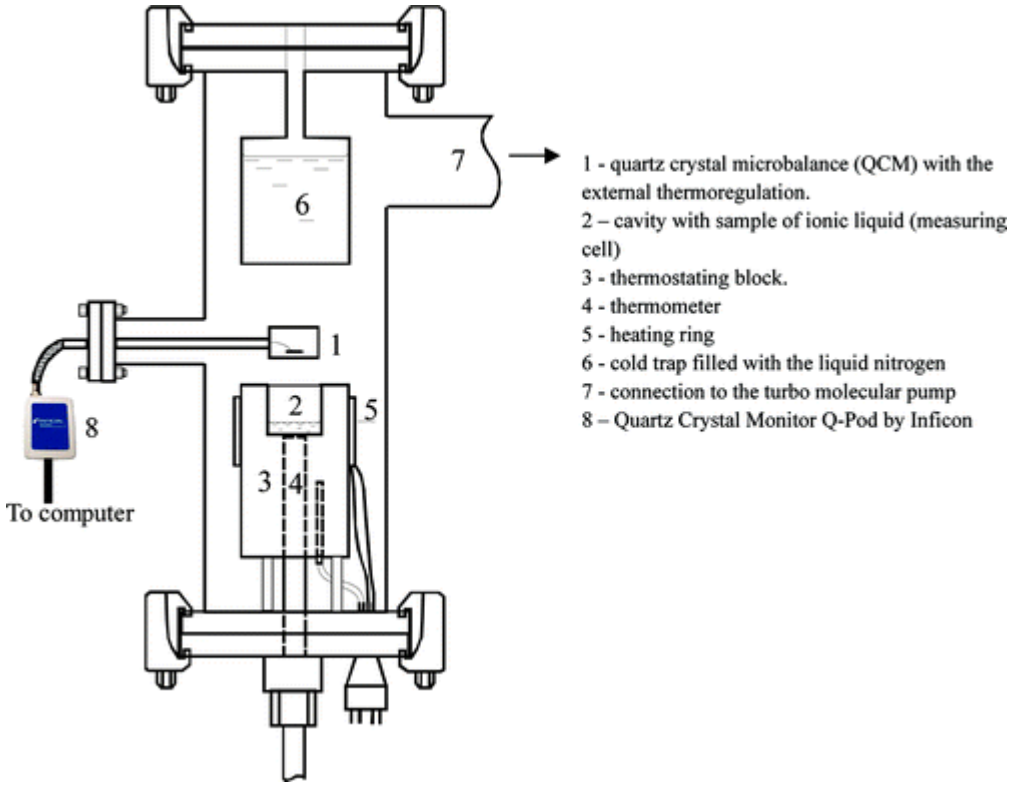

Figure 6.1 The scheme of the experimental QCM setup.

For the experiment sample is loaded to the cavity (2) in the thermostated block (3). Experimental chamber is assembled and evacuated by turbomolecular pump (7). The cooling trap (6) is filled with liquid nitrogen to prevent evaporating substances from getting into pump, as well this also cause to reduce the pressure in the experiment chamber due to gas condensation on the trap. Prior to the experiment runs, sample is conditioned by heating to the temperatures (383-423 K). After the temperature is set to the highest expected temperature of mass depositions experiment, and kept under these conditions for several hours, after that initial sample, residual and condensate are collected and analyzed for a possible traces of decompositions. After that several runs, consisting of several isothermal steps up to maximum temperature are performed.

Depositing process on the quartz-crystal (1) is described by the following equation:

$$\Delta f = -C \cdot f^2 \cdot \Delta m \cdot S_C^{-1} \quad (6.1)$$

where f is the fundamental frequency of the crystal (6 MHz in this case), S_C is the area of the crystal, $C = 2.26 \times 10^{-6}$ cm^2 g^{-1} Hz^{-1} is a constant, and m is the mass, g.

The QCM is capable to detect mass gain higher than 50 pg·s^{-1}. The corresponded mass gain on every step is related to vapor pressure, according to a Langmuir equation:

$$\frac{dm}{dt} = \alpha PS\sqrt{\frac{M}{2\pi RT}} \quad (6.2)$$

where dm/dt – mass loss rate at the specified temperature, kg s^{-1}; α – vaporization (or accommodation) coefficient; P – saturated vapor pressure, Pa; S – the surface of vaporization, m^2; M – molar mass of the substance, kg mol^{-1}; R – universal gas constant; T – temperature of the isothermal experiment, K.

The further combination of eq. 6.2 with Clausius–Clapeyron equation

$$ln(p) = A - \frac{\Delta_l^g H_m^0}{RT} \quad (6.3)$$

and Hess equation:

$$\Delta_l^g H_m^0(T) = \Delta_l^g H_m^0(T_0) + \Delta_l^g C_{p,m}^0(T - T_0) \quad (6.4)$$

produces the final equation for QCM method.

$$ln\left(\frac{df}{dt}\sqrt{T}\right) = A' - \frac{\Delta_l^g H_m^0(T_0) - \Delta_l^g C_{p,m}^0(T_0)}{R}\left(\frac{1}{T} - \frac{1}{T_0}\right) + \frac{\Delta_l^g C_{p,m}^0}{R} ln\left(\frac{T}{T_0}\right) \quad (6.5)$$

After experiment again the residue and the condensate are analysed using IR spectroscopy to confirm the absence of decomposition process.

6.2 Thermogravimetrical analysis (TGA)

We used a computer controlled Perkin Elmer Pyris 6 TGA to measure vaporization enthalpies from the temperature dependence of the mass loss rates measurements. TGA procedure is not complicated. About 50-70 mg of the IL sample is loaded in a plain platinum crucible inside of the measuring head of the TGA under a dry nitrogen flow, to prevent exposure to air, or water contamination. Prior to the measurement of vaporization enthalpy, a careful conditioning of the sample inside the TGA have been performed. A heating ramp of 10 K·min^{-1} was used, followed by a 4 h static hold period at 423 K, allowing for the slow removal of volatile impurities and traces of water prior to a stepwise isothermal runs. The conditioning was repeated until a

reproducible mass loss within two consequent runs was recorded. For the experiment the nitrogen flow is set to rate of 140 ml·min^{-1}. For every experiment the temperature range is chosen in such a manner that at the lowest temperature the sample mass loss should be c.a. 2 orders of magnitude higher than the self-drift of the instrumental balance. For Perkin Elmer 6 TGA this random balance drift do not exceed $1 \cdot 10^{-9}$ g·s^{-1}, so the minimal mass loss rate to achieve < than a 2% mass loss error should be not lower than $5 \cdot 10^{-8}$ g·s^{-1}. The highest temperature is limited by several factors. First, the temperature range for a reliable $\Delta_l^g H_m^0$ determination, should be not less than 60 K, otherwise the uncertainties in the mass loss on the boundary temperature points would have greater contribution. Second, the upper temperature is limited by the temperature of decomposition of the IL. And finally, it is not practical to have mass loss rates higher than $2 \cdot 10^{-6}$ g·s^{-1}, because otherwise the IL level in the crucible would not remain constant during the experiment. An absence of decomposition of the IL in the experimental conditions is confirmed by ATR-IR spectroscopy. The initial sample, crucible residue, and condensate on the top lid of the TGA were collected and stored in hermetical containers for this analysis.So as it was reported in [30], the optimal conditions for the reliable determination of vaporization enthalpies of ILs can be summarized as follows:

- mass loss *dm*/*dt* at each temperature step- 0.1-0.8 mg;
- duration of isothermal steps - at least 10 min;
- temperature range - at least 60 K;

Experiment consists of several runs. Every run consist of equally distributed isothermal steps over the experimental temperature range. An example of the experiment is shown in Figure 6.2

For each step the mass loss *dm*/*dt* is determined as the slope of the mass vs. time dependence, and the correlation coefficient was calculated too. The significant deviations of this coefficient form unity indicate either a complete conditioning procedure or a possible decomposition. Mass loss during each step is related to the vapour pressure of the IL. This is described by the Langmuir equation 6.2:

Further the enthalpy of vaporization is obtained using the Clausius-Clapeyron equation:

$$ln\left(\frac{dm}{dt}\sqrt{T}\right) = A - \frac{\Delta_l^g H_m^0}{RT} \tag{6.6}$$

where A is a parameter. The obtained value of $\Delta_l^g H_m^0$ corresponds to the average temperature of the single run. For every sample the average $\Delta_l^g H_m^0$ with the uncertainly equal to the double standard deviation from the linear regression was calculated.

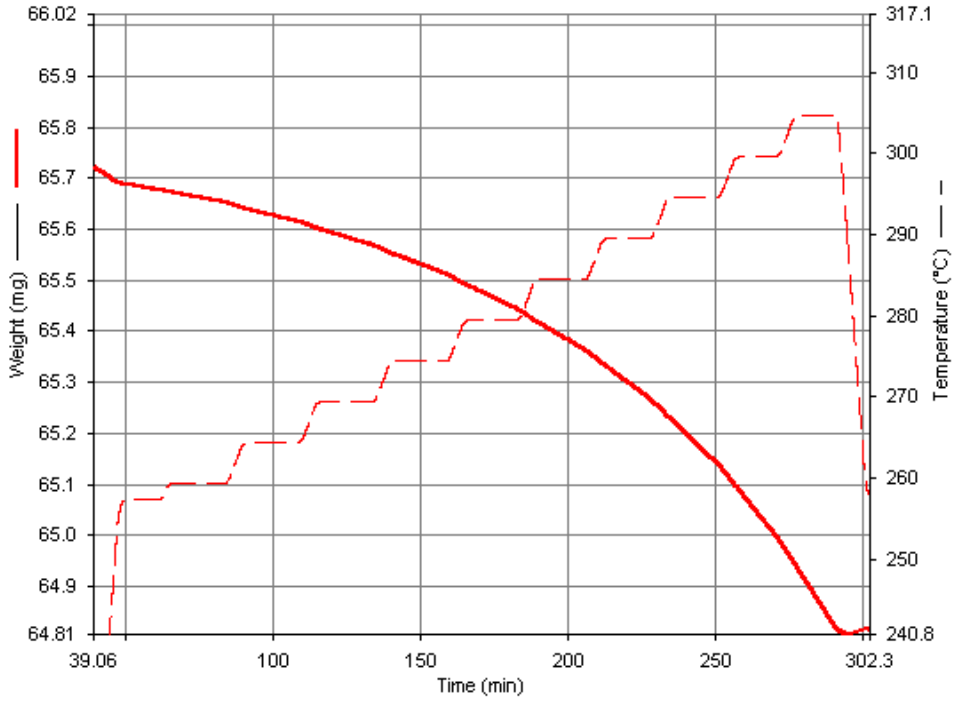

Figure 6.2 The mass loss of the IL during one run, that consists of 10 isothermal steps

6.3 Differential scanning calorimetry (DSC)

Experimental enthalpies of ILs synthesis reactions (according to eq. 1) measured by DSC open the direct way to derive enthalpies of formation of ILs as well as the indirect way to estimate vaporization enthalpies. Enthalpies of reaction were measured using the calibrated computer controlled Mettler-Toledo 822 DSC. About 10-15 mg of starting materials were placed in a 40 μL aluminum pan. As a rule, the DSC-pan was filled with the defined quantity of the first precursor 1-alkyl-halide, then with the layer of the solvent [C_4mim][NTf_2], and finally with the second precursor 1-alkyl-imidazole. We used some excess of 1- alkyl -imidazole in order to reach complete conversion of the alkyl chloride at the end of reaction. The layer of the solvent (about 75-80 wt. %;) was necessary in order to separate precursors and to avoid beginning of the chemical reaction outside of the DSC. The DSC pan was weighed with the resolution of ±0.000005 g and air buoyancy corrections were taken into account. The pan was hermetically sealed with a cover. Measurements were performed in the range 273 - 500 K with scanning rates between 10 and 50 K·min^{-1}. It is well known that ionic liquid synthesis reactions from an amine and an alkylhalide occurs very rapidly already at 353 K. Reactions are also highly exothermic but very selective with conversion over 99%. Under the DSC pan reaction conditions the relatively volatile starting materials (1- alkyl -imidazole and alkylhalides) rapidly produced the very low volatile ionic liquids already in the temperature range 343-373 K. Further heating of the pan only facilitated the complete conversion of starting materials. Completeness of reactions under study in the excess of 1- alkyl -imidazole was over 99% and therefore no volatile materials were present in the pan at elevated temperatures. The mass of the pan was controlled before and

after experiment. Any traces of unconverted starting materials or decomposition products would cause an explosion of the pan, but this was not observed. During the development of the DSC method we determined the degree of conversion in the following way: after completing of the DSC experiment the pan was cooled and a pin hole was made in the cover. The pan was heated in vacuum at 353 K within 12 h and weighed before and after the heating. The mass loss could be ascribed to the volatility of precursors, because the ionic liquid in these conditions has no measurable vapour pressure. In addition we checked the absence of unreacted alkylhalides or decomposition products in the DSC pan by GLC. The degree of conversion determined on both ways was always 99.8± 0.3%. The area of the DSC peak occurring during the chemical reaction was a measure of the reaction enthalpy. A typical reaction peak is shown in Figure 6.3.

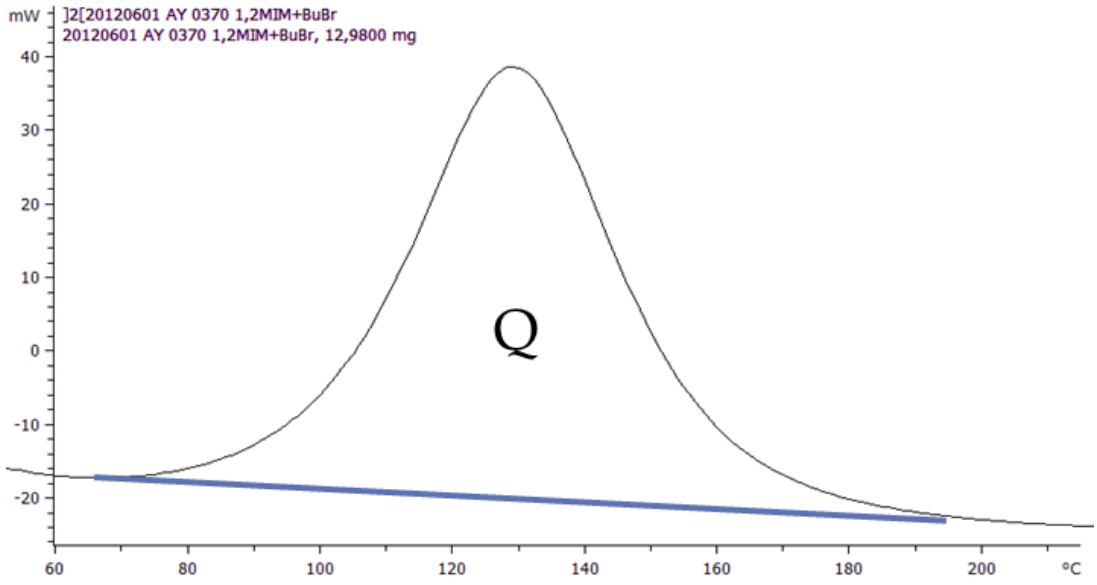

Figure 6.3 Typical synthesis reaction DSC peak, exothermic up

In order to obtain a reaction heat effect in a dynamic temperature scan mode the temperature difference between a sample pan and an empty reference pan was measured and converted into a heat flow value. The peak corresponding to this exothermic heat effect was then integrated over the time range of the effect and a total enthalpy of reaction was determined from the area of the DSC peak. The heat released during the IL synthesis reaction was related to the molar amount of a stoichiometrically deficient reactant in the starting formulation. The experimental procedure has been elaborated in our lab just recently and it was reported elsewhere [58].

6.4 Solution calorimetry

6.4.1 Theoretical background of solution calorimetry.

Solution calorimetry is the method to measure the heats of dissolution for different substances in solvents. During the calorimetrical experiment the well-defined amount of heat liberates, and the temperature change of the calorimetric system is measured. The observed temperature change is related to heat of solution with the basic equation of the calorimetry eq 6.7:

$$Q = c \cdot \Delta T \tag{6.7}$$

where: Q – heat of solution, J; ΔT – temperature change during the experiment; c – calorimetric constant of the system, $J \cdot K^{-1}$.

For practical measurements an electrical calibration is used for determination of the calorimetric constant of the system. It can be expressed in the following form:

$$Q_{exp} = Q_{cal} \frac{\Delta T_{exp}}{\Delta T_{cal}} \tag{6.8}$$

The solution calorimetry using isoperibol calorimeter (e.g. constant bath temperature) require to take into account the heat transfer between the reaction vessel and the thermostatic bath, described with eq 6.9.

$$\frac{dT_{cell}}{dt} = k(T_\infty - T_{cell}) \tag{6.9}$$

where: k – heat leakage constant, s^{-1}; t – time, s; T_{cell} – temperature of calorimetric vessel, K; T_∞ - temperature of the vessel after infinite time.

Heat leakage constant is determined combining formulas for the initial and the final periods for solution experiment:

$$k = \frac{\left(\frac{dT}{dt}\right)_i - \left(\frac{dT}{dt}\right)_f}{T_f - T_i} \tag{6.10}$$

where: $\left(\frac{dT}{dt}\right)_i$ and $\left(\frac{dT}{dt}\right)_f$ are the temperature drifts for initial and final periods respectively.

The experimental correction to the solution temperature change is applied using heat leakage constant k:

$$\Delta T = T_{end} - T_{start} - \int_{t_{start}}^{t_{end}} k(T_\infty - T)dt \tag{6.11}$$

where T_{start} and T_{end} are temperature of the calorimetric system in the beginning and in the end of dissolution of the sample. To calculate an integral we approximated the resulting solution temperature measurement in the main solution period with cubic splines. Integral for each spline

was taken analytically and calculated. No further corrections (e.g. ampoule break heat, solvent evaporation heat, etc.) were used.

The molar solution enthalpies were calculated using the following formula:

$$\Delta_{sol}H = -Q_{exp} \cdot \frac{M}{m} \tag{6.12}$$

where: M – molar mass, g·mol^{-1}; m – sample mass, g

For a further usage in Born-Harber cycle one must to extrapolate obtained values of solution enthalpies to infinite dilution. Different extrapolation procedures to infinite dilution of solution enthalpies were found in the literature. This is usually done using eq. 6.13:

$$\Delta_{sol}H = \Delta_{sol}H^0 + L_\varphi m \tag{6.13}$$

where $L_\varphi m$ is the heat of dilution to infinite dilution. There is two ways to obtain the $L_\varphi m$. First possibility is to measure and integrate the heats of dilution, from the measured concentration toward zero. However as a matter of practice the second way is used. $L_\varphi m$ is calculated according to different analytical equations describing the solution enthalpy dependence on concentration (molality of the solution). Five main methods were found in the literature and described below:

1. The Debye-Hückel limiting law and a linear term:

$$\Delta_{sol}H = \Delta_{sol}H^0 + A_H m^{0.5} + Bm \tag{6.14}$$

where A_H is the limiting slope for the enthalpy and B is adjustable parameter to compensate all deviations. Ref. [124] report the applicability of this equation for concentrations up to 1 mol·kg^{-1}.

2. The Chris and Cobble method is an extended form of Debye-Hückel limiting law [125]:

$$\Delta_{sol}H = \Delta_{sol}H^0 + 1.5A_H m^{0.5}\left[\frac{1}{1+m^{0.5}} + \frac{1}{m^{1.5}} \cdot \left(1 + m^{0.5} - \frac{1}{1+m^{0.5}} - 2\ln(1+m^{0.5})\right)\right] + Bm \tag{6.15}$$

where B is the adjustable parameter. This equation is applicable to concentrations up to 1 mol·kg^{-1}.

3. The Pitzer equation [126] for molality less than 1 mol·kg-1:

$$\Delta_{sol}H = \Delta_{sol}H^0 + v|Z_M Z_X| \frac{A_H}{2b} ln(1 + bI^{0.5}) - 2v_M v_X RT^2 B'_{MX} \tag{6.16}$$

where

$$B'_{MX} = 2\frac{\partial \beta^0}{\partial T} + \frac{2}{\alpha^2 I}\frac{\partial \beta^1}{\partial T}\left[1 - (1 + \alpha I^{0.5})e^{-\alpha I^{0.5}}\right] \tag{6.17}$$

and the ionic strength is expressed as:

$$I = 0.5 \sum_i m_i z_i^2 \quad (6.18)$$

Z_M, Z_X – charge numbers of cation and anion; v_M, v_X – the number of cations and anions in solute molecule; v – total number of ions in solute molecule; $b = 1.2$ for all electrolytes; $\alpha = 2.0$ for all 1-1 and most other electrolytes; $\frac{\partial \beta^0}{\partial T}$ and $\frac{\partial \beta^1}{\partial T}$ are adjustable parameters.

4. Polynomial fit [125]:

$$\Delta_{sol}H = \Delta_{sol}H^0 + Cm^{0.5} + Dm \quad (6.19)$$

where C, D – adjustable parameters. This equation can be used if A_H parameter for solvent is not known.

5. Linear extrapolation [127], [128]:

$$\Delta_{sol}H = \Delta_{sol}H^0 + Bm \quad (6.20)$$

where B is adjustable parameter.

All these extrapolation methods were developed for fairly concentrated solutions. Moreover, in the refs. [124], [125] authors compared the behavior of all extrapolation methods on the KCl. They reported that the quality of extrapolation depends strongly on the quality of initial calorimetric data. Enthalpies of solution at infinity dilution $\Delta_{sol}H^0$ values obtained using different extrapolation methods vary in range ± 1 kJ·mol^{-1} for the same initial experimental dataset.

In our work measure the solution enthalpies of ILs in the concentration range as close to infinite dilution as it were instrumentally possible. In this range we observed no significant concentration dependence of $\Delta_{sol}H^0$ values. Moreover the analysis of the literature showed that the experimental $\Delta_{sol}H$ values for very diluted solutions of ILs are lies in the range ± 0.5 kJ·mol^{-1} in comparison with $\Delta_{sol}H^0$ reported by authors. The theoretical study of solution concentration predicts no strong dependency of $\Delta_{sol}H$ in such diluted range. Thus taking into account 3 factors:

- the $\Delta_{sol}H^0$ values spread caused by selection of the extrapolation method;
- the small difference between $\Delta_{sol}H$ of diluted solutions and $\Delta_{sol}H^0$
- the fact that the uncertainties of solution calorimetry experiment is significantly lower, than uncertainty from other methods (e.g. DSC, TGA, QC)

we decided to take an average values from several experiments. The final estimated uncertainty falls in range of ± 1 kJ·mol^{-1} is totally acceptable in the calculations of $\Delta_l^g H_m^0$

6.4.2 Solution Calorimeter

In this work we used a LKB 8700-2 isoperibol solution calorimeter produced in Sweden. This calorimeter was successfully used by Prof. Heiko Cammenga at the TU Braunschweig ant it was

gifted to the University of Rostock after his retirement. The complete description of original calorimeter can be found in the original LKB 8700 manual. Prior to research we heavily modified the calorimeter to comply with modern demands. It has turned out that the mechanical parts of the calorimeter have been in good order, but the electronic part and the data acquisition have been completely upgraded in our lab. From the original device we kept only thermostatic bath with proportional heat controller and calibrator power block. We installed for the temperature measurements two modern multimeters. A relay card Quancom with a conventional PC was used to switch on/off the calibrator and the trigger for the ampoule breaker.

Figure 6.4. Calorimeric cell and crushing ampoule

New calorimetric cells. The calorimetric 25 ml glass cell and the glass container for sample (ampoule) were manufactured at University of Rostock according to the original LKB design (see Figure 6.4). The original LKB calorimetric cells pockets were made of metal, we manufactured them of glass as the integral part of the cell instead. Test measurements have validated these changes as insignificant. The calorimetric cell was equipped with two pockets. A thermistor for a highly precise temperature measurements was placed in the first pocket. The second pocket was used for a heating element. In order to improve heat exchange rate both pockets were filled with highly thermal conductive composition GELID TC-GC-03-A. This grease was non-corrosive, and non-electrical conductive compound with one of the highest available on the market thermal conductivity (8.5 $W \cdot mK^{-1}$). Pockets were hermetically sealed with the epoxide polymer. Each cell was equipped with 50.4 Ohm self-made resistor as a calibrator and heater. The thermistor and the heating element were connected to the multimeters. Both multimeters were managed by the PC. The general modified scheme of the solution calorimeter is shown on the Figure 6.5.

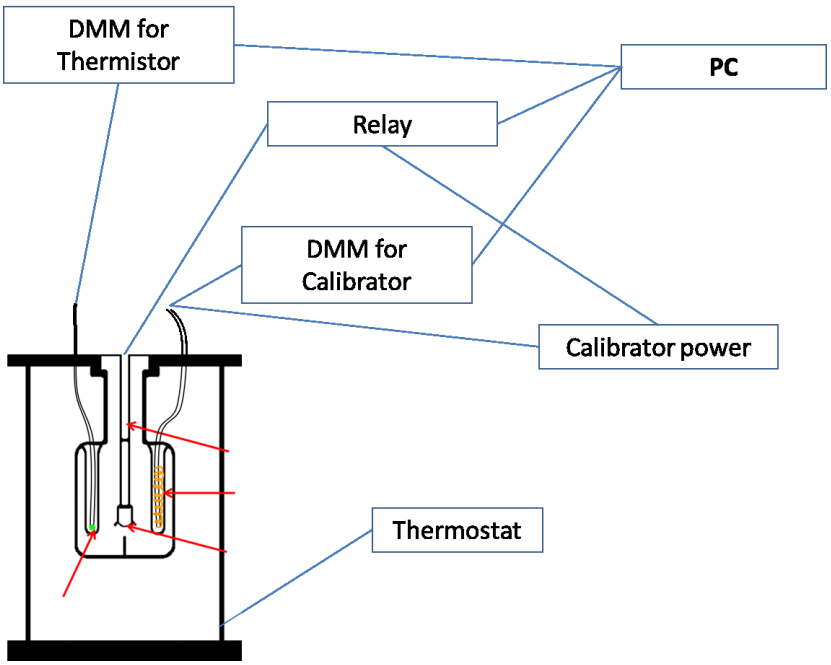

Figure 6.5. New solution calorimeter functional diagramm

New temperature control system. For the precise temperature measurements we used a commercially available thermistor: precision temperature sensor SEMI833ET (Hygrosens), inserted in one of the calorimetric cell pockets. Thermistor had a nominal resistance 50 kOhm at 310 K, and 700 ms. reaction time. In the limits of working range (298.15 ± 0.70 K) thermistor had a linear dependence, so no further corrections in conversion between resistance and temperature were made. Thermistor was connected to the 6.5 digits Keithley Digital Multimeter Model 2700 using 4-wire scheme. We used a cable with individual shields for every wire to minimize the influence of noise pickup. The resistance of thermistor was directly measured with the multimeter. In the course of experiment the multimeter collected one reading in 5 seconds, provided that every reading had 1 second integration time to minimize the noise. Readings were sent from multimeter to the controlling software using RS-232 interface.

Modified heating system. The original LKB calibration and heating systems were modified. We connected the calibration system to the 6.5 digits Prema 5000 multimeter to control and logged the voltage on the calibration resistance during the calibration procedure. This multimeter was connected to the PC via GPIB interface. We used a relay card Quancom USBREL8/LC with 1 ms. switching time to control the calibrator.

New controlling system. We used a PC with Microsoft Windows XP SP2 with .NET 4.0 framework to run and control the experiment. The solution experiment and the data acquisition were fully automated using a homemade software package consisting of 2 packages. First package controlled the experimental run over the relay card, automatically heated the calorimetric system to the initial temperature, prepared both multimeters to the working mode,

logged all experimental data and prepared the short report (see Figure 6.6). This package was written with multiple treads of execution. This allowed to improve stability and reaction time of the software. Second package of the software was designed for the acquisition of the temperature changes during the solution experiment and export of the treated data (see Figure 6.7) in the readable format (to .csv table).

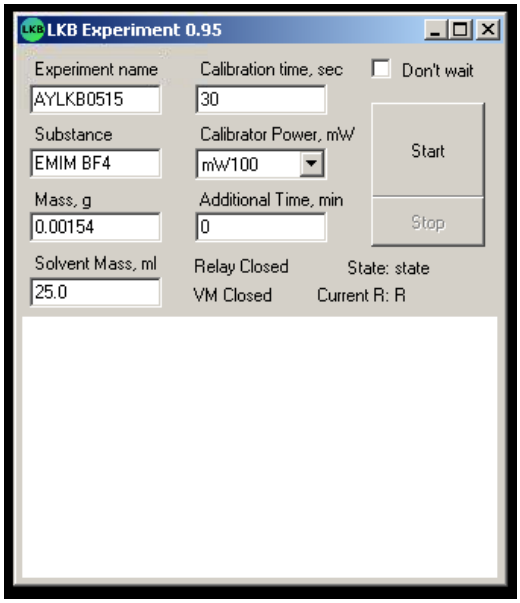

Figure 6.6 The experiment control package

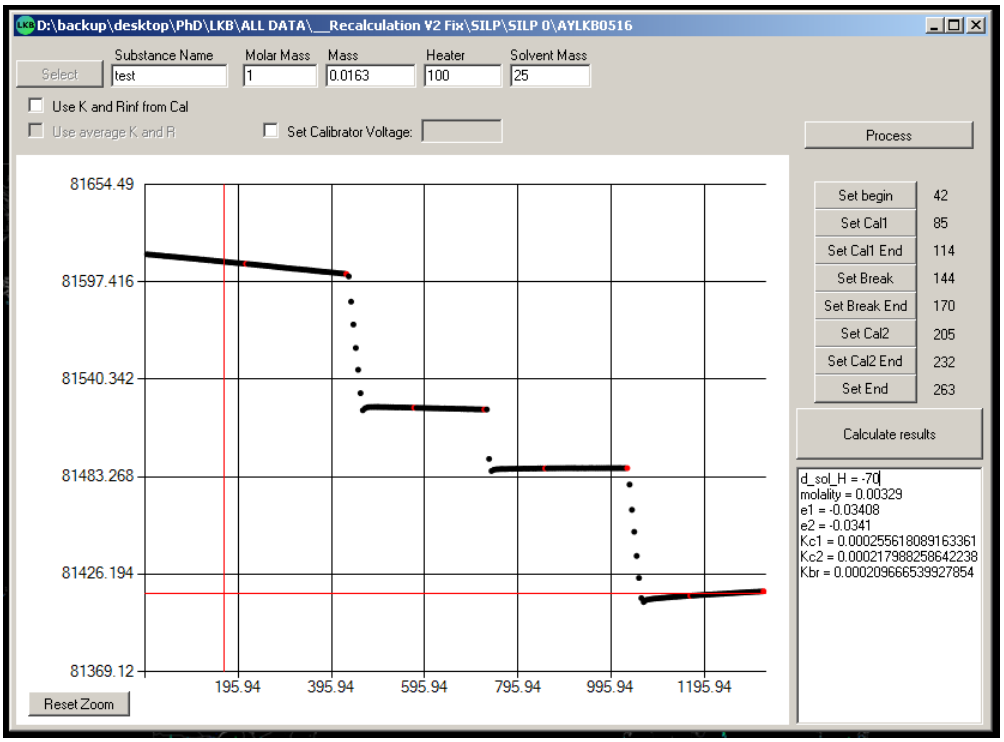

Figure 6.7 Solution curves processing package

The theoretical background of the data processing is explained in chapter 6.4.1. Software was written in C# programming language (.NET v4.0 Server Profile, Microsoft Visual Studio

Express 2010). The C# language is broadly used for enterprise-class projects. It is managed language with big existing codebase, which could be extended with additional libraries, and good community support. It also allows easy and predictable low level programming (e.g. easy access to the RS-232 and GPIB (or IEEE-488))

The calorimeter was calibrated calorimeter at 298.15 K and successfully tested with KCl (reference compound for solution calorimetry). Prior to experiment the potassium chloride was dried at 373 K in vacuum for 24 hours. Solution experiments were performed in the bi-distilled water. The test result of 17.65 ± 0.07 kJ·mol^{-1} was in excellent agreement with recommended in the literature result 17.58 ± 0.02 [129]. The results of calibration are listed in the Table 6.1

Table 6.1 Enthalpies of solution of KCl in water

m(KCl), g	molality, mol·kg^{-1}	$\Delta_{sol}H_m^0$, J·mol^{-1}
0.00879	0.00472	17655
0.03447	0.01849	17705
0.03986	0.02139	17604
0.07334	0.03935	17615
0.09030	0.04845	17651
0.11324	0.06076	17656

Sample Preparation. Prior to experiments, the IL-samples were subjected to vacuum evaporation at 333 K for more than 24 hours to remove possible traces of solvents and moisture. IL samples loaded in ampoules for the solution experiments were additionally kept for 48 h over the P_2O_5 in vacuum in a desiccator connected to a rotary pump. Before an experiment desiccator was filled with the dry nitrogen and ampoules were closed with silicon stoppers.

Solution experiment. Calorimetric procedure. The solution experiment procedure consists of several steps. The 25 ml calorimetric cell is filled with 25.00 ± 0.01 g of bi-distilled water. The sample is loaded into a pre-weighted glass crushing ampoule. Liquids were loaded in the ampoule with a syringe. Solids were loaded as a pallet. The ampoule was closed with a silicon stopper and weighted again in order to determine the mass of the sample. In experiments with volatile compounds a thin wax layer was deposited upon the stopper. In experiments with ILs such precaution was unnecessary. All weightings were made using the Mettler-Toledo balances with the resolution $1 \cdot 10^{-5}$g. The mass of the sample was adjusted to provide the final molality of the solution in the calorimetric cell at the level of 0.02 mol·kg^{-1} and lower.

Assembled ampoules were fixed in the golden ampoule holder, which was inserted in the calorimetric system. Electrical calibrations were performed short before and after solution step. The duration of main period differed significantly for different ILs, ranging from several seconds for [C_2mim][NO_3] to 1 hour for low soluble [C_8mim][BF_4]. Temperature change was determined as a difference between the temperatures of the end and the beginning of main solution period. Temperature change was corrected using integration of cubic splines to take into account the

heat exchange between the calorimetric system and the calorimetric bath according to eq .6.10. The typical solution calorimetric curve is plotted in the Figure 6.8, two calibrations were made before and after the solution period.

6.5 Quantum chemical calculations of $\Delta_f H_m^0(g)(298\ K)$

In this work we performed standard quantum chemical calculations using the Gaussian 09 program package [130]. From 20 to 30 initial conformations of ionic liquids were generated which were optimized on B3LYP/6-31e+(d,p) level of theory. After that the lowest by energy conformation was calculated on CBS-QB3 as well as G3(MP2) level. CBS-QB3 theory uses geometries from B3LYP/6-311G(2d,d,p) calculation, scaled zero-point energies from B3LYP/6-311G(2d,d,p) calculation followed by a series of single-point energy calculations at the MP2/6-311G(3df,2df,2p), MP4(SDQ)/6-31G(d(f),p) and CCSD(T)/6-31G† levels of theory [131]. G3(MP2) theory uses geometries from second-order perturbation theory and scaled zero-point energies from Hartree-Fock theory followed by a series of single-point energy calculations at the MP2(Full)/6-31G(d), QCISD(T)/6-31G(d) and MP2/GTMP2-Large levels of theory (for details see reference [132]). Calculated values of the enthalpies of reaction and enthalpies of formation are based on the electronic energy calculations obtained using standard procedures of statistical thermodynamics [133]. Both CBS-QB3 and G3(MP2) methods provide good results for ILs, but the latter one requires significantly less computing time for such big systems.

The quantum chemical calculations with CBS-QB3 and G3MP2 methods for ILs were checked with the precise experimental [15]. For example, The experimental determination of gaseous enthalpy of formation $\Delta_l^g H_m^0$ of $[C_4mim][N(CN)_2]$ = 363.4±2.7 kJ·mol^{-1} from thermochemical measurements (combustion and transpiration) was in excellent agreement with the $\Delta_l^g H_m^0$ of = 359.63 kJ·mol^{-}1 calculated using the G3MP2 theory. Also QC calculations of the enthalpies of formation in the gaseous phase for the ionic liquids $[C_nMIM][C(CN)_3]$ calculated using the CBS-QB3 and G3MP2 theory were in good agreement (see Table 6.2) with the experimental data (combination of the results obtained from QCM and combustion calorimetry) [59].

Table 6.2 Thermochemical data at T = 298.15 K (p° = 0.1 MPa) for $[C_nMIM][N(CN)_3]$, kJ·mol^{-1}

ILs	$\Delta_c H_m^0$ (l)	$\Delta_f H_m^0$ (l)	$\Delta_l^g H_m^0$	$\Delta_f H_m^0$ (g) exp	$\Delta_f H_m^0$ (g) CBS-QB3	$\Delta_f H_m^0$ (g) G3MP2
$[C_2MIM][C(CN)_3]$	-5849.4±2.2	342.2±2.5	138.8±5.0	481.0±5.6	473.3±5.0	486.0±5.0
$[C_4MIM][C(CN)_3]$	-7145.1±2.1	279.2±2.6	143.2±5.0	422.4±5.6	429.7±5.0	439.8±5.0

7. Aknowledgements

This PhD thesis has been the most challenging academic task I have ever faced. It wouldn't be possible to complete it without tremendous support and invaluable help of the following people to whom I would like to express my deepest appreciation:

- my scientific supervisors **Prof. Sergey Verevkin** and **Prof. Christoph Schick**, for the opportunity to carry out my research, for their competent guidance, continuing support and constructive feedback. I have benefited greatly from their extensive knowledge and reach experience and am indebted to them for my constant personal and scientific development;
- **DFG** and **DAAD**, for their financial support;
- my friend and colleague **Dr. Dzmitry Zaitsau**, for his significant contribution with QCM measurements, meaningful discussions and technical assistance;
- my colleague **Dr. Vladimir Yemel'yanenko**, for his important contribution with QC calculations and helpful advice;
- **Polymer Physics group**, for warm and supportive working environment;
- **Dr. Mikhail Varfolomeev**, for sharing his experience in solution calorimetry;
- **Prof. Heiko Cammenga**, for the opportunity to make solution calorimetry measurements with the calorimeter he presented to our lab;
- **Herr Peter Kumm**, for his technical support;
- **Herr Roland Weihs** and **Herr Patrick Quade**, for producing glass spare parts for solution calorimeter;
- **Prof. Edward Maginn** and **Dr. Hongjun Liu**, for their conciderable contribution with MD simulations;
- **Prof. Ralf Ludwig**, for constructive comments and suggestion during seminars;
- **Frau Anne-Marie Bonza**, for her contribution with conductometric measurements;
- my **family** and especially my wife **Aliona Yermalayeva**, for their love, support and endless patience;
- my chemistry teachers and friends **Elena Buraga** and **Dr. Vasily Linnik**, for introducing me to the world of chemistry
- all my **friends** and **metal band mates**, for their moral support and sincere encouragement during writing this PhD thesis.

References

[1] A. Triolo, O. Russina, H.-J. Bleif, and E. Di Cola, "Nanoscale Segregation in Room Temperature Ionic Liquids," *J. Phys. Chem. B*, vol. 111, no. 18, pp. 4641–4644, May 2007.

[2] S. Gabriel and J. Weiner, "Ueber einige Abkömmlinge des Propylamins," *Berichte Dtsch. Chem. Ges.*, vol. 21, no. 2, pp. 2669–2679, 1888.

[3] P. Walden, *Bull. Acad. Sci. St. Petersburg*, pp. 405–422, 1914.

[4] J. S. Wilkes, J. A. Levisky, R. A. Wilson, and C. L. Hussey, "Dialkylimidazolium chloroaluminate melts: a new class of room-temperature ionic liquids for electrochemistry, spectroscopy and synthesis," *Inorg. Chem.*, vol. 21, no. 3, pp. 1263–1264, 1982.

[5] J. S. Wilkes and M. J. Zaworotko, "Air and water stable 1-ethyl-3-methylimidazolium based ionic liquids," *J. Chem. Soc. Chem. Commun.*, no. 13, pp. 965–967, Jan. 1992.

[6] M. J. Earle, J. M. S. S. Esperança, M. A. Gilea, J. N. Canongia Lopes, L. P. N. Rebelo, J. W. Magee, K. R. Seddon, and J. A. Widegren, "The distillation and volatility of ionic liquids," *Nature*, vol. 439, no. 7078, pp. 831–834, Feb. 2006.

[7] M. Kosmulski, J. Gustafsson, and J. B. Rosenholm, "Thermal stability of low temperature ionic liquids revisited," *Thermochim. Acta*, vol. 412, no. 1–2, pp. 47–53, Mar. 2004.

[8] J. James H. Davis, "Task-Specific Ionic Liquids," *Chem. Lett.*, vol. 33, no. 9, pp. 1072–1077, 2004.

[9] J. P. Hallett and T. Welton, "Room-Temperature Ionic Liquids: Solvents for Synthesis and Catalysis. 2," *Chem. Rev.*, vol. 111, no. 5, pp. 3508–3576, May 2011.

[10] M. E. V. Valkenburg, R. L. Vaughn, M. Williams, and J. S. Wilkes, "Thermochemistry of ionic liquid heat-transfer fluids," *Thermochim. Acta*, vol. 425, no. 1–2, pp. 181–188, Jan. 2005.

[11] M. Galiński, A. Lewandowski, and I. Stępniak, "Ionic liquids as electrolytes," *Electrochim. Acta*, vol. 51, no. 26, pp. 5567–5580, Aug. 2006.

[12] C. Ye, W. Liu, Y. Chen, and L. Yu, "Room-temperature ionic liquids: a novel versatile lubricant," *Chem. Commun.*, no. 21, pp. 2244–2245, Oct. 2001.

[13] D. Dobler, T. Schmidts, I. Klingenhöfer, and F. Runkel, "Ionic liquids as ingredients in topical drug delivery systems," *Int. J. Pharm.*, vol. 441, no. 1–2, pp. 620–627, Jan. 2013.

[14] J. Jeong, N. Aetukuri, T. Graf, T. D. Schladt, M. G. Samant, and S. S. P. Parkin, "Suppression of Metal-Insulator Transition in VO_2 by Electric Field–Induced Oxygen Vacancy Formation," *Science*, vol. 339, no. 6126, pp. 1402–1405, Mar. 2013.

[15] V. N. Emel'yanenko, S. P. Verevkin, and A. Heintz, "The Gaseous Enthalpy of Formation of the Ionic Liquid 1-Butyl-3-methylimidazolium Dicyanamide from Combustion Calorimetry, Vapor Pressure Measurements, and Ab Initio Calculations," *J. Am. Chem. Soc.*, vol. 129, no. 13, pp. 3930–3937, Apr. 2007.

[16] S. P. Verevkin, V. N. Emel'yanenko, D. H. Zaitsau, A. Heintz, C. D. Muzny, and M. Frenkel, "Thermochemistry of imidazolium-based ionic liquids: experiment and first-principles calculations," *Phys. Chem. Chem. Phys.*, vol. 12, no. 45, pp. 14994–15000, Nov. 2010.

[17] M. Knudsen, *The kinetic theory of gases some modern aspects*. London; New York: Metheun & Co. ; Wiley, 1950.

[18] M. Knudsen, "Die Molekularströmung der Gase durch Offnungen und die Effusion," *Ann. Phys.*, vol. 333, no. 5, pp. 999–1016, 1909.

[19] H. Luo, G. A. Baker, and S. Dai, "Isothermogravimetric Determination of the Enthalpies of Vaporization of 1-Alkyl-3-methylimidazolium Ionic Liquids," *J. Phys. Chem. B*, vol. 112, no. 33, pp. 10077–10081, Aug. 2008.

[20] F. Heym, B. J. M. Etzold, C. Kern, and A. Jess, "An improved method to measure the rate of vaporisation and thermal decomposition of high boiling organic and ionic liquids by thermogravimetrical analysis," *Phys. Chem. Chem. Phys.*, vol. 12, no. 38, pp. 12089–12100, Oct. 2010.

[21] A. Seeberger, A.-K. Andresen, and A. Jess, "Prediction of long-term stability of ionic liquids at elevated temperatures by means of non-isothermal thermogravimetrical analysis," *Phys. Chem. Chem. Phys.*, vol. 11, no. 41, pp. 9375–9381, Nov. 2009.

[22] J. P. Armstrong, C. Hurst, R. G. Jones, P. Licence, K. R. J. Lovelock, C. J. Satterley, and I. J. Villar-Garcia, "Vapourisation of ionic liquids," *Phys. Chem. Chem. Phys.*, vol. 9, no. 8, pp. 982–990, Feb. 2007.

[23] V. N. Emel'yanenko, S. P. Verevkin, A. Heintz, J.-A. Corfield, A. Deyko, K. R. J. Lovelock, P. Licence, and R. G. Jones, "Pyrrolidinium-Based Ionic Liquids. 1-Butyl-1-methyl Pyrrolidinium Dicyanoamide: Thermochemical Measurement, Mass Spectrometry, and ab Initio Calculations," *J. Phys. Chem. B*, vol. 112, no. 37, pp. 11734–11742, Sep. 2008.

[24] A. Deyko, K. R. J. Lovelock, J.-A. Corfield, A. W. Taylor, P. N. Gooden, I. J. Villar-Garcia, P. Licence, R. G. Jones, V. G. Krasovskiy, E. A. Chernikova, and L. M. Kustov, "Measuring and predicting $\Delta_{(vap)}H_{298}$ values of ionic liquids," *Phys. Chem. Chem. Phys.*, vol. 11, no. 38, pp. 8544–8555, Oct. 2009.

[25] K. R. J. Lovelock, A. Deyko, P. Licence, and R. G. Jones, "Vaporisation of an ionic liquid near room temperature," *Phys. Chem. Chem. Phys.*, vol. 12, no. 31, pp. 8893–8901, Aug. 2010.

[26] C. Wang, H. Luo, H. Li, and S. Dai, "Direct UV-spectroscopic measurement of selected ionic-liquid vapors," *Phys. Chem. Chem. Phys.*, vol. 12, no. 26, pp. 7246–7250, Jun. 2010.

[27] L. M. N. B. F. Santos, J. N. Canongia Lopes, J. A. P. Coutinho, J. M. S. S. Esperança, L. R. Gomes, I. M. Marrucho, and L. P. N. Rebelo, "Ionic Liquids: First Direct Determination of their Cohesive Energy," *J. Am. Chem. Soc.*, vol. 129, no. 2, pp. 284–285, Jan. 2007.

[28] S. P. Verevkin, D. H. Zaitsau, V. N. Emel'yanenko, and A. Heintz, "A New Method for the Determination of Vaporization Enthalpies of Ionic Liquids at Low Temperatures," *J. Phys. Chem. B*, vol. 115, no. 44, pp. 12889–12895, Nov. 2011.

[29] D. H. Zaitsau, G. J. Kabo, A. A. Strechan, Y. U. Paulechka, A. Tschersich, S. P. Verevkin, and A. Heintz, "Experimental vapor pressures of 1-alkyl-3-methylimidazolium bis(trifluoromethylsulfonyl)imides and a correlation scheme for estimation of vaporization enthalpies of ionic liquids," *J. Phys. Chem. A*, vol. 110, no. 22, pp. 7303–7306, Jun. 2006.

[30] S. P. Verevkin, R. V. Ralys, D. H. Zaitsau, V. N. Emel'yanenko, and C. Schick, "Express thermogravimetric method for the vaporization enthalpies appraisal for very low volatile molecular and ionic compounds," *Thermochim. Acta*, vol. 538, pp. 55–62, Jun. 2012.

[31] M. A. A. Rocha, C. F. R. A. C. Lima, L. R. Gomes, B. Schröder, J. A. P. Coutinho, I. M. Marrucho, J. M. S. S. Esperança, L. P. N. Rebelo, K. Shimizu, J. N. C. Lopes, and L. M. N. B. F. Santos, "High-Accuracy Vapor Pressure Data of the Extended $[C_nC_1im][NTf_2]$ Ionic Liquid Series: Trend Changes and Structural Shifts," *J. Phys. Chem. B*, vol. 115, no. 37, pp. 10919–10926, Sep. 2011.

[32] F. Heym, B. J. M. Etzold, C. Kern, and A. Jess, "Analysis of evaporation and thermal decomposition of ionic liquids by thermogravimetrical analysis at ambient pressure and high vacuum," *Green Chem.*, vol. 13, no. 6, pp. 1453–1466, Jun. 2011.

[33] J. A. Widegren, Y.-M. Wang, W. A. Henderson, and J. W. Magee, "Relative Volatilities of Ionic Liquids by Vacuum Distillation of Mixtures," *J. Phys. Chem. B*, vol. 111, no. 30, pp. 8959–8964, Aug. 2007.

[34] M. Månsson, P. Sellers, G. Stridh, and S. Sunner, "Enthalpies of vaporization of some 1-substituted n-alkanes," *J. Chem. Thermodyn.*, vol. 9, no. 1, pp. 91–97, Jan. 1977.

[35] Y. Wang and G. A. Voth, "Tail Aggregation and Domain Diffusion in Ionic Liquids," *J. Phys. Chem. B*, vol. 110, no. 37, pp. 18601–18608, Sep. 2006.

[36] J. N. A. Canongia Lopes and A. A. H. Pádua, "Nanostructural Organization in Ionic Liquids," *J. Phys. Chem. B*, vol. 110, no. 7, pp. 3330–3335, Feb. 2006.

[37] D. H. Zaitsau, S. P. Verevkin, V. N. Emel'yanenko, and A. Heintz, "Vaporization Enthalpies of Imidazolium Based Ionic Liquids: Dependence on Alkyl Chain Length," *ChemPhysChem*, vol. 12, no. 18, pp. 3609–3613, 2011.

[38] J. M. S. S. Esperança, J. N. Canongia Lopes, M. Tariq, L. M. N. B. F. Santos, J. W. Magee, and L. P. N. Rebelo, "Volatility of Aprotic Ionic Liquids — A Review," *J. Chem. Eng. Data*, vol. 55, no. 1, pp. 3–12, Jan. 2010.

[39] S. P. Verevkin, D. H. Zaitsau, V. N. Emel'yanenko, A. V. Yermalayeu, C. Schick, H. Liu, E. J. Maginn, S. Bulut, I. Krossing, and R. Kalb, "Making Sense of Enthalpy of Vaporization Trends for Ionic Liquids: New Experimental and Simulation Data Show a Simple Linear Relationship and Help Reconcile Previous Data," *J. Phys. Chem. B*, vol. 117, no. 21, pp. 6473–6486, May 2013.

[40] T. Köddermann, D. Paschek, and R. Ludwig, "Ionic Liquids: Dissecting the Enthalpies of Vaporization," *ChemPhysChem*, vol. 9, no. 4, pp. 549–555, 2008.

[41] Y. U. Paulechka, G. J. Kabo, A. V. Blokhin, O. A. Vydrov, J. W. Magee, and M. Frenkel, "Thermodynamic Properties of 1-Butyl-3-methylimidazolium Hexafluorophosphate in the Ideal Gas State†," *J. Chem. Eng. Data*, vol. 48, no. 3, pp. 457–462, May 2003.

[42] N. Rai and E. J. Maginn, "Vapor–Liquid Coexistence and Critical Behavior of Ionic Liquids via Molecular Simulations," *J. Phys. Chem. Lett.*, vol. 2, no. 12, pp. 1439–1443, Jun. 2011.

[43] S. P. Verevkin, D. H. Zaitsau, V. N. Emel'yanenko, R. V. Ralys, A. V. Yermalayeu, and C. Schick, "Vaporization enthalpies of imidazolium based ionic liquids. A thermogravimetric study of the alkyl chain length dependence," *J. Chem. Thermodyn.*, vol. 54, pp. 433–437, Nov. 2012.

[44] J. S. Chickos and W. E. Acree, "Enthalpies of Vaporization of Organic and Organometallic Compounds, 1880–2002," *J. Phys. Chem. Ref. Data*, vol. 32, no. 2, pp. 519–878, Apr. 2003.

[45] Y. U. Paulechka, "Heat Capacity of Room-Temperature Ionic Liquids: A Critical Review," *J. Phys. Chem. Ref. Data*, vol. 39, no. 3, pp. 033108–033108–23, Sep. 2010.

[46] Y. U. Paulechka, G. J. Kabo, and V. N. Emel'yanenko, "Structure, Conformations, Vibrations, and Ideal-Gas Properties of 1-Alkyl-3-methylimidazolium bis(trifluoromethylsulfonyl)imide Ionic Pairs and Constituent Ions," *J. Phys. Chem. B*, vol. 112, no. 49, pp. 15708–15717, Dec. 2008.

[47] E. A. Moelwyn-Hughes, *Physical Chemistry*. Pergamon Press, 1965.

[48] Y. U. Paulechka, D. H. Zaitsau, and G. J. Kabo, "On the difference between isobaric and isochoric heat capacities of liquid cyclohexyl esters," *J. Mol. Liq.*, vol. 115, no. 2–3, pp. 105–111, Nov. 2004.

[49] R. Auerbach, "Oberflächenspannung und Schallgeschwindigkeit," *Kurze Mitteilungen*, pp. 473–474, Dec. 1948.

[50] R. L. Gardas and J. A. P. Coutinho, “Estimation of speed of sound of ionic liquids using surface tensions and densities: A volume based approach,” *Fluid Phase Equilibria*, vol. 267, no. 2, pp. 188–192, May 2008.
[51] T. A. Knotts, W. V. Wilding, J. L. Oscarson, and R. L. Rowley, “Use of the DIPPR Database for Development of QSPR Correlations: Surface Tension,” *J. Chem. Eng. Data*, vol. 46, no. 5, pp. 1007–1012, Sep. 2001.
[52] S. P. Verevkin, D. H. Zaitsau, V. N. Emel’yanenko, R. V. Ralys, A. V. Yermalayeu, and C. Schick, “Does alkyl chain length really matter? Structure–property relationships in thermochemistry of ionic liquids,” *Thermochim. Acta*, vol. 562, pp. 84–95, Jun. 2013.
[53] “Ionic Liquids Database.” .
[54] Y. U. Paulechka, A. G. Kabo, A. V. Blokhin, G. J. Kabo, and M. P. Shevelyova, “Heat Capacity of Ionic Liquids: Experimental Determination and Correlations with Molar Volume,” *J. Chem. Eng. Data*, vol. 55, no. 8, pp. 2719–2724, Aug. 2010.
[55] Y. Shimizu, Y. Ohte, Y. Yamamura, S. Tsuzuki, and K. Saito, “Comparative Study of Imidazolium- and Pyrrolidinium-Based Ionic Liquids: Thermodynamic Properties,” *J. Phys. Chem. B*, vol. 116, no. 18, pp. 5406–5413, May 2012.
[56] D. Waliszewski, I. Stępniak, H. Piekarski, and A. Lewandowski, “Heat capacities of ionic liquids and their heats of solution in molecular liquids,” *Thermochim. Acta*, vol. 433, no. 1–2, pp. 149–152, Aug. 2005.
[57] A. A. Strechan, A. G. Kabo, Y. U. Paulechka, A. V. Blokhin, G. J. Kabo, A. S. Shaplov, and E. I. Lozinskaya, “Thermochemical properties of 1-butyl-3-methylimidazolium nitrate,” *Thermochim. Acta*, vol. 474, no. 1–2, pp. 25–31, Aug. 2008.
[58] S. P. Verevkin, V. N. Emel’yanenko, D. H. Zaitsau, R. V. Ralys, and C. Schick, “Ionic Liquids: Differential Scanning Calorimetry as a New Indirect Method for Determination of Vaporization Enthalpies,” *J. Phys. Chem. B*, vol. 116, no. 14, pp. 4276–4285, Apr. 2012.
[59] V. N. Emel’yanenko, D. H. Zaitsau, S. P. Verevkin, A. Heintz, K. Voß, and A. Schulz, “Vaporization and Formation Enthalpies of 1-Alkyl-3-methylimidazolium Tricyanomethanides,” *J. Phys. Chem. B*, vol. 115, no. 40, pp. 11712–11717, Oct. 2011.
[60] M. Smiglak, W. M. Reichert, J. D. Holbrey, J. S. Wilkes, L. Sun, J. S. Thrasher, K. Kirichenko, S. Singh, A. R. Katritzky, and R. D. Rogers, “Combustible ionic liquids by design: is laboratory safety another ionic liquid myth?,” *Chem. Commun.*, no. 24, pp. 2554–2556, Jun. 2006.
[61] S. Sunner and M. Månsson, *Combustion Calorimetry*. Pergamon Press, 1979.
[62] J. D. Cox, D. D. Wagman, and V. A. Medvedev, *CODATA key values for thermodynamics*. Hemisphere Pub. Corp., 1989.
[63] S. P. Verevkin, V. N. Emel’yanenko, I. Krossing, and R. Kalb, “Thermochemistry of ammonium based ionic liquids: Tetra-alkyl ammonium nitrates – Experiments and computations,” *J. Chem. Thermodyn.*, vol. 51, pp. 107–113, Aug. 2012.
[64] C. Shoifet, E ; Huth, H ; Verevkin, S ; Schick, “Influence of cation size on dynamic glass transition in room temperature ionic liquids,” presented at the 7th International Discussion Meeting on Relaxations in Complex Systems, 2013.
[65] M. A. A. Rocha, J. A. P. Coutinho, and L. M. N. B. F. Santos, “Cation Symmetry effect on the Volatility of Ionic Liquids,” *J. Phys. Chem. B*, vol. 116, no. 35, pp. 10922–10927, Sep. 2012.
[66] S. P. Verevkin, R. V. Ralys, V. N. Emel’yanenko, D. H. Zaitsau, and C. Schick, “Thermochemistry of the pyridinium- and pyrrolidinium-based ionic liquids,” *J. Therm. Anal. Calorim.*, vol. 112, no. 1, pp. 353–358, Apr. 2013.
[67] W. S. Ohlinger, P. E. Klunzinger, B. J. Deppmeier, and W. J. Hehre, “Efficient Calculation of Heats of Formation,” *J. Phys. Chem. A*, vol. 113, no. 10, pp. 2165–2175, Mar. 2009.
[68] V. Majer, V. Svoboda, and J. Pick, *Heats of vaporization of fluids*. Elsevier, 1989.
[69] V. P. Glushko and L. V. Gurvich, *Thermodynamic Properties of Individual Substances: Computation of thermodynamic properties* . Office of Technical Services, U.S. Department of Commerce, 1963.
[70] V. N. Emel’yanenko, S. P. Verevkin, A. Heintz, and C. Schick, “Ionic Liquids. Combination of Combustion Calorimetry with High-Level Quantum Chemical Calculations for Deriving Vaporization Enthalpies,” *J. Phys. Chem. B*, vol. 112, no. 27, pp. 8095–8098, Jul. 2008.
[71] S. P. Verevkin, D. H. Zaitsau, V. N. Emel’yanenko, C. Schick, S. Jayaraman, and E. J. Maginn, “An elegant access to formation and vaporization enthalpies of ionic liquids by indirect DSC experiment and ‘in silico’ calculations,” *Chem. Commun.*, vol. 48, no. 55, pp. 6915–6917, Jun. 2012.
[72] W. Guan, J.-Z. Yang, L. Li, H. Wang, and Q.-G. Zhang, “Thermo-chemical properties of aqueous solution containing ionic liquids: 1. The heat of reaction mixed 1-methyl-3-butylimidazolium chloride with InCl3,” *Fluid Phase Equilibria*, vol. 239, no. 2, pp. 161–165, Jan. 2006.
[73] D. H. Zaitsau, V. N. Emel’yanenko, S. P. Verevkin, and A. Heintz, “Sulfur-Containing Ionic Liquids. Rotating-Bomb Combustion Calorimetry and First-Principles Calculations for 1-Ethyl-3-methylimidazolium Thiocyanate,” *J. Chem. Eng. Data*, vol. 55, no. 12, pp. 5896–5899, Dec. 2010.

[74] J. Vitorino, C. E. S. Bernardes, and M. E. M. da Piedade, “A general strategy for the experimental study of the thermochemistry of protic ionic liquids: enthalpy of formation and vaporisation of 1-methylimidazolium ethanoate,” *Phys. Chem. Chem. Phys.*, vol. 14, no. 13, pp. 4440–4446, Mar. 2012.

[75] V. N. Emel’yanenko, S. P. Verevkin, and A. Heintz, “Pyridinium based ionic liquids. N-Butyl-3-methyl-pyridinium dicyanoamide: Thermochemical measurement and first-principles calculations,” *Thermochim. Acta*, vol. 514, no. 1–2, pp. 28–31, Feb. 2011.

[76] S. D. Chambreau, G. L. Vaghjiani, A. To, C. Koh, D. Strasser, O. Kostko, and S. R. Leone, “Heats of Vaporization of Room Temperature Ionic Liquids by Tunable Vacuum Ultraviolet Photoionization,” *J. Phys. Chem. B*, vol. 114, no. 3, pp. 1361–1367, Jan. 2010.

[77] D. Kulikov, S. P. Verevkin, and A. Heintz, “Enthalpies of vaporization of a series of aliphatic alcohols: Experimental results and values predicted by the ERAS-model,” *Fluid Phase Equilibria*, vol. 192, no. 1–2, pp. 187–207, Dec. 2001.

[78] M. V. Roux, M. Temprado, and J. S. Chickos, “Vaporization, fusion and sublimation enthalpies of the dicarboxylic acids from C4 to C14 and C16,” *J. Chem. Thermodyn.*, vol. 37, no. 9, pp. 941–953, Sep. 2005.

[79] M.-M. Huang, Y. Jiang, P. Sasisanker, G. W. Driver, and H. Weingärtner, “Static Relative Dielectric Permittivities of Ionic Liquids at 25 °C,” *J. Chem. Eng. Data*, vol. 56, no. 4, pp. 1494–1499, Apr. 2011.

[80] P. Eiden, S. Bulut, T. Köchner, C. Friedrich, T. Schubert, and I. Krossing, “In Silico Predictions of the Temperature-Dependent Viscosities and Electrical Conductivities of Functionalized and Nonfunctionalized Ionic Liquids,” *J. Phys. Chem. B*, vol. 115, no. 2, pp. 300–309, Jan. 2011.

[81] C. Reichardt, “Polarity of ionic liquids determined empirically by means of solvatochromic pyridinium N-phenolate betaine dyes,” *Green Chem.*, vol. 7, no. 5, pp. 339–351, May 2005.

[82] C. Chiappe, C. S. Pomelli, and S. Rajamani, “Influence of Structural Variations in Cationic and Anionic Moieties on the Polarity of Ionic Liquids,” *J. Phys. Chem. B*, vol. 115, no. 31, pp. 9653–9661, Aug. 2011.

[83] M. A. A. Rani, A. Brant, L. Crowhurst, A. Dolan, M. Lui, N. H. Hassan, J. P. Hallett, P. A. Hunt, H. Niedermeyer, J. M. Perez-Arlandis, M. Schrems, T. Welton, and R. Wilding, “Understanding the polarity of ionic liquids,” *Phys. Chem. Chem. Phys.*, vol. 13, no. 37, pp. 16831–16840, Sep. 2011.

[84] A. A. Oliferenko, P. V. Oliferenko, K. R. Seddon, and J. S. Torrecilla, “Prediction of gas solubilities in ionic liquids,” *Phys. Chem. Chem. Phys.*, vol. 13, no. 38, pp. 17262–17272, Sep. 2011.

[85] L. Glasser and H. D. B. Jenkins, “Volume-Based Thermodynamics: A Prescription for Its Application and Usage in Approximation and Prediction of Thermodynamic Data,” *J. Chem. Eng. Data*, vol. 56, no. 4, pp. 874–880, Apr. 2011.

[86] M. Tariq, M. G. Freire, B. Saramago, J. A. P. Coutinho, J. N. C. Lopes, and L. P. N. Rebelo, “Surface tension of ionic liquids and ionic liquid solutions,” *Chem. Soc. Rev.*, vol. 41, no. 2, pp. 829–868, Jan. 2012.

[87] R. L. Gardas and J. A. P. Coutinho, “Applying a QSPR correlation to the prediction of surface tensions of ionic liquids,” *Fluid Phase Equilibria*, vol. 265, no. 1–2, pp. 57–65, Mar. 2008.

[88] R. Lungwitz, M. Friedrich, W. Linert, and S. Spange, “New aspects on the hydrogen bond donor (HBD) strength of 1-butyl-3-methylimidazolium room temperature ionic liquids,” *New J. Chem.*, vol. 32, no. 9, pp. 1493–1499, Sep. 2008.

[89] R. Lungwitz and S. Spange, “A hydrogen bond accepting (HBA) scale for anions, including room temperature ionic liquids,” *New J. Chem.*, vol. 32, no. 3, pp. 392–394, Mar. 2008.

[90] T. Cremer, C. Kolbeck, K. R. J. Lovelock, N. Paape, R. Wölfel, P. S. Schulz, P. Wasserscheid, H. Weber, J. Thar, B. Kirchner, F. Maier, and H.-P. Steinrück, “Towards a molecular understanding of cation-anion interactions--probing the electronic structure of imidazolium ionic liquids by NMR spectroscopy, X-ray photoelectron spectroscopy and theoretical calculations,” *Chem. Weinh. Bergstr. Ger.*, vol. 16, no. 30, pp. 9018–9033, Aug. 2010.

[91] A. Wulf, K. Fumino, and R. Ludwig, “Spectroscopic Evidence for an Enhanced Anion–Cation Interaction from Hydrogen Bonding in Pure Imidazolium Ionic Liquids,” *Angew. Chem. Int. Ed.*, vol. 49, no. 2, pp. 449–453, 2010.

[92] K. Fumino, A. Wulf, and R. Ludwig, “The Cation–Anion Interaction in Ionic Liquids Probed by Far-Infrared Spectroscopy,” *Angew. Chem. Int. Ed.*, vol. 47, no. 20, pp. 3830–3834, 2008.

[93] K. Fumino, A. Wulf, and R. Ludwig, “Strong, Localized, and Directional Hydrogen Bonds Fluidize Ionic Liquids,” *Angew. Chem. Int. Ed.*, vol. 47, no. 45, pp. 8731–8734, 2008.

[94] K. Fumino, A. Wulf, S. P. Verevkin, A. Heintz, and R. Ludwig, “Estimating Enthalpies of Vaporization of Imidazolium-Based Ionic Liquids from Far-Infrared Measurements,” *ChemPhysChem*, vol. 11, no. 8, pp. 1623–1626, 2010.

[95] R. L. Gardas and J. A. P. Coutinho, “A group contribution method for viscosity estimation of ionic liquids,” *Fluid Phase Equilibria*, vol. 266, no. 1–2, pp. 195–201, Apr. 2008.

[96] J. A. P. Coutinho and R. L. Gardas, “Predictive Group Contribution Models for the Thermophysical Properties of Ionic Liquids,” in *Ionic Liquids: From Knowledge to Application*, vol. 1030, 0 vols., American Chemical Society, 2009, pp. 385–401.

[97] U. Preiss, S. P. Verevkin, T. Koslowski, and I. Krossing, “Going full circle: phase-transition thermodynamics of ionic liquids,” *Chem. Weinh. Bergstr. Ger.*, vol. 17, no. 23, pp. 6508–6517, May 2011.

[98] S. P. Verevkin, “Predicting Enthalpy of Vaporization of Ionic Liquids: A Simple Rule for a Complex Property,” *Angew. Chem. Int. Ed.*, vol. 47, no. 27, pp. 5071–5074, 2008.
[99] G. N. Roganov, P. N. Pisarev, V. N. Emel’yanenko, and S. P. Verevkin, “Measurement and Prediction of Thermochemical Properties. Improved Benson-Type Increments for the Estimation of Enthalpies of Vaporization and Standard Enthalpies of Formation of Aliphatic Alcohols,” *J. Chem. Eng. Data*, vol. 50, no. 4, pp. 1114–1124, Jul. 2005.
[100] W. M. Haynes, D. R. Lide, and T. J. Bruno, *CRC Handbook of Chemistry and Physics*. CRC Press, 2012.
[101] M. G. Freire, C. M. S. S. Neves, P. J. Carvalho, R. L. Gardas, A. M. Fernandes, I. M. Marrucho, L. M. N. B. F. Santos, and J. A. P. Coutinho, “Mutual Solubilities of Water and Hydrophobic Ionic Liquids,” *J. Phys. Chem. B*, vol. 111, no. 45, pp. 13082–13089, Nov. 2007.
[102] D. S. H. Wong, J. P. Chen, J. M. Chang, and C. H. Chou, “Phase equilibria of water and ionic liquids [emim][PF6] and [bmim][PF6],” *Fluid Phase Equilibria*, vol. 194–197, pp. 1089–1095, Mar. 2002.
[103] J.-Z. Yang, Z.-H. Zhang, D.-W. Fang, J.-G. Li, W. Guan, and J. Tong, “Studies on enthalpy of solution for ionic liquid: The system of 1-methyl-3-ethylimidazolium tetrafluoroborate (EMIBF4),” *Fluid Phase Equilibria*, vol. 247, no. 1–2, pp. 80–83, Sep. 2006.
[104] D. W. Fang et al, “Study on Solution Enthalpies of Ionic Liquids of C3MIBF4and C5MIBF4,” *Acta Chim. Sin.*, vol. 66, no. 4, p. 408, 2008.
[105] K.-S. Kim, B.-K. Shin, and H. Lee, “Physical and electrochemical properties of 1-butyl-3-methylimidazolium bromide, 1-butyl-3-methylimidazolium iodide, and 1-butyl-3-methylimidazolium tetrafluoroborate,” *Korean J. Chem. Eng.*, vol. 21, no. 5, pp. 1010–1014, Sep. 2004.
[106] W. Guan, H. Wang, L. Li, Q.-G. Zhang, and J.-Z. Yang, “Enthalpy of solution of the ionic liquid BMIBF4 in water,” *Thermochim. Acta*, vol. 437, no. 1–2, pp. 196–197, Oct. 2005.
[107] D. G. Archer, J. A. Widegren, D. R. Kirklin, and J. W. Magee, “Enthalpy of Solution of 1-Octyl-3-methylimidazolium Tetrafluoroborate in Water and in Aqueous Sodium Fluoride,” *J. Chem. Eng. Data*, vol. 50, no. 4, pp. 1484–1491, Jul. 2005.
[108] M. Reis, R. E. Leitão, and F. Martins, “Enthalpies of Solution of 1-Butyl-3-methylimidazolium Tetrafluoroborate in 15 Solvents at 298.15 K,” *J. Chem. Eng. Data*, vol. 55, no. 2, pp. 616–620, Feb. 2010.
[109] V. D. Kiselev, H. A. Kashaeva, I. I. Shakirova, L. N. Potapova, and A. I. Konovalov, “Solvent Effect on the Enthalpy of Solution and Partial Molar Volume of the Ionic Liquid 1-Butyl-3-methylimidazolium Tetrafluoroborate,” *J. Solut. Chem.*, vol. 41, no. 8, pp. 1375–1387, Sep. 2012.
[110] Y. Zhao, Z. Chen, J. Wang, and K. Zhuo, “Solution Thermodynamics of some Imidazolium-based Ionic Liquids in Water and Aliphatic Alcohols,” *Z. Für Phys. Chem.*, vol. 223, no. 8, pp. 857–868, Aug. 2009.
[111] U. Domańska, “Solubilities and thermophysical properties of ionic liquids,” *Pure Appl. Chem.*, vol. 77, no. 3, pp. 543–557, 2005.
[112] C. M. S. S. Neves, M. L. S. Batista, A. F. M. Cláudio, L. M. N. B. F. Santos, I. M. Marrucho, M. G. Freire, and J. A. P. Coutinho, “Thermophysical Properties and Water Saturation of [PF6]-Based Ionic Liquids,” *J. Chem. Eng. Data*, vol. 55, no. 11, pp. 5065–5073, Nov. 2010.
[113] Y. Li, L.-S. Wang, and S.-F. Cai, “Mutual Solubility of Alkyl Imidazolium Hexafluorophosphate Ionic Liquids and Water,” *J. Chem. Eng. Data*, vol. 55, no. 11, pp. 5289–5293, Nov. 2010.
[114] König, “Proceedings of the 13th International Workshop on Industrial Crystallization BIWIC 2006,” Delft, The Netherlands, 2006, p. 79.
[115] J.-Z. Yang et al, “Studies on Thermochemical Properties of Ionic Liquid EMIInCl4 Based on Scattered Metal Indium,” *Acta Chim. Sin.*, vol. 64, no. 13, p. 1385, 2006.
[116] E. A. Turner, C. C. Pye, and R. D. Singer, “Use of ab Initio Calculations toward the Rational Design of Room Temperature Ionic Liquids,” *J. Phys. Chem. A*, vol. 107, no. 13, pp. 2277–2288, Apr. 2003.
[117] U. Domańska and L. Mazurowska, “Solubility of 1,3-dialkylimidazolium chloride or hexafluorophosphate or methylsulfonate in organic solvents: effect of the anions on solubility,” *Fluid Phase Equilibria*, vol. 221, no. 1–2, pp. 73–82, Jul. 2004.
[118] J.-Z. Yang, W. Guan, J. Tong, H. Wang, and L. Li, “Studies of Thermochemical Properties of a New Ionic Liquid Prepared by Mixing 1-Methyl- 3-Pentylimidazolium Chloride with InCl3,” *J. Solut. Chem.*, vol. 35, no. 6, pp. 845–852, Jun. 2006.
[119] D.-W. Fang, Y.-C. Sun, and Z.-W. Wang, “Solution Enthalpies of Ionic Liquid 1-Hexyl-3-methylimidazolium Chloride,” *J. Chem. Eng. Data*, vol. 53, no. 1, pp. 259–261, Jan. 2008.
[120] Y. U. Paulechka, G. J. Kabo, A. V. Blokhin, A. S. Shaplov, E. I. Lozinskaya, and Y. S. Vygodskii, “Thermodynamic properties of 1-alkyl-3-methylimidazolium bromide ionic liquids,” *J. Chem. Thermodyn.*, vol. 39, no. 1, pp. 158–166, Jan. 2007.
[121] K. Nishikawa, S. Wang, H. Katayanagi, S. Hayashi, H. Hamaguchi, Y. Koga, and K. Tozaki, “Melting and Freezing Behaviors of Prototype Ionic Liquids, 1-Butyl-3-methylimidazolium Bromide and Its Chloride, Studied by Using a Nano-Watt Differential Scanning Calorimeter†,” *J. Phys. Chem. B*, vol. 111, no. 18, pp. 4894–4900, May 2007.
[122] Z.-C. Tan and Z.-H. Zhang, “Study on Thermochemistry of Room Temperature Ionic Liquid,” *Acta Chim. Sin.*, vol. 62, no. 21, pp. 2161–2164, 2004.

[123] M. Leskiv, C. E. S. Bernardes, M. E. Minas da Piedade, and J. N. Canongia Lopes, “Energetics of Aqueous Solutions of the Ionic Liquid 1-Ethyl-3-methylimidazolium Ethylsulfate,” *J. Phys. Chem. B*, vol. 114, no. 41, pp. 13179–13188, Oct. 2010.
[124] A. Sanahuja and J. L. Gómez-Estévez, “The influence of the extrapolation method on enthalpies of solution at infinite dilution,” *Thermochim. Acta*, vol. 94, no. 2, pp. 223–279, Oct. 1985.
[125] A. Sanahuja and J. . Gómez-Estévez, “Determination of the enthalpies of solution at infinite dilution of KCl and NaCl in water at 303.15, 308.15, and 313.15 K,” *J. Chem. Thermodyn.*, vol. 18, no. 7, pp. 623–628, Jul. 1986.
[126] L. F. Silvester and K. S. Pitzer, “Thermodynamics of electrolytes. 8. High-temperature properties, including enthalpy and heat capacity, with application to sodium chloride,” *J. Phys. Chem.*, vol. 81, no. 19, pp. 1822–1828, Sep. 1977.
[127] F. J. Mompean, J. Perrone, and M. Illemassène, *Chemical Thermodynamics of Thorium*. OECD Publishing, 2008.
[128] S. Taniewska-Osińska, M. Tkaczyk, and A. Apelblat, “Enthalpies of dilution and solution of succinic, malonic, and glutaric acids in water at 298.15 K,” *J. Chem. Thermodyn.*, vol. 22, no. 7, pp. 715–720, Jul. 1990.
[129] M. V. Kilday, “The enthalpy of solution of SRM 1655 (KCl) in H2O,” *J. Res. Natl. Bur. Stand.*, vol. 85, no. 6, p. 467, Nov. 1980.
[130] M. J. Frisch, *Gaussian 09 Revision A.1*. .
[131] J. A. Montgomery, M. J. Frisch, J. W. Ochterski, and G. A. Petersson, “A complete basis set model chemistry. VII. Use of the minimum population localization method,” *J. Chem. Phys.*, vol. 112, no. 15, pp. 6532–6542, Apr. 2000.
[132] L. A. Curtiss, P. C. Redfern, K. Raghavachari, V. Rassolov, and J. A. Pople, “Gaussian-3 theory using reduced Møller-Plesset order,” *J. Chem. Phys.*, vol. 110, no. 10, pp. 4703–4709, Mar. 1999.
[133] D. A. McQuarrie, *Statistical Mechanics*. University Science Books, 2000.

Supplementary

Table S1. The volumetric properties of $[C_n mim][NTf_2]$ used in C_P-C_V(l, 298 K) calculations.

Compound	M, kg·mol^{-1}	$10^4 V_m$, m^3·mol^{-1}	$10^4 \alpha_T$, K^{-1}	W, m·s^{-1}	$10^{10} \kappa_T$, Pa^{-1}	C_P-C_V, J·K^{-1}·mol^{-1}	Reference
$[C_2mim][NTf_2]$	391.32	**2.576**	**6.714**				2002Kruwas
		2.566					2002HeiKul
		2.571	**6.571**				2005TokHay
		2.578	**6.683**				2006JacHus
		2.574	5.984				2004frecro
		2.574	7.565				2007GarFre
		2.577	**6.664**				2008WanLeh
		2.576	**6.571**				2010SchZug
				1240			2006fredie
		2.575	6.641	1240	4.950	68.41	average
$[C_3mim][NTf_2]$	405.34	**2.747**	**5.930**	**1235**	**5.080**	56.70	2006EspVis
$[C_4mim][NTf_2]$	419.36	**2.916**	**6.377**				2004frecro
		2.918	**6.509**	**1228.8**			2005azeesp
		2.917	**6.677**				2002kruwas
		2.913	**6.529**				2005TokHay
		2.933					2001hudvis
		2.916	**6.693**		4.980	76.18	2006JacHus
		2.918	**6.243**				2006toktsu
		2.924	**6.677**				2006TroCer
		2.921	**6.674**				2006TroCer
		2.917	**6.605**				2007JacHus
		2.916	**6.641**				2007JacHus2
		2.919	**6.657**				2007HarKan
		2.919	**6.724**				2008WanLeh
		2.917	**6.607**				2009PalKan
		2.919	**6.377**				2010AndArc
				1227			2006fredie
		2.919	6.586	1228.8	5.277	71.82	average
$[C_5mim][NTf_2]$	434.40	**3.093**	**6.477**	**1230.7**	**5.331**	72.57	2006EspVis
$[C_6mim][NTf_2]$		3.240	6.443				2010BocHef
		3.266					2004FitKne
		3.276	7.468				2005TokHay
		3.266	**6.569**				2005KatGme
		3.264	**6.701**		5.410	80.77	2005azeesp
		3.265	**6.714**				2006LacMor
		3.263	7.586				2006toktsu
		3.262	**6.600**				2006KumKam
		3.262	**6.530**				2007WidMag
		3.261	**6.694**	**1226.85**			2007WidMag
		3.263	**6.710**		5.340	82.05	2007KanMar
		3.265					2008DomMar
		3.261	**6.611**				2008Sed
		3.249	**6.810**		5.155	87.15	2008EspGue
		3.261	8.143				2008MuhMut
		3.264	7.822				2010AhoSen
				1232			2006fredie
		3.262	6.660	1226.85	5.527	78.05	average
$[C_7mim][NTf_2]$	461.45	3.426	7.424		5.677	96.15	2007GarFre
$[C_8mim][NTf_2]$	475.48	3.686					2004FitKne
		3.597	**7.565**				2005TokHay
		3.589	**8.188**				2005KatGme
		3.599	**8.383**				2006ZaiKab
		3.602	**7.519**				2006toktsu
		3.600					2007AloArc

		3.597	**8.701**		5.407	141.3	2007GarFre
		3.603					2008AloArc
				1232			2006Fredie
		3.598	8.071	1232	6.134	107.2	average
$[C_{10}mim][NTf_2]$	499.5	**3.908**	6.685		6.142	75.94	2008TomCar

In bold listed the chosen values.

2004 frecro Fredlake, C. P.; Crosthwaite, J. M.; Hert, D. G.; Aki, S. N. V. K.; Brennecke, J. F. J. Chem. Eng. Data 2004, 49 , 954-964

2006 fredie Frez, C.; Diebold, G. J.; Tran, C. D.; Yu, S. J. Chem. Eng. Data 2006, 51 , 1250-1255

2002Kruwas Krummen, M.; Wasserscheid, P.; Gmehling, J. J. Chem. Eng. Data 2002, 47 , 1411-1417

2002HeiKul Heintz, A.; Kulikov, D. V.; Verevkin, S. P. J. Chem. Eng. Data 2002, 47 , 894-899

2005TokHay Tokuda, H.; Hayamizu, K.; Ishii, K.; Susan, M. A. B. H.; Watanabe, M. J. Phys. Chem. B 2005, 109 (13), 6103-6110

2006JacHus Jacquemin, J.; Husson, P.; Padua, A. A. H.; Majer, V. Green Chem. 2006, 8 , 172-180

2007GarFre Gardas, R. L.; Freire, M. G.; Carvalho, P. J.; Marrucho, I. M.; Fonseca, I. M. A.; Ferreira, A. G. M.; Coutinho, J. A. P. J. Chem. Eng. Data 2007, 52 , 1881-1888

2008WanLeh Wandschneider, A.; Lehmann, J. K.; Heintz, A. J. Chem. Eng. Data 2008, 53 , 596-599

2010SchZug Schreiner, C.; Zugmann, S.; Hartl, R.; Gores, H. J. J. Chem. Eng. Data 2010, 55 (5), 1784-1788

2006TroCer Troncoso, J.; Cerdeirina, C. A.; Sanmamed, Y. A.; Romani, L.; Rebelo, L. P. N. J. Chem. Eng. Data 2006, 51 , 1856-1859

2005azeesp de Azevedo, R. G.; Esperanca, J. M. S. S.; Szydlowski, J.; Visak, Z. P.; Pires, P. F.; Guedes, H. J. R.; Rebelo, L. P. N. J. Chem. Thermodyn. 2005, 37 , 888-899

2001hudvis Huddleston, J. G.; Visser, A. E.; Reichert, W. M.; Willauer, H. D.; Broker, G. A.; Rogers, R. D. Green Chem. 2001 (3), 156-164

2006toktsu Tokuda, H.; Tsuzuki, S.; Susan, M. A. B. H.; Hayamizu, K.; Watanabe, M. J. Phys. Chem. B 2006, 110 (39), 19593-19600

2007JacHus Jacquemin, J.; Husson, P.; Mayer, V.; Cibulka, I. J. Chem. Eng. Data 2007, 52 , 2204-2211

2007JacHus2 Jacquemin, J.; Husson, P.; Majer, V.; Gomes, M. F. C. J. Solution Chem. 2007, 36 , 967-979

2007HarKan Harris, K. R.; Kanakubo, M.; Woolf, L. J. Chem. Eng. Data 2007, 52 (3), 1080-1085

2009PalKan Palgunadi, J.; Kang, J. E.; Nguyen, D. Q.; Kim, J. H.; Min, B. K.; Lee, S. D.; Kim, H.; Kim, H. S. Thermochim. Acta 2009, 494 , 94-98

2010AndArc Andreatta, A. E.; Arce, A.; Rodil, E.; Soto, A. J. Solution Chem. 2010, 39 (3), 371-383

2006Zaikab Zaitsau Dz. H.; Kabo G. J.; Strechan A. A.; Paulechka Y. U.; Tschersich A.; Verevkin S. P.; Heintz A. J. Chem. Phys. A, 2006, 110, 22, 7303 - 7306.

2006EspVis Esperanca, J. M. S. S.; Visak, Z. P.; Plechkova, N. V.; Seddon, K. R.; Guedes, H. J. R.; Rebelo, L. P. N. J. Chem. Eng. Data 2006, 51 , 2009-2015

2007WidMag Widegren, J. A.; Magee, J. W. J. Chem. Eng. Data 2007, 52 , 2331-2338

2004FitKne Fitchett, B. D.; Knepp, T. N.; Conboy, J. C. J. Electrochem. Soc. 2004, 151 (7), E219-E225

2005KatGme Kato, R.; Gmehling, J. J. Chem. Thermodyn.2005, 37 , 603-619

2006LacMor Lachwa, J.; Morgado, P.; Esperanca, J. M. S. S.; Guedes, H. J. R.; Lopes, J. N. C.; Rebelo, L. P. N. J. Chem. Eng. Data 2006, 51 , 2215-2221

2006KumKam Kumelan, J.; Kamps, A. P. -S.; Tuma, D.; Maurer, G. J. Chem. Thermodyn. 2006, 38 (11), 1396-1401

2007KanMar Kandil, M. E.; Marsh, K. N.; Goodwin, A. R. H. J. Chem. Eng. Data 2007, 52 , 2382-2387

2008DomMar Domanska, U.; Marciniak, A. http://Ilthermo.boulder.nist.gov

2008Sed Seddon, K. R. Densities of Ionic Liquid for IUPAC Project. http://Ilthermo.boulder.nist.gov

2008EspGue Esperanca, J. M. S. S.; Guedes, H. J. R.; Lopes, J. N. C.; Rebelo, L. P. N. J. Chem. Eng. Data 2008, 53 , 867-870

2008MuhMut Muhammad, A.; Mutalib, M. I. A.; Wilfred, C. D.; Murugesan, T.; Shafeeq, A. J. Chem. Thermodyn. 2008, 40 , 1433-1438

2010AhoSen Ahosseini, A.; Sensenich, B.; Weatherley, L. R.; Scurto, A. M. J. Chem. Eng. Data 2010, 55 (4), 1611-1617

2007AloArc Alonso, L.; Arce, A.; Francisco, M.; Soto, A. J. Chem. Eng. Data 2007, 52 , 2409-2412

2008AloArc Alonso, L.; Arce, A.; Francisco, M.; Soto, A. J. Chem. Eng. Data 2008, 53 , 1750-1755

2008TomCar Tome, L. I. N.; Carvalho, P. J.; Freire, M. G.; Marrucho, I. M.; Fonseca, I. M. A.; Ferreira, A. G. M.; Coutinho, J. A. P.; Gardas, R. L. J. Chem. Eng. Data 2008, 53 , 1914-1921

Table S2 List of abbreviations of ILs and precursors in this work

Abbreviation	IUPAC Name
[$C_n$mim]	1-alkyl-3-methylimidazolium
[C_{n1}Pyrr]	1-alkyl-1-methylpyrrolidinium
[C_nPy]	1-alkylpyridinium
[$C_n$mmim]	1-alkyl-2,3-dimethylimidazolium
[$C_nC_n$im]	1,3-dialkylimidazolium
[N_{nnnn}]	tetraalkylammonium
[Hmim]	1-alkylimidazolium
3Me-C_nPy	3-methyl-1-alkylpyridinium
[NTf_2]	bis(trifluoromethylsulfonyl)imide
[Br]	bromide
[Cl]	chloride
[I]	iodide
[SCN]	thiocyanate
[C_nSO_4]	ethylsulfate
[CF_3CO_2]	trifluoroacetate
[CF_3SO_3]	trifluoromethanesulfonate
[$(C_2H_5O)_2PO_2$]	diethylphosphate
[PF_6]	hexafluorophosphate
[BF_4]	tetrafluoroborate
[$C(CN)_3$]	tricyanomethanide
[$N(CN)_2$]	dicyanamide
[$B(CN)_4$]	tetracyanoborate
[FAP]	tris(pentafluoroethyl)trifluorophosphate
[NO_3]	nitrate
[beti]	bis(pentafluoroethylsulfonyl)amide
[TOS]	tosylate
C_nBr	n-alkylbromide
C_nIm	n-alkylimidazole
1,2-diMeIm	1,2 -dimethylimidazole

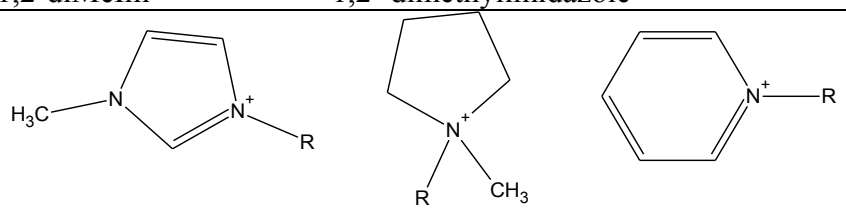

Figure S1 imidazolium, pyrrolidinium and pyridinium based cations.

Table S3 Initial solution calorimetry data measure in this work

IL	m sample, g	m, mol·kg^{-1}	$\Delta_{sol}H_m^0$, kJ·mol^{-1}
[C_2mim][BF_4]	0.0465	0.00940	18.27
	0.0919	0.01857	18.08
	0.1193	0.02410	18.08
	0.2041	0.04124	18.11
	0.0286	0.00578	18.28
[C_4mim][BF_4]	0.0125	0.00221	17.27
	0.0187	0.00331	17.38
	0.0461	0.00816	17.31
	0.0554	0.00980	16.92
	0.0799	0.01414	17.44

	0.1111	0.01966	16.67
$[C_8mim][BF_4]$	0.09480	0.01344	16.10
	0.05700	0.00808	17.34
	0.04020	0.00570	16.57
	0.09990	0.01416	18.48
	0.10334	0.01465	17.42
	0.04628	0.00656	18.84
	0.02231	0.00316	19.25
	0.18894	0.02679	17.18
	0.02598	0.00368	18.00
	0.01204	0.00171	18.31
$[C_2mim][PF_6]$	0.04381	0.00684	46.36
	0.06349	0.00992	45.85
	0.04737	0.00740	45.54
	0.09036	0.01411	45.82
	0.05681	0.00887	46.45
$[C_4mim][PF_6]$	0.10917	0.01537	19.84
	0.16056	0.02260	19.99
$[C_2mim][Cl]$	0.06861	0.01872	-16.16
	0.03414	0.00931	-16.88
$[C_4mim][Cl]$	0.04138	0.00948	1.74
	0.04338	0.00993	1.79
	0.03236	0.00741	1.87
	0.09093	0.02082	1.70
	0.03489	0.00799	1.60
$[C_2mim][Br]$	0.01205	0.00252	11.59
	0.00836	0.00175	10.71
	0.03793	0.00794	1.96 (l)
$[C_4mim][Br]$	0.03420	0.00716	10.00
	0.03107	0.00650	9.56
	0.06279	0.01314	10.29
	0.08532	0.01786	10.63
$[C_2mim][NO_3]$	0.11134	0.02572	1.78 (l)
	0.07840	0.01811	2.62 (l)
	0.09879	0.02282	1.67 (l)
	0.03629	0.00838	17.41
	0.05274	0.01218	17.23
	0.14885	0.03438	16.72
$[C_4mim][NO_3]$	0.03677	0.00731	0.40
	0.05431	0.01080	0.23
	0.08023	0.01595	0.14
	0.04557	0.00906	0.24
	0.03116	0.00619	0.21
$[C_2mim][SCN]$	0.10671	0.02522	7.80
	0.03803	0.00899	7.85
	0.06176	0.01460	7.86
	0.02136	0.00505	7.88
	0.07211	0.01704	7.83
$[C_4mim][SCN]$	0.04376	0.00887	7.76
	0.07149	0.01449	7.63
	0.04215	0.00855	7.81
	0.05632	0.01142	7.71
	0.04314	0.00875	7.66
$[C_2mim][C_1SO_4]$	0.06722	0.01210	-13.92
	0.12167	0.02190	-13.60
	0.06942	0.01249	-13.65
	0.04986	0.00897	-14.86
	0.08288	0.01492	-14.45
	0.05706	0.01027	-14.71
$[C_4mim][C_1SO_4]$	0.07280	0.0116	-11.21
	0.04936	0.0079	-10.59
	0.04827	0.0077	-10.85

	0.02990	0.0048	-11.06
	0.08397	0.0134	-11.49
$[C_2mim][C_2SO_4]$	0.10444	0.01768	-10.97
	0.09570	0.01620	-10.87
	0.04308	0.00729	-10.64
	0.03931	0.00665	-10.84
	0.04371	0.00740	-10.85
$[C_2mim][C_4SO_4]$	0.03044	0.00461	-11.56
	0.05265	0.00797	-11.63
	0.10219	0.01546	-11.52
	0.07557	0.01144	-11.90
	0.03526	0.00534	-11.81
$[C_2mim][C_8SO_4]$	0.04039	0.00504	-6.28
	0.01237	0.00154	-6.00
	0.04116	0.00514	-6.07
	0.02104	0.00263	-6.00
	0.02965	0.00370	-6.10
$[C_2mim][CF_3SO_3]$	0.03489	0.00536	2.56
	0.09093	0.01398	2.53
	0.03236	0.00497	2.77
	0.04338	0.00667	2.67
	0.04138	0.00636	2.61
$[C_4mim][CF_3SO_3]$	0.05469	0.00759	1.87
	0.09767	0.01355	1.77
	0.11417	0.01584	1.76
	0.07373	0.01023	1.74
$[C_2mim][N(CN)_2]$	0.05220	0.01178	3.49
	0.03436	0.00776	3.22
	0.01680	0.00379	3.24
	0.03942	0.00890	3.30
	0.02156	0.00487	3.49
$[C_2mim][C(CN)_3]$	0.01325	0.00263	12.25
	0.12405	0.02466	12.46
	0.11420	0.02270	12.51
	0.07268	0.01445	12.77
$[C_4mim][C(CN)_3]$	0.06721	0.01173	12.26
	0.09524	0.01662	12.29
	0.04773	0.00833	11.63
$[C_4C_4im][BF4]$	0.03722	0.00323	21.35
	0.02327	0.00202	21.56
	0.01810	0.00157	21.50
	0.01082	0.00094	21.91
	0.04080	0.00354	21.27
$[C_{41}Pyrr][N(CN)_2]$	0.02475	0.00475	-1.75
	0.02391	0.00459	-1.21
	0.04278	0.00822	-1.07
$[3Me\text{-}C_4Py][N(CN)_2]$	0.02276	0.00421	-0.46
	0.04786	0.00885	-0.45
	0.02487	0.00460	-0.30
$[N_{1111}][BF_4]$	0.01375	0.00342	42.92
	0.01374	0.00341	43.30
	0.00790	0.00196	43.27
	0.00846	0.00210	42.81
$[N_{4444}][BF_4]$	0.01103	0.00134	6.84
	0.02251	0.00273	6.29
	0.01335	0.00162	6.66
	0.01313	0.00160	6.75

Table S4. The volumetric properties of $[C_nmim][NTf_2]$ used in $\Delta_l^g C_p^{o}{}_m$ (l, 298 K) calculations.

Compound	M, kg·mol^{-1}	$C_P^{o}{}_m$(l), J·K^{-1}·mol^{-1}	$10^4 V_m$, m^3·mol^{-1}	$10^4 \alpha_T$, K^{-1}	W, m·s^{-1}	$10^{10} \kappa_T$, Pa^{-1}	C_P-C_V, J·K^{-1}·mol^{-1}	$\Delta_l^g C_p^{o}{}_m$, J·K^{-1}·mol^{-1}	Reference
$[C_2Py][NTf_2]$	**0.38832**	**518**				**5.44**	**-43.8**	**-60**	30, 31
			2.526	**5.630**	**1142.5**				S5
			2.528						S1
$[C_3Py][NTf_2]$	**0.40235**	**550**				**5.87**	**-49.5**	**-66**	30, 31
			2.694	**6.012**	**1120**[a]				S6
$[C_4Py][NTf_2]$	**0.41637**	**582**							30
			2.891						S3
			2.862	5.990	**1099.2**	6.22	-49.3	-66	S5
			2.800	6.489		6.17	-57	-74	S4
								-70	average
$[C_5Py][NTf_2]$	**0.43040**	**614**				**6.44**	**-56**	**-73**	30, 31
			3.029	**6.300**	**1096.2**				S5
$[C_6Py][NTf_2]$	**0.44442**	620							S2
		646							30, 31
			3.203	**6.455**	**1095.5**	**6.62**	**-60**	**-77**	S6
			3.188	**6.455**		**6.59**	**-60**	**-77**	S4

[a] interpolated between $[C_2Py][NTf_2]$ and $[C_4Py][NTf_2]$

In bold listed the chosen values.

S1 Kato, R.; Gmehling, J. Fluid Phase Equilib., 2004, 226, 37-44

S2 J. M. Crosthwaite, M. J. Muldoon, J. K. Dixon, J. L. Anderson, and J. F. Brennecke, J. Chem. Thermodyn. 37, 559 2005 .

S3 Tokuda, H.; Tsuzuki, S.; Susan, M. A. B. H.; Hayamizu, K.; Watanabe, M. J. Phys. Chem. B, 2006, 110(39), 19593-19600

S4 Oliveira, F. S.; Freire, M. G.; Carvalho, P. J.; Coutinho, J. A. P.; Lopes, J. N. C.; Rebelo, L. P. N.; Marrucho, I. M. J. Chem. Eng. Data, 2010, 55(10), 4514-4520

S5 Liu, Q.-S.; Yang, M.; Yan, P.-F.; Liu, X.-M.; Tan, Z.-C.; Welz-Biermann, U. J. Chem. Eng. Data, 2010, 55(11), 4928-4930

S6 Q. Liu, M. Yang, S. Sun, U. Welz-biermann, Z. Tan, Q. Zhang. J. Chem. Eng. Data 2011, 56, 4094-4101

Table S5. The dataset for calculation of the $(C_p\text{-}C_v)_l$ for $[C_{41}Pyrr][NTf_2]$

$C_p^{\circ}{}_m$ (l, 298 K), J·K^{-1}·mol^{-1}	W, m·s^{-1}	ρ, kg·m^{-3}	$10^4\,V$, m^3·mol^{-1}	$10^4\,a_P$, K^{-1}	$10^{10}\,k_T$, Pa^{-1}	Reference
588						Paulechka
	1269	1394.66	3.029		5.071	2012seocor
	1269	1394.59	3.029	6.237	5.068	2009pervei
		1393.99	3.030	6.180	4.470	2008jacnan
		1394	3.030	7.461		2005antand
		1395	3.028	6.452		2006tok
		1394	3.030	3.484		2005katgme
		1394.57	3.029	6.487		2012vradoz
		1394.51	3.029	6.345	4.194	2011harwoo
		1404.19	3.008	7.038	5.263	2008garcos
588	**1269**	**1394.69**	**3.029**	**6.358**	**5.069**	Selected

$(C_p\text{-}C_v)_l$, J·K^{-1}·mol^{-1}	$\Delta_l{}^g C_p^{\circ}{}_m$, J·K^{-1}·mol^{-1}
72	-89

[Paulechka] Y.U. Paulechka, Heat Capacity of Room-Temperature Ionic Liquids: A Critical Review, J. Phys. Chem. Ref. Data 39, 3 (2010) 033108-1-033107-23.

[2012seocor] R.G. Seoane, S. Corderí, E. Gómez, N. Calvar, E.J. González, E.A. Macedo, Á. Domínguez, Temperature Dependence and Structural Influence on the Thermophysical Properties of Eleven Commercial Ionic Liquids, Ind. Eng. Chem. Res. 51 (2012) 2492−2504.

[2009pervei] A.B. Pereiro, H.I.M. Veiga, J.M.S.S. Esperanca, A. Rodriguez, Effect of temperature on the physical properties of two ionic liquids, J. Chem. Thermodyn. 41 (2009) 1419-1423.

[2008jacnan] J. Jacquemin, R. Ge, P. Nancarrow, D.W. Rooney,M.F. Costa Gomes, A.A.H. Pádua,C. Hardacre, Prediction of Ionic Liquid Properties. I. Volumetric Properties as a Function of Temperature at 0.1 MPa, J Chem. Eng. Data 53 (2008) 2473-2473.

[2005antand] J.L. Anthony, J.L. Anderson, E.J. Maginn, J.F. Brennecke, Anion Effects on Gas Solubility in Ionic Liquids, J. Phys. Chem. B 109 (2005) 6366-6374.

[2006tok] H. Tokuda, S. Tsuzuki, M.A.B.H. Susan, K. Hayamizu, M. Watanabe, How Ionic Are Room-Temperature Ionic Liquids? An Indicator of the Physicochemical Properties, J Phys. Chem. B 110 (2006) 19593-19600

[2005katgme] R. Kato, J. Gmehling, Systems with ionic liquids: Measurement of VLE and □8 data and prediction of their thermodynamic behavior using original UNIFAC, mod. UNIFAC(Do) and COSMO-RS(Ol) J. Chem. Thermodyn. 37 (2005) 603-619.

[2012vradoz] M. Vranes, S. Dozic, V. Djeric, S. Gadzuric, Physicochemical Characterization of 1-Butyl-3-methylimidazolium and 1-Butyl-1-methylpyrrolidinium Bis(trifluoromethylsulfonyl)imide, J Chem. Eng. Data 57 (2012) 1072-1077.

[2011harwoo] K.R. Harris, L.A. Woolf, M. Kanakubo, T. Rüther, Transport Properties of N-butyl-N-methylpyrrolidinium Bis(trifluoromethylsulfonyl)amide. J Chem. Eng. Data 56 (2011) 4672-4685.

[2008garcos] R.L. Gardas, H.F. Costa, M.G. Freire, P.J. Carvalho, I.M. Marrucho, I.M.A. Fonseca, A.G.M. Ferreira, J.A.P. Coutinho, Densities and Derived Thermodynamic Properties of Imidazolium-, Pyridinium-, Pyrrolidinium-, and Piperidinium-Based Ionic Liquids, J Chem. Eng. Data 53 (2008) 805-811.

Table S6 The $\Delta_l^g H_m^0$ of n-alkylhalides used for calculations [C1]. e – extrapolated with equation $\Delta_l^g H_m^0$ (Alkyliodide) = 4.4n +23.1, derived from n = 2-6.

Alkyl	$\Delta_l^g H_m^0$ (298 K), kJ·mol^{-1}		
	Cl	Br	I
methyl	20.5	23.2	-
ethyl	24.7	28.3	32.1
n-propyl	28.7	31.9	36.3
n-butyl	33.5	36.7	40.7
n-pentyl	38.2	41.1	45.3
n-hexyl	42.8	46.1	49.8
n-heptyl	47.7	50.8	-
n-octyl	52.4	55.8	58.3[e]

[C1] V. Majer, V. Svoboda, and J. Pick, *Heats of vaporization of fluids*. Elsevier, 1989

Table S7 The $\Delta_l^g H_m^0$ of imidazoles used for calculations (a – interpolated values)

	$\Delta_l^g H_m^0$ (298 K), kJ·mol^{-1}
1,2-dimethylimidazole	58.9 ± 0.2 [B1]
butylimidazole	65.1 ± 0.5[a][B2]
pentylimidazole	69.1 ± 0.5[B2]
octylimidazole	81.2 ± 0.5[a][B2]

[B1] D. H. Zaitsau, A. V. Yermalayeu, V. N. Emel'yanenko, C. Schick, S. P. Verevkin, A. A. Samarov, S. Schlenk, and P. Wasserscheid, "Structure-property relations in ionic liquids: 1,2,3-trimethyl-imidazolium and 1,2,3-trimethylbenzimidazolium bis-(trifluorsulfonyl)imide," *Z. Phys. Chem.*, vol. 227, no. 2–3, pp. 205–215, 2013.
[B2] V. N. Emel'yanenko, S. V. Portnova, S. P. Verevkin, A. Skrzypczak, and T. Schubert, "Building blocks for ionic liquids: Vapor pressures and vaporization enthalpies of 1-(n-alkyl)-imidazoles," *J. Chem. Thermodyn.*, vol. 43, no. 10, pp. 1500–1505, Oct. 2011

Table S8 Conductometric study of diluted EMIM NTf2 solutions

m([EMIM][NTf_2]) / g	m(H_2O) / g	σ / μS/cm
0.0049	30.055	30
0.0104	30.1041	64.6
0.0135	30.1324	76.2
0.0239	30.1316	139.4
0.0463	29.9931	257.4
0.0566	29.9245	319
0.113	29.5634	618
0.5153	30.1286	2282
0	∞	1.8

Table S9 Conductometric study of diluted Na NTf2 solutions

m([Na][NTf_2]) / g	**m(H_2O) / g**	**σ / μS/cm**
0.0031	79.7837	13.3
0.031	26.7368	300
0.0199	30.2423	188.5
0.0623	30.0782	521
0.0062	30.1257	55.5
0.0515	29.7408	440
0.0124	36.6499	95.6
0.0392	29.4356	344

Table S10 DSC synthesis reaction for [$C_nC_n$im][Hal]

System	m solvent, mg	m imidazole, mg	m alkylhalogenide, mg	Q, mJ	$\Delta_r H_m^0$ kJ/mol
C_4Im+ C_4Br	-	2.77	1.80	1310.47	99.8
	-	2.77	1.94	1384.38	97.8
	-	2.54	1.92	1379.51	98.4
	-	1.69	1.31	942.08	98.5
	-	3.22	1.96	1433.81	100.2
	-	3.38	2.29	1651.01	98.8
C_5Im+ C_5Br	-	2.35	1.87	1271.94	102.7
	-	2.67	1.96	1350.1	104.0
	-	2.52	1.84	1243.58	102.1
	-	2.95	2.08	1391.92	101.1

	-	3.20	2.58	1731.87	101.4
	-	3.96	1.41	964.53	103.3
$C_8Im+ C_8Br$	-	1.59	1.29	658.24	98.5
	-	2.70	2.11	1096.04	100.3
	-	2.86	2.18	1124.51	99.6
	-	2.59	1.61	850.81	102.1
	-	3.09	2.33	1206.24	100.0
	-	3.22	2.42	1258.05	100.4
$C_4Im+ C_4I$	4.31	3.05	2.74	1591.00	106.9
	4.64	3.28	2.30	1343.58	107.5
	3.27	2.32	1.91	1085.14	104.5
	4.25	3.00	2.27	1310.95	106.3
	4.93	3.48	2.97	1672.24	103.6
	4.55	3.22	2.86	1609.39	103.6
$C_5Im+ C_5I$	3.73	3.72	2.51	1310.58	103.4
	3.38	3.36	2.37	1268.48	106.0
	4.33	4.30	2.17	1131.09	103.2
	4.22	4.19	2.82	1459.72	102.5
	4.81	4.79	2.77	1447.14	103.5
	3.00	2.99	1.35	711.32	104.4
$C_8Im+ C_8I$	4.17	1.71	0.99	432.2	104.8
	6.05	2.49	1.31	564.74	103.5
	4.10	1.68	1.14	481.21	101.4

Table S11 DSC synthesis reaction for [$C_n$mmim][Hal]

System	m solvent, mg	m imidazole, mg	m alkylhalogenide, mg	Q, mJ	$\Delta_r H_m^0$ kJ/mol
1,2diMeIm+ C_4Br	4.60	3.83	3.36	2403.81	98.0
	5.15	4.29	2.26	1577.37	95.6
	4.07	3.39	3.38	2421.03	98.1
	4.88	4.07	4.03	2860.11	97.2
	4.84	4.03	2.95	2075.98	96.4
	4.40	3.67	3.83	2704.38	96.8
	3.70	3.09	4.54	3032.77	94.4
1,2diMeIm+ C_5Br	3.83	3.20	1.59	1019.17	96.8
	5.33	4.44	2.71	1737.74	96.9
	3.76	3.13	1.58	985.78	94.2
	3.46	2.88	2.26	1445.57	96.6
	5.16	4.30	3.61	2311.65	96.7
	4.13	3.44	1.83	1167.32	96.3
	5.34	4.45	2.25	1440.97	96.7
1,2diMeIm+ C_8Br	4.60	3.83	3.36	2403.81	98.0
	5.15	4.29	2.26	1577.37	95.6
	4.07	3.39	3.38	2421.03	98.1
	4.88	4.07	4.03	2860.11	97.2
	4.84	4.03	2.95	2075.98	96.4
	4.40	3.67	3.83	2704.38	96.8
	3.70	3.09	4.54	3032.77	94.4
12MIm+ C_4I	5.46	0.46	1.67	520.39	109.6
	6.77	0.57	0.56	325.13	106.8
	8.64	0.72	0.71	412.75	107.0
	8.98	0.75	0.87	498.35	105.4
	10.27	0.86	0.71	410.15	106.3
	10.36	0.87	0.87	511.00	108.1
	9.54	0.80	0.86	497.93	106.5
12MIM+ C_5I	5.93	3.26	2.89	1553.10	106.4
	6.03	3.31	2.94	1571.31	105.8
	5.97	3.28	2.61	1420.29	107.8
	6.00	3.30	2.71	1457.61	106.5
	6.40	3.51	2.82	1527.77	107.3

	6.01	3.30	2.86	1533.24	106.2
	6.00	3.29	2.68	1438.79	106.3
	4.50	2.47	1.32	715.49	107.4
	6.04	3.32	1.36	730.87	106.4
	5.95	3.27	2.72	1211.55	107.0
	6.14	3.38	2.52	1130.81	107.8
	6.08	3.34	2.53	1111.52	105.5
	6.02	3.31	2.51	1129.64	108.1
12MIM+ C_8I	6.16	3.39	2.60	1174.24	108.5
	6.03	3.31	2.60	1170.77	108.1
	5.93	3.26	2.60	1143.82	105.6
	6.09	3.34	2.71	1232.55	109.2
	5.15	2.83	2.65	1197.63	108.5